

**TNO report****TNO 2021 R10526****Identification and quantification of risks of  
subsurface hydrogen storage in salt caverns**

Leeghwaterstraat 44  
2628 CA Delft  
P.O. Box 6012  
2600 JA Delft  
The Netherlands

[www.tno.nl](http://www.tno.nl)

T +31 88 866 22 00  
F +31 88 866 06 30

Date	30 June 2021
Number of pages	84 (incl. appendices)
Number of appendices	3
Project name	Testen van opslag waterstof in zoutcaverne ter flexibilisering duurzaam energiesysteem
Project number	060.36820, subsidy reference: DEI4819001

All rights reserved.

No part of this publication may be reproduced and/or published by print, photoprint, microfilm or any other means without the previous written consent of TNO.

In case this report was drafted on instructions, the rights and obligations of contracting parties are subject to either the General Terms and Conditions for commissions to TNO, or the relevant agreement concluded between the contracting parties. Submitting the report for inspection to parties who have a direct interest is permitted.

© 2021 TNO

# Contents

<b>1</b>	<b>Introduction .....</b>	<b>3</b>
1.1	List of abbreviations .....	5
<b>2</b>	<b>BowTie analysis for hydrogen storage in a salt cavern .....</b>	<b>6</b>
2.1	BowTie methodology .....	6
2.2	Notional design of hydrogen storage system and set-up of test procedures .....	9
2.3	BowTie analysis for top event leakage of hydrogen in the subsurface .....	15
2.4	BowTie analysis for top event leakage of hydrogen at the surface .....	27
2.5	Towards failure scenarios for hydrogen storage in a salt cavern .....	35
<b>3</b>	<b>Physical effects of accidental hydrogen release at the wellhead .....</b>	<b>38</b>
3.1	Set-up of outflow and effect calculations .....	38
3.2	Discussion of study results .....	47
<b>4</b>	<b>Conclusion .....</b>	<b>61</b>
4.1	BowTie analysis for hydrogen storage in a salt cavern .....	61
4.2	Physical effects of accidental hydrogen release at the wellhead .....	62
4.3	Recommendations .....	64
<b>5</b>	<b>References .....</b>	<b>65</b>

## Appendices

- A BowTie diagram
- B Effect of well geometry
- C Detailed results OLGA-old well path

# 1 Introduction

This report describes the research contribution of TNO to the project “*Testen van opslag waterstof in zoutcaverne ter flexibilisering duurzaam energiesysteem*” with subsidy reference DEI4819001. TNO performed this research during 2020 and the beginning of 2021 in cooperation with EnergyStock.

The scope of the project contributes to the aim of EnergyStock to develop one of the first locations in western-Europe for subsurface hydrogen storage in a salt cavern. The specific location where facilities and installation are under development is close to Zuidwending in the upper north-east of the Netherlands. For project partner EnergyStock this development is foreseen to contribute to establishing a hydrogen hub in the north of the Netherlands where excess electricity from wind farms is converted to green hydrogen to be stored in the subsurface, see also Figure 1. The stored hydrogen then serves as energy buffer and as source to reconvert to electricity at moments of electricity shortage.

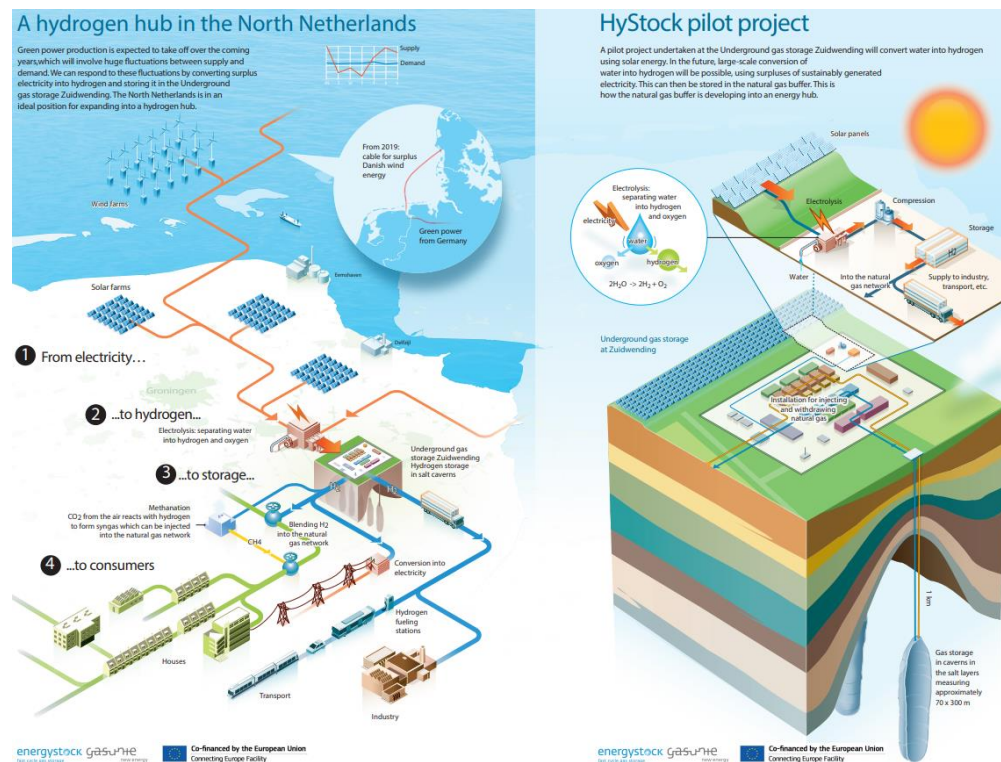


Figure 1: Schematic diagram of a hydrogen hub for the North of The Netherlands, source: EnergyStock.

The project “*Testen van opslag waterstof in zoutcaverne ter flexibilisering duurzaam energiesysteem*” consists of three main activities. The first two activities are carried out under supervision of EnergyStock (together with several service providers and other third parties) and with no involvement from TNO. These two activities concern:

- Development and realisation of a pilot-installation in a small salt cavern on the Zuidwending location (gas storage facilities) of EnergyStock,

- Execution of field tests with associated safety barriers where hydrogen is injected and withdrawn. These tests have the purpose of validation, monitoring and analysis of foreseen innovations under realistic conditions.

The field tests consist of two steps for a well at the aforementioned location:

- 1) An MIT (Mechanical Integrity Test) with nitrogen followed by an MIT with hydrogen to test the leak tightness of the casing and Last Cemented Casing Shoe (without completion),
- 2) Cyclic hydrogen injection and withdrawal tests with a completion (production tubing, packer and wellhead) installed.

Where the field tests are also referred to as the pilot phase in this report, it is expected to be followed by a second phase (in case this pilot phase is successful), as follow-up of this project, in which hydrogen will be injected into a full-scale cavern at the Zuidwending location.

The third activity of this project, the research contribution of TNO, is subject of this report and concerns:

- Development of a generic methodology for identification and quantification of risks that come with subsurface hydrogen storage in salt caverns.

It consists of the following two studies:

- I. Performing a so-called BowTie analysis targeted at events that can cause a loss of integrity and with leakage of hydrogen as a consequence, provision of examples of relevant high-risk failure scenarios (which describe potential future situations and developments of the storage system and that can lead to undesirable events), and formulation of applicable risk-mitigation measures and suitable monitoring techniques.
- II. A modelling study to quantify the risk associated with uncontrolled partial or full free outflow of hydrogen due to leakage at the wellhead (from tubing, casing) or as an extreme case due to a blow-out.

The two studies I and II consider both a pilot phase and a subsequent second full-scale cavern phase for subsurface hydrogen storage in salt caverns. The notional design for the subsurface hydrogen storage system (i.e. cavern and well design) used in both studies are derived and modified from the salt caverns at the Zuidwending location. These caverns are considered representative for a typical cavern in a subsurface storage system for hydrogen. Both studies, however, are generic and do not consist of a specific evaluation for the location of Zuidwending, but results of the studies may guide an approach to evaluate specific locations. Any decisions and further choices regarding a location-specific application of this generic methodology are outside the scope of this study. This will be the responsibility of the licence holder and operator of a hydrogen storage location.

The risk inventorization and subsequent BowTie analysis performed in part I is described in chapter 2, whereas chapter 3 discusses the approach applied and the

results obtained for part II. Chapter 4 discusses the conclusions from both part I and part II, whereas the report is completed with a chapter with references. Furthermore, the content of this report is supported by three appendices.

Throughout the chapters and appendices of this report several abbreviations are being used and a listing of these abbreviations is found below.

## 1.1 List of abbreviations

ATEX	Atmospheres Explosible
H <sub>2</sub>	Hydrogen
H <sub>2</sub> S	Hydrogen sulphide
IR	Infrared
JT	Joule-Thompson
LCCS	Last-Cemented Casing Shoe
MD	Measured depth (along-hole)
MIC	Microbiologically influenced corrosion
MIT	Mechanical Integrity Test
P	Pressure
QRA	Quantitative risk assessment
SSSV	Subsurface Safety Valve
T	Temperature
TVD	True vertical depth
UGS	Underground Gas Storage
UV	Ultraviolet

## 2 BowTie analysis for hydrogen storage in a salt cavern

A BowTie analysis is a risk evaluation and management method that can be used to represent the risks associated with a hazard and analyse and demonstrate the causal relationships in failure scenarios. A hazard concerns an activity that has the potential to cause damage and which in this research concerns the subsurface storage of hydrogen in a salt cavern. In section 2.1 the BowTie methodology is first explained, whereas in section 2.2 the design and set-up of the studied hydrogen storage system are described. In sections 2.3 and 2.4, the results of the BowTie analysis are discussed for two “loss of control” top events. The chapter concludes with section 2.5 in which the findings from the analysis are summarized and examples of possible high-risk failure scenarios are highlighted.

### 2.1 BowTie methodology

A literature review was conducted to inventorize risks associated with subsurface hydrogen storage in salt caverns and to identify potential mitigations and monitoring techniques to reduce risks. The term “risk” is defined as the probability of occurrence of a potentially hazardous event times its effect. The latter concerns the consequence(s) of the occurrence of the hazardous event for the environment and (in particular) human health and safety. Accordingly, risks can be classified by the nature of their causes and consequences according to the TEECOPS<sup>1</sup> method. In this study, we focus on the technical risks and the health, safety and environmental risks. That is, we study risks that are caused by technical failure and their effects on humans and the environment.

Prior to the BowTie analysis, risks were identified and reviewed, and the potential causes and consequences were defined. Additionally, an exploratory discussion was held on the barriers. This was done together with experts, such as from EnergyStock and TNO, during a one-day workshop end of June 2020. This served as a starting point for:

- Performing a BowTie analysis targeted at hazardous events that can cause a loss of integrity, with leakage of hydrogen as a consequence. From this examples are provided of relevant high-risk failure scenarios that describe potential future situations and developments of the storage system that can lead to undesirable events.
- Formulation of applicable risk-mitigation measures and suitable monitoring techniques.

The BowTie analysis focused on two potentially hazardous events: (i) leakage of hydrogen in the subsurface, and (ii) leakage of hydrogen at the surface. A third potentially hazardous event is induced seismicity, and which concerns earthquakes induced by the solution mining and/or storage activities. In salt however, stress build-up leading to faulting is highly unlikely as salt behaves visco-plastically, and therefore it bends rather than breaks, [Li et al., 2016]. Earthquakes that have the potential to cause harm and/or damage are therefore extremely unlikely to occur. Hence, induced seismicity was not included in the BowTie analysis. As a potential threat to the integrity (leak tightness) of the storage system, seismicity is considered though.

---

<sup>1</sup> TEECOPS: Technical, Economic, Environmental, Commercial, Organizational, Political, Societal

A 'BowTie' is a diagram that visualizes the risks associated with a hazard in one easy to understand picture as is shown in Figure 2. The diagram is shaped like a BowTie, creating a clear differentiation between proactive and reactive risk management. The power of a BowTie diagram is that it provides an overview of multiple plausible failure scenarios in a single picture. It provides a simple, visual explanation of a risk, the causes that lead to the risk occurring and the possible consequences and effects when the risk occurs. Such explanation would be much more difficult to provide otherwise. The diagram is a result of an analysis known as BowTie analysis and which is further explained below referring to the generic diagram shown in Figure 2.

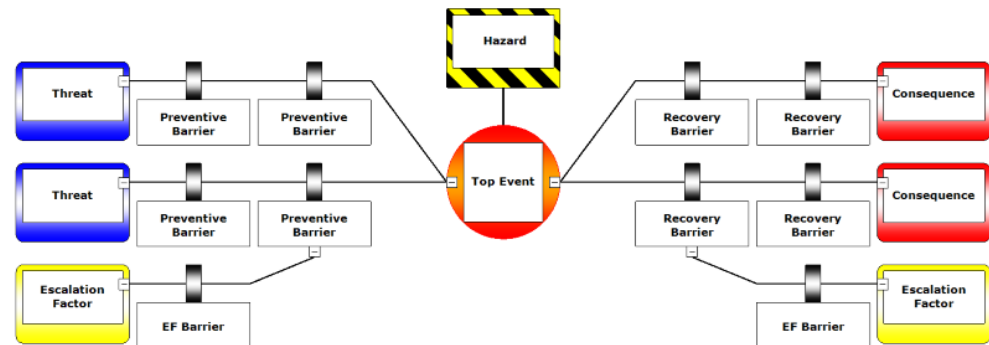


Figure 2: Illustration of a generic BowTie diagram<sup>2</sup>.

The start of any BowTie analysis is to choose the '**hazard**'. This is something in, around or part of the organization, which has the potential to cause damage. Here damage needs to be understood as the negative impact when control over the hazard is lost. As stated earlier, in this study the hazard is the injection and subsurface storage of hydrogen in a salt cavern.

Once the hazard is chosen, the next step is to define the so called '**top event**'. This is the moment when control is lost over the hazard. There is no damage or negative impact yet, but it is imminent. This means that the top event is chosen to occur in time just before events start causing actual damage. As introduced before in this chapter, we focus on the two top events: (i) *leakage of hydrogen in the subsurface*, and (ii) *leakage of hydrogen at the surface*.

Following the definition of the top event, threats and consequences are identified. '**Threats**' (or causes) are whatever will cause the top event, and '**consequences**' (effects) are the result from the top event potentially leading to damage. There can be multiple threats that could lead to occurrence of the top event, and there can also be multiple consequences when a top event occurs.

Once the hazard, top event, threats and consequences are in the BowTie diagram, there is a clear understanding of the risks associated with the hazard and what needs to be controlled to prevent the risk from occurring or to lower the risk to acceptable ALARA<sup>3</sup> levels. Every line through the BowTie represents an incident (failure) scenario that relates the causes of the failure and the consequences to the top event. To control these scenarios barriers are defined, to either prevent scenarios to happen or to mitigate the consequences.

<sup>2</sup> [https://www.cgerisk.com/knowledgebase/The\\_bowtie\\_method](https://www.cgerisk.com/knowledgebase/The_bowtie_method)

<sup>3</sup> ALARA: As Low As Reasonably Achievable

'Safety measures referred to as **Barriers**' in the BowTie diagram appear on both sides of the top event. Barriers on the left side interrupt the scenario so that the threats do not occur (preventive barriers), or do not result in a loss of control of the hazard (control barriers), leading to the top event occurring. Barriers on the right side make sure that, if the top event occurs, the scenario does not escalate into an actual impact (the consequence) and/or the impact (recovery barriers) is mitigated. Once the barriers are identified it also becomes clear how the risks can be managed. There are different types of barriers, which are mainly a combination of human behaviour and/or hardware/technology. Barriers are never perfect as even the best hardware barrier can fail. Why a barrier will fail is reflected in the BowTie diagram with the '**escalation factor**'. Anything that will make a barrier fail can be described in an escalation factor. In the analysis presented here, escalation factors are not included.

Prior to detailing the results of the BowTie analysis, in the next section the notional design of the subsurface storage system under study is described.

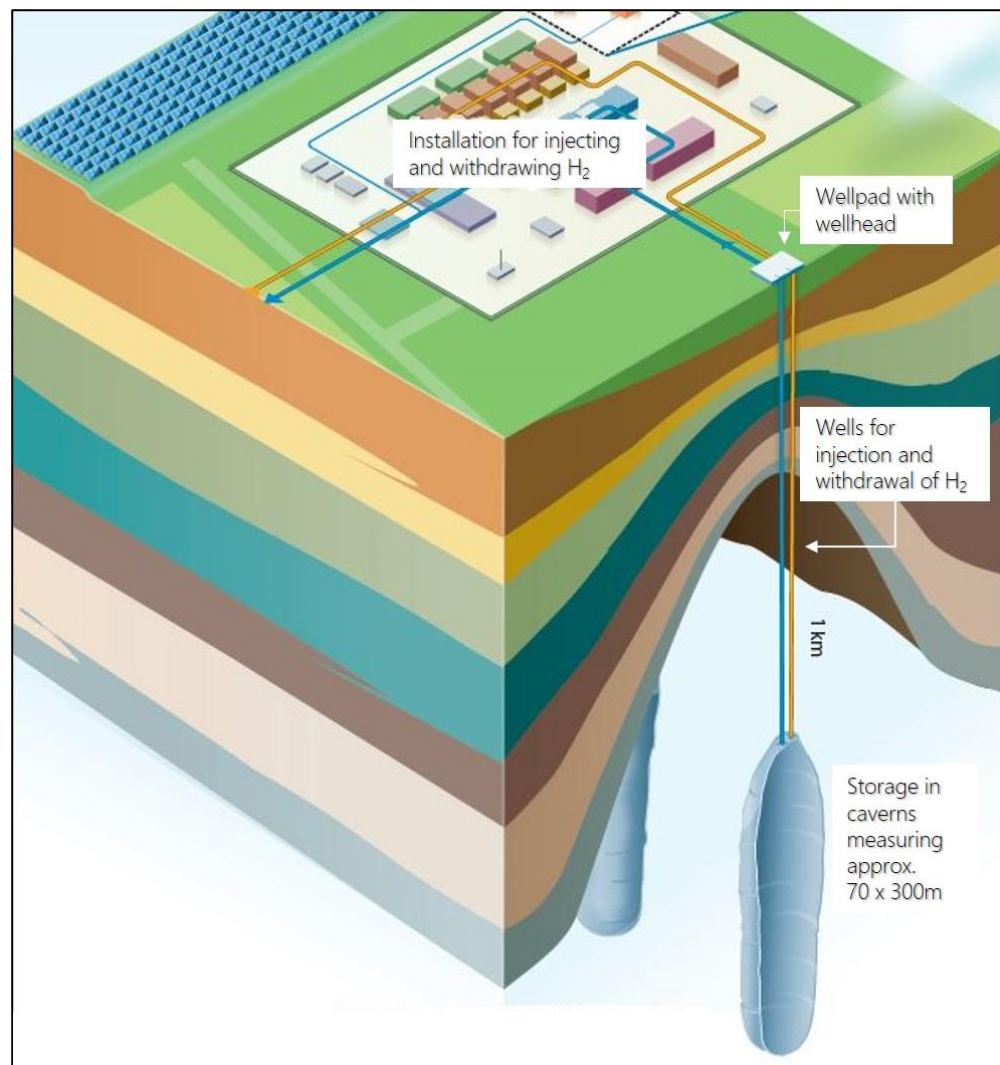


Figure 3: Schematic illustration of a salt cavern storage facility for hydrogen (modified, original by EnergyStock).



## **2.2 Notional design of hydrogen storage system and set-up of test procedures**

The notional design of the subsurface storage system under study as described in this section is based, amongst others, on discussions with project partner EnergyStock, and is illustrated via several displays which have been obtained from our partner. Also, the set-up is discussed of test procedures that will be executed during the field tests introduced in the first chapter. Furthermore, based on the notional design, the boundaries of the storage system will be defined within which the stored hydrogen is considered to be contained. That is as long as the hydrogen remains inside those boundaries, it is considered not to have leaked, and thus the top event(s) analysed have not occurred.

A facility for subsurface storage of hydrogen in a salt cavern is comprised of subsurface and surface components as is shown in Figure 3. The two main subsurface components are the salt cavern, where the hydrogen is stored in compressed form under a pressure of 80-200 bar, and the well that connects the salt cavern with the surface and through which the hydrogen is injected and withdrawn. At the surface, the wellhead on the wellpad is connected to the facilities for compression (prior to injection) and gas treatment (cleaning and drying, after withdrawal).

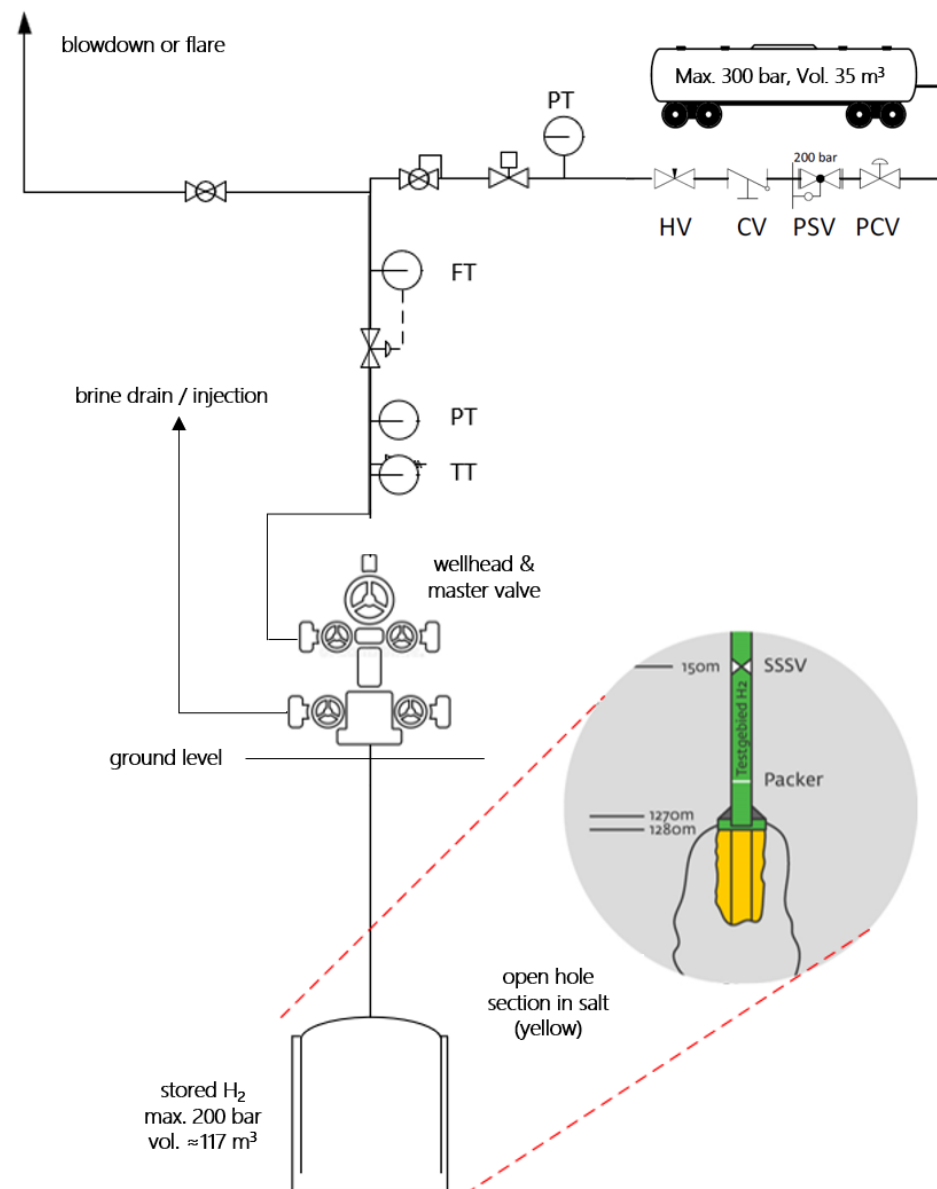


Figure 4: Schematic illustration of test set-up for field tests (source: EnergyStock). H<sub>2</sub>-filled sections are indicated in green, while brine-filled sections are indicated in orange/yellow. TT – Temperature Transmitter; PT – Pressure Transmitter; FT – Flow Transmitter; HV – Hand Valve; CV – Control Valve; PSV – Pressure Safety Valve; PCV – Pressure Control Valve.

For the field tests, introduced in the first chapter of this report, a commercial-scale facility for storage of hydrogen as depicted in Figure 3 will not be present yet. Instead, to be able to conduct the field tests with hydrogen in this pilot-phase, a set-up as schematically shown in Figure 4 will be installed at the wellpad of well A8a that is disconnected from the main storage facility for natural gas. At the surface, the hydrogen that is to be injected is stored in a tube trailer at a pressure of maximum 300 bar that is connected to the wellhead, with a master valve in-between to shut in the well. Multiple flow (head, control) and pressure (safety, control) valves will be installed. Additionally, a pressure and/or temperature and/or flow transmitter will be installed to transmit measured pressure (P), temperature (T), and flow rate to the control room. In the subsurface, the casing of well A8a ends at the Last Cemented Casing Shoe (LCCS) at 1270 m measured depth (MD), corresponding to 1220 m true vertical depth (TVD). Below this the open-hole section of the wellbore in the Zechstein

salt runs down to a depth of 1757 m MD, corresponding to 1700 m TVD, see Figure 4. Base salt is located deeper and not observed in this well. A schematic illustration of the design of the well is shown in Figure 5. It shows the well state during the second step for the field tests when the completion (production tubing, packer, Subsurface Safety Valve (SSSV), and wellhead) has been installed and hydrogen (red colours) is cyclically injected, stored, and withdrawn. Currently though, no completion is installed, and the well and open-hole section are filled with brine (orange colour). During the field tests, the upper 10 m of the open-hole section will be debrined (brine will be evacuated) to make room for the hydrogen. As such, the tested area that will be filled with hydrogen during the tests includes the well itself and the upper 10 m of the open-hole section. This is indicated in red in Figure 5, and in green in Figure 4.

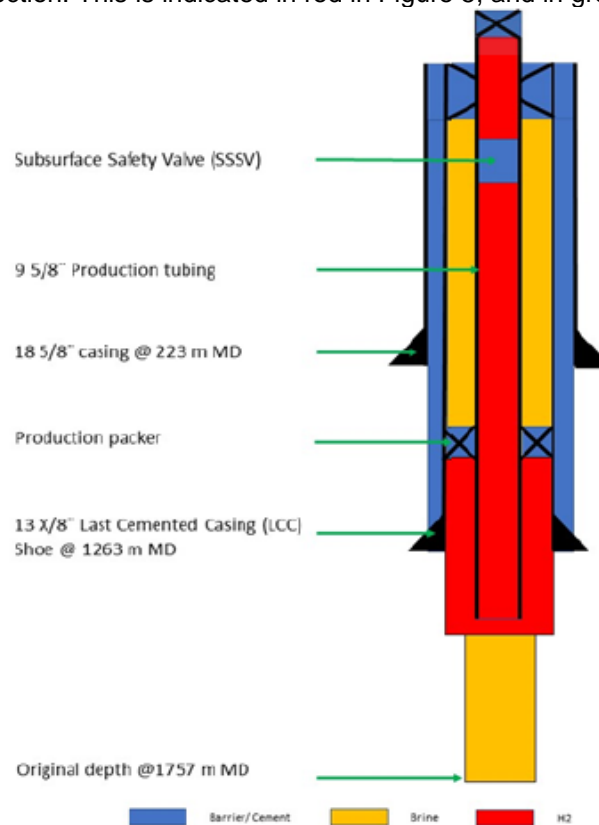


Figure 5: Schematic illustration of design of A8a test well (hydrogen storage state, source: EnergyStock).

The well design as shown in Figure 5 contains multiple barriers (blue colors) to prevent uncontrolled fluid flow (leakage) into the subsurface and through the wellbore towards the surface. These barriers can be divided into **primary barriers** and **secondary barriers**. Primary barriers are the production casing, liner and liner cement below the production packer, the production packer, the completion string below the SSSV, and the SSSV itself. The SSSV is a key component of a gas storage well. Its sole purpose is to automatically close off the well in the event of loss of hydraulic control pressure that would lead to uncontrolled release of the gas (i.e. blow-out). Secondary barriers are the production casing, liner and liner cement above the production packer, the completion string above the SSSV, the wellhead (including casing hanger with seals and wellhead valves, not shown in Figure 5), and the production tree (body and master valves).

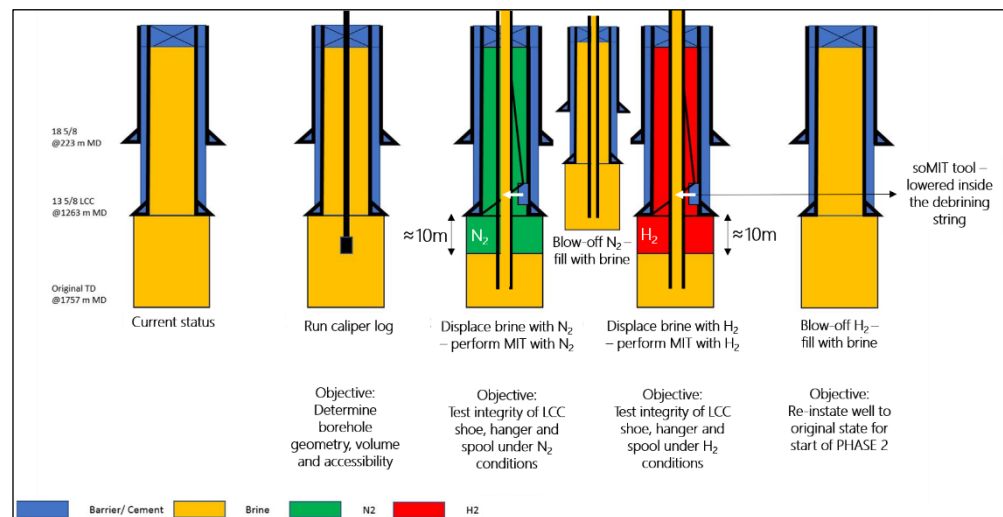


Figure 6: Schematic illustration of test procedure during the 1<sup>st</sup> step for the field tests (source: EnergyStock)

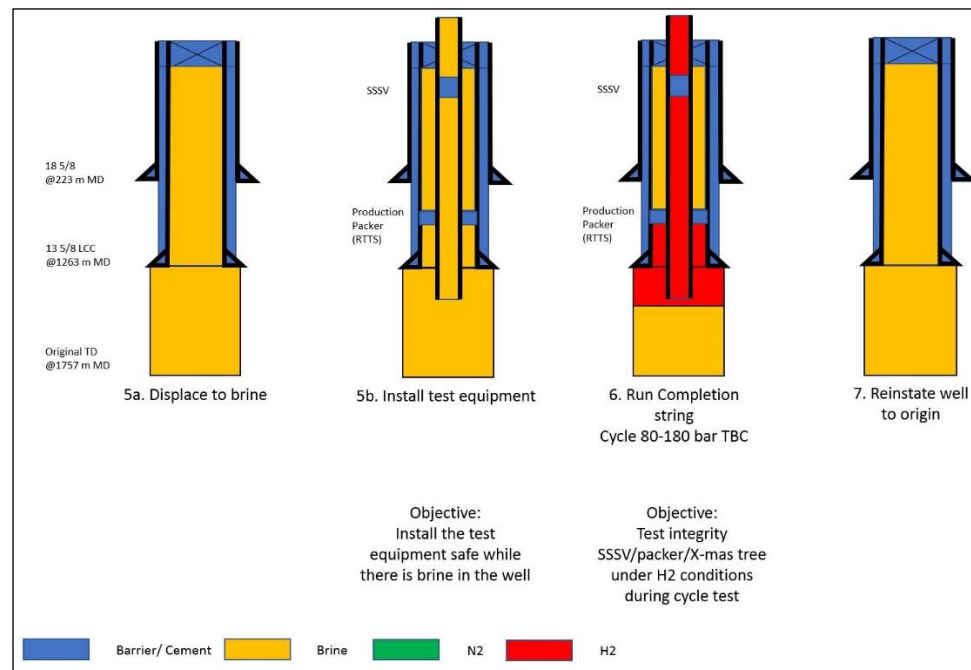


Figure 7: Schematic illustration of test procedure during the 2<sup>nd</sup> step for the tests (source: EnergyStock)

The field tests, introduced in the first chapter of this report, will be executed under supervision of EnergyStock in two steps. Step 1, being an MIT with nitrogen followed by one with hydrogen, is depicted in Figure 6, whereas step 2, the cyclic hydrogen injection and withdrawal tests, is depicted in Figure 7.

The so-called “containment boundary” of the subsurface part of the storage system for conducting the field tests in step 2 is formed by the walls (and base) of the open-hole section, the rock-cement-casing interface at the LCCS, the production packer, the walls of the tubing, the wellhead and the wellhead master valve. At the surface the containment boundary is formed by the walls of the tube trailers, the walls of the compression and drying equipment, and by the hoses that connect the wellhead to the tube trailers and the trailers to the equipment. However, these boundaries are not explicitly taken into account in the BowTie analysis.

For our study we considered the storage system for a pilot phase and for a full-scale cavern phase. This means that for the first one there is no cavern and only an open-hole section with a small storage space, for which we assume a volume of 117 m<sup>3</sup>. For the system of a full-scale cavern phase there is a large storage space, and which we assume to be up to 1 million m<sup>3</sup>, whereas the walls and base of the cavern are part of the containment boundary.

It must be noted that for our study we only considered a single-cavern case and that it does not take into account the influence of activities in the direct surroundings of a cavern. Such activities could e.g. consist of salt mining and subsurface storage of energy (such as via natural gas, hydrogen and compressed air).

### 2.2.1 Overview for further reading

In the next two sections the results of the Bowtie analysis will be detailed for each of the two top events introduced in the previous section: (i) leakage of hydrogen in the subsurface, and (ii) leakage of hydrogen at the surface. The analysis was done for the storage system introduced for both a pilot phase and a full-scale cavern phase. Where this impacts the Bowties, the differences will be highlighted for the two phases. The BowTie analysis has resulted in a considerable set of threats, consequences and barriers for the two top events, and which results are nicely depicted via the BowTie diagram available in Appendix A. Here it should be noted that the barriers are categorized, and visualized as such, in Appendix A to be of the types *monitoring measure* and *prevention measure* or *recovery measure*. The latter two correspond to measures for the left and the right-side of the BowTie diagram, respectively. Because of this subdivision of barriers over these types one may find in the next sections (for several threats and consequences) measures of different types and for which the reader may argue that these contribute to, and form together, one barrier. For others it needs to be recognized that a barrier has the specific standalone scope of the type as indicated in Appendix A.

While threats and consequences are unique, several barriers and recovery measures occur multiple times in the BowTie diagram and in the descriptions of the two next sections. However, a description for each of the barriers and for each of the recovery measures is only given once where it first appears. For successive appearances of each a document reference is given to the description at first appearance. Table 1 provides a listing of all threats, consequences, barriers and recovery measures from the BowTie analysis and which are preceded with a reference to the threat / consequence / barrier / measure number & character where descriptions have been introduced. Each such reference in the table is clickable and takes the reader to the description of the item in the document. In this way, it serves as a look-up table and enables quick navigation to the description of a specific threat, consequence, barrier or recovery measure.

Table 1: Overview of results of BowTie analysis with reference to under which threat / consequence number descriptions are introduced

Threats	Preventive barriers	Recovery measures	Consequences
1 - H <sub>2</sub> embrittlement of well materials	1.a - Use of austenitic steels with appropriate hardness 1.b - Avoid damaging oxide coating layer 1.c - Keep P, T within safe operating limits to avoid large thermo-mechanical stresses 1.d - P, T monitoring	17.a - Prevent accumulation of H <sub>2</sub> close to the surface  17.b - P, T monitoring  17.c - Install/use leakage detection and H <sub>2</sub> gas presence monitoring equipment at surface	17 - Explosion of near-surface H <sub>2</sub> accumulations leading to damage or injury
2 - Internal corrosion of steel components exposed to brine, H <sub>2</sub> S, and MIC	2.a - Use of corrosion resistant steel 2.b - Applying anti-corrosion measures 2.c - Protection of casing with tubing and packer 2.d - Periodic caliper log and/or downhole camera inspection 2.e - Monitor gas and brine composition periodically 2.f - Laboratory experiments to assess the risk of H <sub>2</sub> S formation 2.g - Laboratory experiments to assess the risk of microbiologically influenced corrosion 2.h - H <sub>2</sub> S formation - add microbial growth- and reaction-inhibiting additives	18.a - Warn (drinking water) authorities  18.b - Determine cause of leakage and repair it  18.c - Soil zone remediation  18.d - Groundwater quality monitoring	18 - Adverse effects of H <sub>2</sub> pollution on groundwater quality, vegetation and animals
3 - Connections not H <sub>2</sub> tight	3.a - Use of welded connections 3.b - Test welds before running down casing 3.c - Minimize vertical strain on casing 3.e - Performing an MIT	26.a - Minimize volume and flow rate during release  26.b - Minimize presence of humans and animals in vicinity of site	26 - Adverse effects to humans and animals due to air pollution with H <sub>2</sub>
4 - Mechanical failure of the casing (fatigue)	4.a - Use existing design standards	26.c - Execute emergency response plan	
5 - Poor quality and/or bonding of the cement	5.a - Use of flexible cements 5.b - Test cements 5.c - Stimulate natural sealing behavior of halite 5.e - Cement bond logging	26.d - Warn local stakeholders and authorities	
6 - Cement degradation	6.f - Monitor downhole chemical conditions	27.b - Use proper Personal Protective Equipment	27 - Extreme noise levels leading to hearing damage
7 - Integrity failure of last-cemented casing shoe	7.f - Leach a cavern neck 8.a - Use of hydrogen-resistant packer materials	28.a - Prevent accumulation of a high-concentration H <sub>2</sub> cloud	28 - Shockwave from explosion causing structural damage, injury or death
8 - Packer integrity failure	8.b - Increase weight below packer 8.c - Avoid slip at top of packer	28.b - Stimulate immediate ignition on release to prevent explosion	
9 - Degrading durability of materials due to scaling	9.a - Implementing measures to avoid scaling 9.b - Periodic removal of scaling 9.c - Monitor injection and withdrawal performance	29.a - Execute fire prevention plan	29 - Heat radiating from flash fire or jet flame causing structural damage, injury, or death
10 - External corrosion of the casing (including conductor, anchor casing)	10.a - Upfront site characterization 10.c - Implement multiple barriers to leakage 10.e - Install/use leakage detection and H <sub>2</sub> gas presence monitoring equipment at surface	30.a - Perform a QRA	30 - Injury or death – occurring in combination with other consequences (fire, explosion)
11 - Faults or leaky interbeds intersecting the cavern	11.a - Geological mapping of the internal composition of dome 11.b - Minimize/avoid presence of faults and non-halite interbeds 11.c - Faults in halite seal naturally 11.d - Drill deeper 11.e - Test open-hole section by pressurization	30.b - Reconsidering the ATEX zonation	
12 - Roof fall	12.b - Adhere to geomechanical cavern stability criteria 12.d - Micro-seismic monitoring 12.e - Periodic sonar measurement	30.f - Record incidents and follow-up with additional measures	
13 - H <sub>2</sub> permeation into the wall of the cavern	13.a - Assess/quantify permeation effect during characterization phase		
14 - Integrity loss caused by drilling activities	14.a - Careful site selection 14.b - Only drill a single well per wellpad 14.c - Carefully monitor directional surveys during drilling		
15 - Overpressurization due to malfunctioning equipment	15.a - Applying safety margins to maximum operational pressure 15.b - Install reliable well-functioning safety valves		

16 - Large sub-zero temperatures leading to failure of materials or components	15.c - Monitor position of valves 15.d - Monitor pressure, temperature and flow rates 15.e - Check functioning of safety valves 16.a - Quantify (adiabatic) expansion effect and define safety margins 16.b - Control/tune pressure, injection temperature and flow rates to limit expansion effect 16.c - Absorb/control expansion effects by manipulating the safety valves		
19 - Catastrophic x-mas tree damage due to collision	19.a - Enforcing a no-drive zone around wellhead 19.b - Completely submerge wellhead cellar 19.c - Install a functioning SSSV 19.d - Periodically check SSSV		
20 - Catastrophic x-mas tree damage due to vandalism/terrorism	20.a - Security fence around the wellpad 20.e - Security surveillance 20.f - Video surveillance		
21 - Failing wellhead flange or hose connection	21.b - Use H <sub>2</sub> -tested wellhead, components and materials		
22 - Improperly closed wellhead valve	22.a - Using a pressure control system on the tube trailer 22.b - Enable remote control of valves 22.d - Repeated performance tests of valves		
23 - Integrity failure during workover under pressure	23.a - Use H <sub>2</sub> -tested well intervention equipment, tools and materials 23.b - Use H <sub>2</sub> compliant intervention techniques 23.c - Perform well intervention with qualified and competent staff 23.d - Perform detailed and dedicated risk assessment 23.e - Test debrining procedure		
24 - H <sub>2</sub> dissolved in brine coming to surface during debrining	24.a - Quantify/measure volume of hydrogen that will dissolve into brine 24.b - Install separator to de-hydrogenate the brine		
25 - Migration of H <sub>2</sub> via overburden to surface	25.a - Characterize overburden to assess migration pathways and risk		

## 2.3 BowTie analysis for top event leakage of hydrogen in the subsurface

In the remainder of this section the well-related threats and barriers, the threats related to the cavern, and the potential consequences of leakage and possible recovery measures are described for the first top event. Each of these descriptions have been placed in a separate subsection, which are numbered 2.3.1 to 2.3.3.

### 2.3.1 Well-related threats and barriers

The well-related threats that have been identified in the BowTie analysis for the first top event, and the potential barriers that can be put in place to prevent the threat from occurring, are subject of this subsection.

#### 1. Hydrogen embrittlement of well materials

Hydrogen embrittlement (also known as hydrogen-induced cracking) occurs when metals become brittle as a result of the intrusion and diffusion of hydrogen into the material, whereby the degree of embrittlement is influenced both by the amount of hydrogen absorbed and the microstructure of the material [Robertson et al., 2015]. In combination with repeated mechanical and thermal loading and unloading it can lead to failure of the steel or alloy components of the well

completion that are in direct contact with the hydrogen. These components involve the casing and shoe, production tubing, liner & hanger, SSSV and packers, and which all need to be hydrogen resistant under a wide range of temperatures [DBIGUT, 2017]. Embrittlement is primarily influenced by temperature, pressure, hydrogen concentration and stress fields [Reitenbach et al., 2014]. Additionally, corrosion could play a role, as is also described for the next threat, and if that takes place defects can be created on which cracks could develop due to tensile stress build up, and which could subsequently result in leakage [Gonzalez-Diez et al., 2020]. High-strength steels (with tensile strength above 900 MPa) are particularly affected by hydrogen embrittlement.

Embrittlement is a threat for which the following barriers can be put in place:

- a. *Use of austenitic steels with appropriate hardness* that have been tested by exposure to hydrogen under expected P and T conditions for a prolonged period of time. Corrosion-resistant alloys, such as 13 Cr (UNS Nr. S42000), which are commonly used in the oil industry for severe corrosion conditions, exhibit martensitic structure and provide better resistance against H<sub>2</sub>S or CO<sub>2</sub>, but they are susceptible to the effect of H<sub>2</sub>. Steels having an austenitic structure can have a lower or higher stability, depending on their composition. These austenitic structures can prevent hydrogen diffusion much better than the above-mentioned martensitic or ferritic phases, which act as a path for hydrogen atoms in the structure. Austenitic stainless steels have a nickel content higher than 7% and a chromium content higher than 16% [Reitenbach et al., 2015].
- b. *Avoiding damaging the oxide coating layer* on the inside of the steel components that are exposed to hydrogen that prevents/delays the diffusion of hydrogen into the metal, thereby avoiding (amongst others) embrittlement.
- c. *Keep P, T within safe operating limits to avoid large thermo-mechanical stresses* that exceed the design criteria by controlling and monitoring them. Additionally, avoid exposure of well materials to large subzero temperatures during injection and withdrawal.
- d. *P, T monitoring* to ensure that preventive barriers on safe operating limits, like for this threat under c), can be properly applied.

It must be noted here that the barrier “*Periodic caliper log and/or downhole camera inspection*” that is proposed for threat 2 under d), could also (indirectly) help to reduce the risk of embrittlement. Monitoring the degree of wear and tear by these methods may pinpoint defects that could be more susceptible to embrittlement.

## 2. Internal corrosion of steel components exposed to brine, H<sub>2</sub>S, and MIC

A well contains many steel components such as casing, casing shoes, production tubing, wellhead and x-mas tree. These components may corrode and during the lifetime of the well (30 years) this may lead to failure. In the case of hydrogen storage in a cavern, the specific conditions that require attention are the presence of salt and hydrogen. At injection, the hydrogen is dry, and while being stored in the cavern, it will become wet with water vapor from the brine at the bottom of the cavern. At withdrawal, the hydrogen will therefore contain water (with lower pH, i.e., somewhat acidic, due to the presence of hydrogen) that may condense again while flowing up the well to the surface and into the above-ground facilities. Furthermore, especially in the lower section of the well, some brine may be



sucked into the well at withdrawal, which comes in contact with the casing shoe, packer, and lowermost reaches of the tubing. Corrosion creates defects, known as pitting corrosion, on which cracking can develop due to tensile stress (see also threat 1), eventually leading to leakage and failure [Gonzalez-Diez et al., 2020]. Hydrogen may activate defects that were dormant so far, of which the impact is linked to fatigue, see also threat 4.

Two related threats that may pose a risk in this context are:

- *Formation of corrosive gases (e.g.  $H_2S$ ) by geo- and biochemical reactions* of hydrogen with minerals that are dissolved in the brine or present in sump material (insoluble material in salt that sinks to the base of the cavern) and microbes that live in the cavern. Such corrosive fluids, in particular hydrogen sulphide, can negatively impact the integrity and durability of steel components.
- *Microbiologically influenced corrosion (MIC)* meaning the influence of microorganisms on the kinetics of corrosion processes of metals and non-metallic materials, caused by adhering to the interfaces and which is usually referred to as “biofilms”.

Internal corrosion is a threat for which the following barriers can be put in place:

- a. *Use of (verified/tested) corrosion-resistant steel*, meaning adopting a material selection process where the expected pressure, temperature and environmental conditions, such as exposure to  $H_2S$ ,  $CO_2$ , and highly saline brine, form the basis for the selection.
- b. *Apply anti-corrosion measures* to protect against corrosion such as via coatings and inhibitors.
- c. *Protection of casing with tubing and packer*, as the casing above the packer is a secondary barrier that is protected from exposure to hydrogen by the production tubing, and by the packer that closes off the annular space between the tubing and the casing. Below the packer, the casing and shoe are part of the primary barrier envelope.
- d. *Periodic caliper log and/or downhole camera inspection* are monitoring measures to assess the degree of wear and tear (e.g. by corrosion) of the casing, tubing and other steel components of the well. A caliper log measures the rugosity of a surface, in this case the inner side of the casing.
- e. *Monitor gas and brine composition periodically* during full-scale commercial operations to detect the presence of hazardous, corrosive gases. In a pilot phase, samples of the stored hydrogen and the brine in the open-hole section can be taken before, during and after the tests. By analyzing the differences in gas and brine composition (geochemical, microbiological) before and after storage a lot can be learnt about the possible reaction of hydrogen with minerals and microbes in the cavern.
- f. *Laboratory experiments to assess the risk of  $H_2S$  formation* by geochemical reactions or microbial activity is a measure that can be executed prior to field-scale tests to learn what types of reactions occur, what their products might be, and what controls them. This is done to gain insight into possible mitigations, in case these reactions actually pose a threat.
- g. *Laboratory experiments to assess the risk of microbiologically influenced corrosion* as a measure that can be executed prior to field-scale tests to assess if MIC occurs, what the effects might be, and what controls it. This will gain insight into possible mitigation options in case it actually poses a threat.

- h. *H<sub>2</sub>S formation - add microbial growth- and reaction-inhibiting additives to cavern to minimize risks of hydrogen sulphide formation and MIC by microbial activity and geochemical interaction of hydrogen with rocks and formation water constituents.*

### 3. **Connections not hydrogen-tight (casing, tubing, SSSV)**

Casings and tubings consist of sections of pipe that are joined together by welding or by a screw connection. If the connections between individual sections of the casing or tubing are not leak-tight for hydrogen, this might lead to leakage of hydrogen out of the storage system.

A connection not being hydrogen-tight is a threat that can be prevented/mitigated by:

- a. *Use of welded connections* to prevent leakage through failing connections is very common in underground gas storage (UGS) and can be considered best practice.
- b. *Test welds before running down casing* to make sure that they are leak-tight and contain no weld defects.
- c. *Minimize vertical strain on casing* during the installation in the hole to avoid failing connections.
- d. *Keep P, T within safe operating limits to avoid large thermo-mechanical stresses* (see barrier description introduced for threat 1 under c).
- e. *Perform an MIT*: An MIT with nitrogen is a standard procedure in UGS to test the integrity and leak-tightness of the interfaces between the rock, cement and casing at the last cemented casing shoe and the casing (including connection) itself over its entire length. In the pilot phase, this MIT is performed first as a standard MIT with nitrogen and then with hydrogen.
- f. *P, T monitoring* (see barrier description introduced for threat 1 under d).

### 4. **Mechanical failure of the casing (fatigue)**

Fatigue is failure induced by repeated mechanical and thermal loading and unloading (cyclic loading). A series of events needs to take place before hydrogen is able to influence the fatigue behaviour of steel. First, gaseous hydrogen has to be transported into the tip region of an existing crack/defect tip region. This is followed by the physical adsorption of the hydrogen, which dissociates into two hydrogen atoms at the surface. Next, the hydrogen has to enter the material for hydrogen embrittlement to happen, at which the hydrogen atom is transported from the surface to the bulk material (absorption). Finally, stress-assisted diffusion of the hydrogen atoms in the bulk material takes place, whereby the hydrogen atoms move to the region of high triaxial stresses just ahead of a notch or a crack tip at which the mechanism of hydrogen embrittlement happens [Gonzales-Diez et al., 2020]. The EU-project NATURALHY (2004-2009) tested hydrogen-enhanced fatigue crack growth in pipelines for the material range X42 to X70 (low- to medium-grade steel alloys). It also studied the fatigue properties of the base and weld material, which is also relevant in relation to threat 3. No difference was observed between the fatigue behaviour of the base and weld materials as the latter have the same fatigue properties. However, it might be more prone to crack initiation by weld defects or other damage mechanisms [Van Wortel, 2019]. It is worth noting here though that in applications, such as oil & gas production and gas storage, general purpose carbon steel pipe manufactured to API specification 5CT (N80) is commonly used for casings. Whereas a controlled

yield strength material with a hardness testing requirement (L80) is used for tubings, especially in sour (H<sub>2</sub>S) environments.

Fatigue is a threat that can be prevented/mitigated by:

- a. *Use existing design standards* such as API and Norsok, and best-practices from UGS and oil & gas industry in material selection. Furthermore, it is common practice to over-dimension casings and connections, and which means applying safety margins in such manner that they can withstand pressures larger than operational ones.
- b. *Keep P, T within safe operating limits to avoid large thermo-mechanical stresses* (see barrier description introduced for threat 1 under c).
- c. *P, T monitoring* (see barrier description introduced for threat 1 under d), with in particular also pressure monitoring of the annulus as a leak in the casing will result in a pressure and fluid change in the annulus because fluids present in the subsurface on the outside of the casing can enter the annular space.

## 5. Poor quality and/or bonding of the cement

The cement that surrounds and fixates the casing is a barrier to leakage. The cement around the casing shoe (below the packer) is part of the primary barrier envelope, while the cement around the casing above the packer forms a secondary barrier to leakage. It prevents and/or retards flow of hydrogen along the outside of the casing. The cement that is used may be incompatible for use with hydrogen, because it reacts with it, or is insufficiently tight. If the cement is incompatible, is improperly placed and/or insufficiently bonded with the rock and casing while hardening after placement, this can pose a threat. Therefore, cementation operations are a critical aspect of well integrity and specific requirements are stated in the NOGEPA 41 standard on well integrity [NOGEPA OPCOM, 2016].

Poor quality and/or bonding of the cement is a threat that can be prevented/mitigated by:

- a. *Use flexible cements* such as flexstone and pozo to avoid formation of cracks in cement and micro-annuli at interfaces with casing and rock by repeated mechanical and thermal loading and unloading.
- b. *Test cements* under operational P, T and geochemical conditions and exposure to hydrogen. As hydrogen has a smaller size and higher diffusivity compared to methane, the cement must be adjusted in order to prevent migration of the hydrogen through the cement. The review study [DBIGUT, 2017] indicates that the risk of chemical alteration of the cement as a consequence of contact with hydrogen is considered to be low.
- c. *Stimulate natural sealing behavior of halite*: As halite, commonly known as rock salt, behaves increasingly visco-plastic at higher pressures and temperatures, it “flows” more easily and which is a process known as salt creep. Therefore, it has the ability to seal or close-off voids and cracks such as remain between the cement and the rock after hardening. This natural sealing behaviour can be stimulated e.g. by applying elevated pressures and temperatures for a period of time after the cement is placed. In such a way the leak tightness of the interface between the cement and the salt can be further improved. However, the integrity of the interface between the casing and the cement may be negatively impacted in the process. For instance, the release of the elevated pressure after cementing may reduce the ballooning effect of the casing, which

may potentially lead to debonding of the casing from the cement and/or the formation of micro-annuli. Further research is required to assess such adverse effects.

- d. *Perform an MIT* (see barrier description introduced for threat 3 under e) during which (amongst others) the integrity and leak-tightness are tested of the interfaces between the rock, cement and casing at the LCCS that are in direct contact with hydrogen.
- e. *Cement bond logging* is a logging technique to measure the quality of the bond between cement and casing. It is a standard logging tool that is run on the inside of the casing to measure the integrity of the cement job, especially whether the cement is adhering solidly to the outside of the casing.

## 6. Cement degradation

It is well-known that cement can mechanically and/or chemically degrade over the lifetime of a well due to a combination of geomechanical processes and geochemical interactions with fluids in the cavern and in the subsurface, such as  $\text{H}_2\text{S}$ ,  $\text{CO}_2$ ,  $\text{O}_2$ , and potentially also  $\text{H}_2$ . However, the review study [DBI-GUT, 2017] concludes that the risk of chemical alteration of the cement as a consequence of contact with hydrogen is considered to be low. Likewise, on the possible chemical effects of hydrogen on the sealing properties of cement in [Reitenbach et al., 2014] it is concluded that the effect of hydrogen on the solubility of cement minerals can be estimated to be very low as the  $\text{H}_2/\text{H}_2\text{O}$  redox system is not very active at low temperatures. At higher temperatures of 60 to 90 °C though, the potential electron donor hydrogen can behave more actively to support metal oxidation processes, such as the reduction of Fe(III)-phases. At the contact areas the casing–cement bond, cement–formation rock and the geochemical environment can also be affected by the redox reaction of  $\text{FeO}/\text{Fe}_3\text{O}_4$ ,  $\text{Fe}_2^{2+}/\text{Fe}_3\text{O}_4$ ,  $\text{Fe}_2^{2+}/\text{green rust (fougerite)}$  and  $\text{H}_2/\text{H}_2\text{O}$ . The activity of these processes greatly depends on the water saturation, salinity of the formation water, hydraulic transmissibility of the formation rock, temperature, pH value, and the presence and concentration of oxygen. Microbiological activity can promote these reactions, whereas the presence of minerals, such as siderite, dolomite and calcite, can inhibit them [Reitenbach et al., 2014]. Furthermore, particularly in gas storage, the (progressive) formation of micro-annuli in cement or between cement and casing/rock caused by repeated mechanical and thermal loading is an important mechanism that can negatively impact the mechanical integrity and leak-tightness of the cement.

Cement degradation is a threat that can be prevented/mitigated by:

- a. *Use flexible cements* (see barrier description introduced for threat 5 under a).
- b. *Test cements* (see barrier description introduced for threat 5 under b).
- c. *Stimulate natural sealing behavior of halite* (see barrier description introduced for threat 5 under c).
- d. *Keep  $P$ ,  $T$  within safe operating limits to avoid large thermo-mechanical stresses* (see barrier description introduced for threat 1 under c).
- e.  *$P$ ,  $T$  monitoring* (see barrier description introduced for threat 1 under d).
- f. *Monitor downhole chemical conditions* to detect the presence of fluids that can negatively impact the mechanical integrity and leak-tightness of the cement.

## 7. Integrity failure of the last-cemented casing shoe

At the LCCS, the hydrogen is in direct contact with the interfaces between rock, cement and casing, and serves as a primary barrier against leakage. Integrity failure of the LCCS can be caused by insufficient bonding of cement with rock and casing, and/or repeated mechanical and thermal loading, and/or due to pressures exceeding safe operational limits. Such failure very likely results in migration of hydrogen through the outer envelope of this barrier. An important operational criterion to safeguard the mechanical integrity of the LCCS is the maximum pressure to be exerted on it. This pressure is commonly calculated by taking the hydraulic fracture pressure gradient at which the rock at the LCCS fractures or breaks and which is equal to the lithostatic pressure gradient, being 0.216 bar/m for the Zuidwending site. Applying a safety margin of around 15% would give approximately 0.18 bar/m for the maximum pressure gradient to be used in calculating the maximum pressure to be exerted on the LCCS. This maximum Pressure is then obtained by multiplying the gradient with the depth of the LCCS.

Integrity failure of the LCCS is a threat that can be prevented/mitigated by:

- a. *Use flexible cements* (see barrier description introduced for threat 5 under a).
- b. *Stimulate natural sealing behavior of halite* (see barrier description introduced for threat 5 under c).
- c. *Keeping P, T within safe operating limits to avoid large thermo-mechanical stresses* (see barrier description introduced for threat 1 under b), here in particular to ensure that the maximum Pressure at the LCCS is not exceeded.
- d. *Perform an MIT* (see barrier description introduced for threat 3 under e) to verify the integrity of the LCCS prior to start of operations.
- e. *P, T monitoring* (see barrier description introduced for threat 1 under d).
- f. *Leach a cavern neck* to distribute stresses and confine LCCS such that it can withstand high pressures. Such a neck is a narrow radial opening in the roof of the cavern below the LCCS.

## 8. Packer integrity failure

The packer is a primary barrier in the storage system. It closes off the annular space between the production tubing and the casing at the LCCS, thereby preventing the hydrogen from entering the annulus. Improper placement or incompatibility of packer materials (steels, elastomers) for use with hydrogen may result in integrity failure of the packer. In particular for elastomers, further investigation must be done in order to define their resistance to the higher diffusivity of hydrogen compared to methane [DBI-GUT, 2017]. Furthermore, during the placement of the packer care must be taken to avoid slippage as this may result in improper functioning.

Packer integrity failure is a threat that can be prevented/mitigated by:

- a. *Use hydrogen-resistant packer materials* and which concern steel components and elastomers. These need to be tested by exposure to hydrogen under expected P, T, and environmental conditions.
- b. *Increasing weight below packer* to improve effectiveness of packer anti-slip clamps at install.
- c. *Avoid slip at top of packer below the elastomer.*
- d. *Keep P, T within safe operating limits to avoid large thermo-mechanical stresses* (see barrier description introduced for threat 1 under c).

- e. *P, T monitoring* (see barrier description introduced for threat 1 under d), in particular pressure monitoring of the annulus, to detect a failing packer. The annulus is commonly filled with brine and/or a corrosion inhibitor and is kept at a certain pressure. As a consequence, any hydrogen entering the annulus will immediately migrate to the top and cause a measurable pressure change. Also, by sampling fluid from the annulus at the top, the presence of hydrogen can be detected.

#### 9. **Degrading durability of materials due to scaling**

When scaling occurs, it causes degrading flow performance, and which can potentially deteriorate the tubing material integrity. This may ultimately lead to mechanical failure of the tubing. Furthermore, scaling may jeopardize the proper functioning of the SSSV. In UGS, scaling is not known to be a serious issue, which has been concluded in the aforementioned one-day workshop with relevant experts, end of June 2020.

Degrading materials durability due to scaling is a threat that can be prevented/mitigated by:

- a. *Implement measures to avoid scaling* on tubing walls and SSSV.
- b. *Periodic removal of scaling*.
- c. *Monitor injection and withdrawal performance* to detect degrading performance that might be caused by scaling.
- d. *Periodic caliper log and/or downhole camera inspection* (see barrier description introduced for threat 2 under d).

#### 10. **External corrosion of the casing (including conductor, anchor casing)**

Over the 30-year lifetime of the well, corrosion on the outside of the casing (including conductor and anchor casing at shallow depth) in combination with a degrading cement sheath can lead to loss of integrity of these secondary or higher order barriers.

External corrosion is a threat that can be mitigated by:

- a. *Upfront site characterization* e.g. to identify microbiological activity that might cause MIC, and to measure the composition of the groundwater and how this may influence corrosion.
- b. *Use (verified/tested) corrosion-resistant steel* (see barrier description introduced for threat 2 under a)
- c. *Implement multiple barriers to leakage* via conductor casing, anchor casing and production casing following criteria and best practices in well design.
- d. *P, T monitoring* (see barrier description introduced for threat 1 under d), especially pressure monitoring of the annulus (see also additional description under threat 4 and barrier c).
- e. *Install/use leakage detection and H<sub>2</sub>-gas presence monitoring equipment at surface* to detect hydrogen that leaked in the subsurface escaping above-ground. In case of any leakage of hydrogen at surface, early detection is important in taking recovery measures as to enable a swift response, limit the volume of the leak and thereby the potential impact on health, safety and the environment. For this the reader is also further referred to section 2.3.3 on consequences and recovery measures. However, both gaseous hydrogen and methane are undetectable by human senses as both gasses are colourless, odourless and tasteless. In order to be able to detect natural gas

a sulphur-containing odorant has been added. Unfortunately, there are no known odorants light enough to “travel with” hydrogen at the same dispersion rate, making it difficult to detect hydrogen gas, [H2Tools, 2020]. At hydrocarbon (gas) production platforms several types of gas leakage and flame detectors are used. These for instance concern ultrasonic gas leak detector, open path gas detector, infrared (IR) gas detector and IR flame detectors, [Koelewijn et al., 2020]. However, these detectors are not suited for detecting hydrogen. Specific detectors for hydrogen do exist, for example the catalytic bead detector that is suitable for detecting hydrogen at lower flammable limit levels. These sensors can detect any combustible gas that combines with oxygen to generate heat. Additionally, when hydrogen ignites it has an almost invisible pale blue flame and has low radiant heat, which results in decreased detectability of ignited hydrogen compared to methane. Detectors with the ability to sense hydrogen flames include thermal detectors, ultraviolet (UV) detectors and/or multispectral IR detectors, which have the ability to sense the non-visible spectrum of electromagnetic radiation [Koelewijn et al., 2020].

### 2.3.2 *Cavern-related threats and barriers*

In this subsection, the cavern-related threats that have been identified for the first top event, and the potential barriers that can be put in place to prevent the threat from occurring, will be described.

#### **11. Faults or leaky interbeds intersecting the cavern**

Faults and leaky interbeds with elevated porosity, a higher permeability and different rheological behaviour under stress, such as anhydrites and carbonates, potentially provide a pathway for hydrogen to leak out of the cavern when the pressure inside the cavern exceeds the hydrostatic pressure in the surrounding rock. While faults in salt are known to heal naturally, the presence of (faults in) non-halite interbeds may pose a threat to the leak-tightness of the cavern.

Leakage through faults or leaky interbeds can be prevented/mitigated by:

- a. *Geological mapping of the internal composition of dome* to locate non-halite intervals such that they can be avoided during cavern development.
- b. *Minimize/avoid presence of faults and non-halite interbeds* during site selection and which could be connected with the previous barrier introduced under a.
- c. *Faults in halite seal naturally*, meaning that although present they have a negligible permeability and do not allow flow.
- d. *Drilling deeper* such that higher permeability interbeds in the salt are above the LCCS and do not intersect the cavern.
- e. *Test open-hole section by pressurization*, which is effectively done during the pilot phase, whereby the upper 10 meters of the open-hole section is tested for leak-tightness to hydrogen. Although this could potentially also be done for a longer open-hole section, to cover the entire interval where the cavern will be leached, it does not provide a guarantee that away from this section there are no interbeds that might pose a threat.
- f. *Install/use leakage detection and H<sub>2</sub>-gas presence monitoring equipment at surface* (see barrier description introduced for threat 10 under e).

## 12. Roof fall

Roof fall is a known threat in salt solution mining and cavern storage. Slabs of rock can detach from the roof and fall to the base of the cavern, and this may lead to degraded integrity of the seal, i.e. the roof above the cavern, and/or the LCCS. It also creates a weak but measurable seismic signal that might be perceived as a seismic event induced by the storage operations.

Roof fall is a threat that can be prevented/mitigated by:

- a. *Minimize/avoid presence of faults and non-halite interbeds* (see barrier description introduced for threat 11 under b) intersecting the cavern roof
- b. *Adhere to geomechanical cavern stability criteria* during the development of the cavern, in particular by making sure that the cavern develops according to a geomechanically stable geometry, with limited roof span, and with a cavern neck at the LCCS (the latter can be seen in relation with the barrier below under c)
- c. *Leach cavern neck* (see barrier description introduced for threat 7 under f)
- d. *Micro-seismic monitoring* is a measure that can potentially detect roof fall events, and if detected can be followed up with a sonar measurement (see barrier below under e) and if needed with a closer inspection of the LCCS for damage.
- e. *Periodic sonar measurement* is a monitoring measure that can be applied to obtain an image the 3D geometry of the cavern and neck. With this technique the development of the cavern can be monitored, and changes to the geometry of the cavern can be detected by comparing measurements from different moments in time.

## 13. H<sub>2</sub> permeation into the wall

Although salt is proven to be tight for gases, repeated mechanical and thermal loading may cause dilation in the salt. This may lead to the formation of a damage zone in the salt surrounding the cavern, into which hydrogen can permeate. While it can lead to (perceived) loss of hydrogen, at least temporarily, it is not expected to lead to actual leakage, unless the zone is intersected by non-halite interbeds that provide an actual pathway that can sustain the leakage. It is worth mentioning that this threat is also relevant in natural gas storage, where it has not been proven to give rise to significant risk.

Hydrogen permeation can be prevented/reduced/mitigated by:

- a. *Assess/quantify permeation effect during characterization phase* by experimental testing on core material combined with numerical geomechanical modelling.
- b. *Keep P, T within safe operating limits to avoid large thermo-mechanical stresses* (see barrier description introduced for threat 1 under c).
- c. *P, T monitoring* (see barrier description introduced for threat 1 under d).

## 14. Integrity loss caused by drilling activities

On-site drilling activities for a new cavern, or in the vicinity of the storage facility, can potentially result in integrity loss of a cavern (into which hydrogen is stored) at the moment when the cavern is intersected during drilling. In the past several accidents happened in such a way [Evans, 2008].

Integrity loss caused by drilling activities can be prevented/mitigated by:



- a. *Careful site selection* based on adequate geological study with up-to-date subsurface data on wells and activities in the area, and with close collaboration and communication between different mining companies working in the same area on well planning.
- b. *Only drill a single well per wellpad* to avoid that boreholes for new caverns must be drilled close to existing wells and caverns.
- c. *Carefully monitor directional surveys during drilling* to prevent penetrating unexpected subsurface locations.

For The Netherlands it may be argued that this threat is also prevented by a) the public availability of subsurface data, b) permitting procedures, and c) the large body of expertise of regulating authorities and of companies that use the subsurface for oil and gas production, geothermal, and storage.

#### 15. **Overpressurization due to malfunctioning equipment**

Exceeding safe operating pressures (overpressurization), can occur as a result of malfunctioning pressure monitoring and/or safety valves. This can cause damage to the LCCS (and potentially lead to failure) as the pressure exceeds the maximum allowable pressure. The cement sheath around the casing shoe can break and/or the rock formation around the LCCS can fracture (hydrofracturing).

Overpressurization is a threat that can be prevented/mitigated by:

- a. *Apply safety margins to maximum operational pressure* to reduce risk of damaging the LCCS. This involves measuring the hydraulic fracture pressure (gradient) at the LCCS with a Formation Integrity Test and applying a safety margin (e.g. 15%).
- b. *Install reliable well-functioning safety valves* that are proven suitable for use with hydrogen at the expected storage pressures to prevent injection above the maximum working pressure (which is well below the absolute maximum permissible pressure) and/or that bleed-off pressure when a certain maximum pressure is exceeded.
- c. *Monitor position of valves* meaning automatically record whether these are in open or closed position and have this information available at the location (such as the control room) where the valve position can be manipulated.
- d. *Monitor pressure, temperature and flow rates* at the wellhead/x-mas tree and/or bottom-hole and compare observed values to modelled ranges to validate measurements and models and detect anomalies.
- e. *Check functioning of safety valves* periodically and perform preventive maintenance if necessary.

#### 16. **Large sub-zero temperatures leading to failure of materials or components**

In particular in a pilot phase, the rapid depressurization of hydrogen during withdrawal from the very small storage volume can lead to large negative temperatures in the tubing and at the wellhead due to (adiabatic) thermal expansion of hydrogen. This is further explained in chapter 3 where some potential physical effects have been studied in more detail. These low temperatures can negatively impact their integrity in combination with a mechanical load. In a full-scale cavern phase, this threat is expected to be less relevant because the pressure drop will be much less rapid as a consequence of the large volume. Therefore, the hydrogen in the cavern will expand adiabatically and the temperature is not expected to reach strongly negative values.

Large sub-zero temperatures can be prevented/reduced/mitigated by:

- a. *Quantify (adiabatic) expansion effect and define safety margins* for injection temperature (and pressure) to limit it during the pilot phase.
- b. *Control/tune pressure, injection temperature and flow rates to limit expansion effect.*
- c. *Absorb/control expansion effects by manipulating the safety valves*
- d. *Monitor pressure, temperature and flow rates* at wellhead and/or bottom-hole and signal anomalies (see barrier description introduced for threat 15 under d).

### 2.3.3 Consequences and recovery measures

In this subsection, the potential consequences of the first top event that have been identified, and the potential recovery measures that can be put in place to mitigate and/or remediate the consequences, are described.

#### 17. Explosion of near-surface hydrogen accumulations leading to damage or injury

Hydrogen has a much wider flammability range and a much lower ignition energy compared to methane. Therefore, hydrogen is more prone to ignite when released as it requires very little external energy to ignite. In case of leakage of hydrogen (or methane) in confined spaces where it can accumulate without being detected, there is an elevated risk of explosion. An example of this is the slow leakage of hydrogen from the storage system and upward migration through the (shallow) subsurface, which may lead to accumulations of hydrogen such as in pockets in the shallow subsurface just below the ground. If such accumulations were to ignite this could potentially result in an explosion, and lead to damage and/or injury. However, explosion of hydrogen accumulations in the subsurface is unlikely due to the unfavorable (shallow) subsurface conditions with no or very limited free oxygen and no ignition source.

Explosion of near-surface hydrogen accumulations is a threat that can be prevented/mitigated by:

- a. *Prevent accumulation of hydrogen close to surface* is effectively done by implementing proper barriers to subsurface leakage (see the description for threat 25).
- b. *P, T monitoring* (see barrier description introduced for threat 1 under d), especially pressure monitoring of the annulus (see also additional description under threat 4 and barrier c).
- c. *Install/use leakage detection and H<sub>2</sub>-gas presence monitoring equipment at surface* (see barrier description introduced for threat 10 under e).

#### 18. Adverse effects of hydrogen pollution on groundwater quality, vegetation and animals

Hydrogen leaking from the storage system in the subsurface will migrate upward through the subsurface until it either gets trapped or reaches fresh groundwater-bearing layers (aquifers) in the shallow subsurface. In shallow aquifers, redox reactions that are catalysed by bacteria can oxidize the leaked hydrogen by iron (Fe<sup>3+</sup>) reduction, sulphate (SO<sub>4</sub><sup>2-</sup>) reduction, and methanogenesis (reducing carbonate, CO<sub>3</sub><sup>2-</sup>), and thereby can enhance unwanted changes in the groundwater chemistry. However, the influence of excess hydrogen on the geochemistry of shallow aquifers is poorly investigated. In [Berta et al., 2018] it is

shown experimentally that hydrogen is consumed rapidly via sulphate reduction and acetate production (no methanogenesis). Furthermore, in laboratory experiments described in [Molema, 2021] hydrogen was also completely consumed within 2 days for brackish groundwater and within 7 days for fresh groundwater, but the process responsible for the consumption of hydrogen was found to be enigmatic.

Adverse effects of the pollution of groundwater with hydrogen on groundwater quality, vegetation and animals can be prevented/mitigated by:

- a. *Warn (drinking water) authorities* to implement additional mitigation measures when significant groundwater pollution is expected/observed.
- b. *Determine cause of leakage and repair it*, meaning locating the leak, determine the cause and repair it.
- c. *Soil zone remediation*, meaning taking steps to lower the (elevated) concentrations of hydrogen from the groundwater.
- d. *Groundwater quality monitoring* is a (periodic) monitoring technique that can be used to detect changes in the composition of the groundwater.
- e. *Install/use leakage detection and H<sub>2</sub>-gas presence monitoring equipment at surface* (see barrier description introduced for threat 10 under e).

## 2.4 BowTie analysis for top event leakage of hydrogen at the surface

In this section the results of the BowTie analysis will be detailed for the second top event as follow. In section 2.4.1 the threats and barriers are described, whereas in section 2.4.2 the potential consequences of leakage and possible recovery measures are described.

### 2.4.1 Threats and barriers

In this subsection, the threats that have been identified, and the potential barriers that can be put in place to prevent the threat from occurring, will be described.

#### 19. Catastrophic x-mas tree damage due to collision

Severe catastrophic damage to the wellhead and/or x-mas tree can be caused by a collision with a heavy truck during a workover. In case of such damage the highly pressurized hydrogen (up to 200 bar) can potentially flow out of the storage system into the atmosphere at very high flow rates through the tubing, or casing during the MIT with hydrogen. In a pilot phase the volume of stored hydrogen that is small ( $\approx 20,000 \text{ Nm}^3$ ), and therefore the duration of sustained outflow is short (up to  $\approx 3$  minutes). In a full-scale cavern phase though, the volume of hydrogen is very large,  $\approx 150$  million  $\text{Nm}^3$  for a cavern with a geometric volume of 1 million  $\text{m}^3$ . Therefore, the duration of sustained outflow is very long (up to  $\approx 13$  days). In chapter 3, results are presented of detailed outflow calculations for several scenarios of free outflow at the wellhead, and their physical effects and consequences.

Catastrophic x-mas tree damage due to collision leading to leakage of hydrogen from the well can be prevented/mitigated by:

- a. *Enforce a no-drive zone around wellhead* with reinforced concrete blocks
- b. *Completely submerge wellhead cellar* and close it off.
- c. *Install a functioning SSSV* that is tested after installation under operational storage pressures, as a second barrier to leakage in case a primary barrier

at the wellhead or x-mas tree fails. An SSSV is a key component of a gas storage well. Its sole purpose is to automatically close off the well in the event of loss of hydraulic control pressure and which would lead to uncontrolled release of the gas, i.e. a blow-out. It is failsafe as hydraulic pressure is required to force the valve to its open position, and when the pressure in the hydraulic system drops, the valve will automatically return to the closed (safe) position. It must be installed at the correct depth in the well, and which depth concerns one below crater depth. It is only accepted as a functional barrier after having been installed in the well and tested under operational conditions and when being active at all times during the storage operation. However, it must be removed when a workover of the well must be performed. In such case, an alternative blow-out prevention barrier should be installed and which can be done in the form of a blow-out preventer that is suitable to close upon contact with hydrogen gas. Although SSSV's are extensively used in oil and gas industry, their effectiveness in shutting in a (fast) flowing hydrogen storage well is yet to be confirmed. In fact, it is likely that acceptable leakage rates for hydrogen and hence verification criteria will be different. In such case an SSSV may have to be designed specifically for the purpose of hydrogen storage [Van der Valk et al., 2020].

- d. *Periodically check SSSV*, meaning periodical checks on proper functioning including a pressure test/inflow test to verify that it is sealing.

## 20. Catastrophic x-mas tree damage due to vandalism/terrorism

This threat is very similar in nature to the one with number 19, as would be the same for the consequences. However, instead of (unintentional) collision being the cause, here the cause would be intentional such as vandalism or a terrorist attack.

Catastrophic x-mas tree damage due to vandalism/terrorism can be prevented/mitigated by:

- a. *Security fence around wellpad* that can be closed off to prevent unauthorized personnel to access the wellpad.
- b. *Completely submerge wellhead cellar* (see barrier introduced for threat 19 under b).
- c. *Install a functioning SSSV, tested after installation* under operational storage pressures (see barrier description introduced for threat 19 under c)
- d. *Periodically check SSSV* (see barrier description introduced for threat 19 under d)
- e. *Security surveillance*, meaning regular, periodic patrolling of the area.
- f. *Video surveillance*, meaning visual monitoring of the site with one or more video cameras, for instance as part of a closed-circuit television system, and with a control room involved.

## 21. Failing wellhead flange or hose connection

On the wellhead/x-mas tree flanges are present to which pipelines or hoses can be connected. In a pilot phase, hoses will be connected to enable the hydrogen to flow under pressure from the tube trailer to the well and vice versa. In a full-scale cavern phase, the hydrogen will flow through steel pipelines between the well and the gas processing facility. In case of a failing flange or hose/pipeline connection at the wellhead/x-mas tree, hydrogen can leak into the atmosphere,

whereby the rate of leakage will depend on the size of the leak and the pressure (see chapter 3).

A failing wellhead/x-mas tree flange or hose connection is a threat that can be prevented/mitigated by:

- a. *Use austenitic steels with appropriate hardness* (see barrier description introduced for threat 1 under a)
- b. *Use of H<sub>2</sub>-tested wellhead, components and materials* (steels, elastomers, etc.) that have been tested and proven suitable for use under exposure to hydrogen under expected P, T, and environmental conditions.
- c. *Install a functioning SSSV*, tested after installation under operational storage pressures (see barrier description introduced for threat 19 under c) as a second barrier to leakage in case this primary barrier (flange or connection) fails.
- d. *Install/use leakage detection and H<sub>2</sub>-gas presence monitoring equipment at surface* to detect hydrogen that leaked into the atmosphere (see barrier description introduced for threat 10 under e).
- e. *Periodically check SSSV*, i.e., periodically checking that it properly functions (see barrier description introduced for threat 19 under d).

## 22. Improperly closed wellhead valve

An improperly closed wellhead valve can lead to leakage of hydrogen at the wellhead when it fails to completely close (or open) or when its state is not correctly audited. For example, the state of the valve can be recorded as open, i.e., ready for flow through of hydrogen from the tube trailer (during a pilot phase) or gas processing facility (in a full-scale cavern phase) while in fact it is still closed, which may lead to rapid pressure buildup at the valve leading to failure.

An improperly closed valve is a threat that can be prevented/mitigated by:

- a. *Use a pressure control system on tube trailer*: During a pilot phase, the hydrogen will be stored above-ground in a tube trailer that has a pressure control system (with P, T, and flow sensors) that can open and close valves and keep track of position.
- b. *Enable remote control of valves* from the control room of the facility (during a full-scale cavern phase) by qualified and competent staff.
- c. *Install a functioning SSSV* tested after installation under operational storage pressures (see barrier description introduced for threat 19 under c) as a second barrier to leakage in case this primary barrier (wellhead valve) fails.
- d. *Repeated performance tests of valves* to test their proper functioning.
- e. *Monitor position of valves* (see barrier description introduced for threat 15 under c).
- f. *P, T (and flow) monitoring* (see barrier description introduced for threat 1 under d).
- g. *Periodically check SSSV* (see barrier description introduced for threat 21 under e under c).

## 23. Integrity failure during workover under pressure

In a full-scale cavern phase, when hydrogen is stored under pressure in the cavern, maintenance must sometimes be performed such as on the well. Instead of completely emptying the cavern, which takes time and is costly, such workovers are usually performed under pressure and when the hydrogen is still

in the cavern. It may also involve (partial) rebrining and/or debrining, for which a so-called debrining string (or coiled tubing) must be installed and removed again while the cavern is under high pressure up to 200 bar. If something goes wrong during this operation, and which is known as snubbing, the integrity of the storage system may potentially be compromised leading to leakage of hydrogen into the atmosphere at the surface at (potentially) high flow rate as a consequence of the high pressure. Such workovers are a standard procedure in gas storage operations, and the required tools and equipment have extensively been used for decades in workovers for natural gas storage. There is, however, very little experience with workovers for hydrogen storage, and steps must be taken to test the required equipment, tools and procedures and gain experience in performing such workovers with hydrogen.

Integrity failure during a workover under pressure is a threat that can be prevented/mitigated by:

- a. *Use  $H_2$ -tested well intervention equipment, tools and materials* such as steels, rubbers and elastomers that have been tested and proven suitable for use under exposure to hydrogen under expected P, T, and environmental conditions.
- b. *Use  $H_2$ -compliant intervention techniques* that are based on intervention techniques used in natural gas storage and are adapted where required and tested for hydrogen storage.
- c. *Perform well intervention with qualified and competent staff* that is fully aware of difference between operations with natural gas/oil and hydrogen.
- d. *Perform detailed and dedicated risk assessment* before all well intervention operations.
- e. *Test debrining procedure* during the pilot phase with a debrining string, coiled tubing, or via annulus.

#### **24. Hydrogen dissolved in brine coming to surface during debrining**

At first gas fill of the cavern for a full-scale cavern phase or during a pilot phase, the hydrogen that is injected is in contact with the brine in the cavern. The solubility of hydrogen in pure water is low [Panfilov, 2016], and even lower in saturated brine because of the so-called salting-out effect [Chabab et al., 2020], reaching an absolute minimum value at 57 °C. It is also significantly lower than the solubility of methane in low concentration brines, [Lopez-Lazaro et al., 2019] and [Van der Valk et al., 2020], at least for the depth and related temperature range for storage of hydrogen in caverns (down to maximum 1500 m depth). It is not negligible though as some hydrogen must be expected to dissolve in the brine as does methane.

As more and more hydrogen is injected, the pressure builds up, and at some point it exceeds the halmostatic pressure and brine with dissolved hydrogen is pushed out through the debrining string. As such, hydrogen dissolved in brine is produced during debrining and comes out of solution at surface. If no mitigating measures are taken, the uncontrolled release of this hydrogen gas may potentially cause fire or explosion leading to damage of surface facilities and/or harm to humans and animals.

Uncontrolled release of hydrogen by de-hydrogenation of brine at the surface can be prevented/mitigated by:

- a. *Quantify/measure volume of hydrogen that will dissolve into brine* in the cavern at operational conditions to assess to what extent this poses a risk, and to better understand what mitigating measures to take. This can be done for instance by installing hydrogen gas detection sensors in the brine storage tanks that will be used in a pilot phase to store the brine as hydrogen is injected.
- b. *Install separator to de-hydrogenate the brine* in a controlled environment without ignition sources, similar to what is done with methane in natural gas storage.

## 25. Migration of hydrogen via overburden to surface

This threat is related to the one in the BowTie diagram on subsurface leakage as it concerns the migration of hydrogen that leaked from the storage system in the subsurface. Once leaked, the hydrogen can potentially migrate upward through the layers of rock above the cavern, referred to as the overburden, and via shallow aquifers all the way to the surface.

Above-ground risks associated with hydrogen that leaked in the subsurface, and that migrated via the overburden to the surface, is a threat that can be prevented/mitigated by:

- a. *Characterize overburden to assess migration pathways and risk*, meaning detailed geological mapping of the layers in the overburden section of the subsurface, and characterization of their flow properties, the potential migration pathways for leaked hydrogen, and of areas where it might come to surface and where monitoring measures can be applied (see also next barrier).
- b. *Install/use leakage detection and H<sub>2</sub>-gas presence monitoring equipment at surface* (see barrier description introduced for threat 10 under e).

### 2.4.2 Consequences and recovery measures

In this subsection, the potential consequences of the second top event and the potential recovery measures that can be put in place to mitigate and/or remediate the consequences, will be described.

## 26. Adverse effects to humans and animals due to air pollution with hydrogen

When a gas is released into the atmosphere, it pollutes the air by locally changing the composition of the air. Air is composed of 78% nitrogen and 21% oxygen. In particular a change in oxygen content will cause breathing problems for humans and animals and may ultimately lead to suffocation. As such, the release of hydrogen into the atmosphere poses a threat to humans and animals as there is a risk of suffocation, especially when it is released in large quantities and high flow rate such that it forms a hydrogen cloud, or when it accumulates in confined spaces where humans and/or animals are also present. In a pilot phase, the volume of hydrogen that is used is small and as the tests will be executed on the wellpad in an open field, the risk of air pollution is considered small. In a full-scale cavern phase though, hydrogen can potentially be released in large volumes and at high rates, either at the wellpad or in the connected processing facilities, and the risk must be considered higher. However, since hydrogen is a very light and highly diffusive gas, it will typically rise upward quickly and disperse rapidly (several meters per second) when released into the open atmosphere (unconfined), more rapidly for instance than methane [H2Tools, 2020], which makes it less likely that significant amounts of hydrogen could accumulate.

Adverse effects to humans and animals due to air pollution with hydrogen can be prevented/mitigated by:

- a. *Minimize volume and flow rate during release*, as the lower the volume of leaked hydrogen and rate of leakage, the less likely it is that significant amounts of hydrogen locally pollute the air to a level where it leads to breathing problems for humans and animals. Volume can be minimized for instance by installing safety valves that close off the well, and by monitoring for the presence of hydrogen gas with detectors that detect release of hydrogen into the atmosphere such that leakage can be stopped at an early stage (see recovery measure below under f).
- b. *Minimize presence of humans and animals in vicinity of site*, meaning fencing off the site, maintaining a safety zone around the site, and minimizing the need for personnel to be on the site (e.g. remote operation).
- c. *Execute emergency response plan*, and which details the order of actions to be executed for different types of calamities, such as communication with (local) stakeholders and authorities, and evacuation of humans and/or animals. This is especially important for a full-scale cavern phase.
- d. *Warn local stakeholders and authorities* when significant air pollution is expected such that people living in the area can be informed and advised to take preventive measures to get themselves and animals out of harm's way.
- e. *Determine cause of leakage and repair* (see recovery measure introduced for consequence 18 under b).
- f. *Install/use leakage detection and H<sub>2</sub>-gas presence monitoring equipment at surface* (see barrier description introduced for threat 10 under e).

## **27. Extreme noise levels leading to hearing damage**

Outflow of hydrogen at very high flow rates can be the consequence of a calamity at the wellhead (blow-out), or due to a rupture in a pipeline or hose connecting the wellhead with the tube trailer (pilot phase) or processing facilities (full-scale cavern phase). In such a case extreme noise levels of up to 85 dB can occur and which can cause hearing damage to humans and/or animals nearby. The severity of the damage can be expected to depend on the level of noise and the duration of exposure. In a pilot phase the duration of the noise is limited to about 3 minutes (duration of outflow, see chapter 3), and the level of noise will decrease rapidly (within tens of seconds) due to the rapidly decreasing flow rate (as a result of pressure depletion). In a full-scale cavern phase though, there will be a prolonged period of several days to potentially weeks during which noise levels are extreme. This will severely complicate any remediation action in the vicinity of the leak.

Hearing damage due to extreme noise can be prevented/mitigated by:

- a. *Minimize presence of humans and animals in vicinity of site* (see recovery measure description introduced for consequence 26 under b).
- b. *Use proper Personal Protective Equipment* for all staff working in the vicinity of the well. In this case, the use of hearing protection can help to prevent hearing damage.
- c. *Execute emergency response plan* (see recovery measure description introduced for consequence 26 under c).
- d. *Warn local stakeholders and authorities* when extreme noise levels are expected such that people living in the area can be informed and advised to take preventive measures for themselves and animals living in the area.



- e. *Determine the cause of leakage and repair it* (see recovery measure introduced for consequence 18 under b).

### **28. Shockwave from explosion causing structural damage, injury or death**

If hydrogen is released in an unconfined open environment it will typically rise and disperse more rapidly (several meters per second) in air compared to the heavier methane, [H2Tools, 2020]. This makes it less likely (than for methane) for significant amounts of hydrogen to accumulate and cause an explosion in case of ignition. In case of leakage of hydrogen in confined spaces however, the risks are likely to be more severe than for methane [Van der Valk et al., 2020]. Although both gases, when mixed with air in a combustible gas cloud, can explode when ignited, hydrogen is expected to be more prone to ignite because of the lower ignition energy and wider flammability range (vol% of hydrogen vs. air). However, as little is known on the actual ignition behavior of hydrogen and how this compares to methane, further research on this topic is advised.

When a mixture of hydrogen and air explodes, the higher flame propagation speed potentially generates high pressures that could result in an explosion and a pressure shock wave with massive burst damage. This could result in damage to buildings and even collapse, injury or death, [H2Tools, 2020] and [Hyde and Ellis, 2019]. When a mixture of methane and air explodes, the potential for burst damage is lower. However, the longer duration of the flame, in combination with the heat that it radiates, also has the potential to cause damage, injury or death [Li et al., 2015]. In chapter 3, the potential physical effects of an explosion are further detailed for several outflow scenarios representative for a pilot phase and a full-scale cavern phase. In the absence of confinement and congestion, no overpressures are generated, and the consequence of ignition is limited to a jet flame or flash fire, the consequences of which are described under the one with number 29.

Explosion of leaked hydrogen can be prevented/mitigated by:

- a. *Prevent accumulation of a high-concentration hydrogen cloud*, and which can be done by early detection of leakage (see barrier description introduced for threat 10 under e), minimizing the presence of confined spaces, and air flow and ventilation.
- b. *Stimulate immediate ignition on release to prevent explosion*: Although hydrogen has a very low ignition energy, and is expected to ignite spontaneously, a short delay in ignition in combination with a high flow rate (e.g. 10 to 100 kg/s) may effectively lead to congestion at the location of release. In such a situation even a minor delay of tenths of seconds to seconds in ignition could result in an explosion, because significant amounts of hydrogen would have already been released. To prevent this, measures can be taken to ensure that the hydrogen immediately ignites on release such that a jet fire forms, the consequences of which are described below (see consequence with number 29).
- c. *Execute emergency response plan* (see recovery measure description introduced for consequence 26 under c).
- d. *Install/use leakage detection and H<sub>2</sub>-gas presence monitoring equipment at surface* (see barrier description introduced for threat 10 under e), including the use of gas detectors by personnel as part of the Personal Protective Equipment.

### **29. Heat radiating from flash fire or jet flame causing structural damage, injury or death**

Ignition of hydrogen upon release into the open atmosphere leads to the formation of a jet flame or a flash fire. A jet flame occurs in case of leakage at high flow rate (e.g., directly at the wellhead) or through a hole/rupture, and with highly-concentrated hydrogen, whereas a flash fire occurs at lower rate and a lower concentration of hydrogen in the mix. While burning methane radiates a lot of heat and creates a flame that is clearly visible, burning hydrogen radiates little IR heat, but emits substantial UV radiation. The lack of IR gives little sensation of heat but the exposure to a hydrogen flame still causes severe burns because of the UV radiation. As a burning hydrogen flame is also not easily detectable, it increases the risks associated with hydrogen when it ignites to form a flame (see barrier description introduced for threat 10 under e).

In chapter 3, the potential physical effects of a jet fire are further detailed for several outflow scenarios representative for a pilot phase and a full-scale cavern phase of the hydrogen storage system. From the results obtained it is observed that for the pilot phase the intensity of the jet flame or flash fire (and heat exposure) will decrease rapidly (within tens of seconds) and the event will be short-lived (up to about 3 minutes). In the full-scale cavern phase, however, there will be a prolonged period of several days to (potentially) weeks during which extreme heat is radiated, and this will severely complicate any remediation action in the vicinity of the leak.

Adverse effects of heat radiation by a jet flame or flash fire can be prevented/mitigated by:

- a. *Execute fire prevention plan*, which details the order of actions to be executed to prevent the fire from spreading and mitigate consequences such as harm to humans and animals, and damage to facilities.
- b. *Execute emergency response plan* (see recovery measure description introduced for consequence 26 under c).
- c. *Warn local stakeholders and authorities* when a calamity occurs that causes a jet fire or flash fire such that people living in the area can be informed and advised to take preventive measures to get themselves and animals out of harm's way.
- d. *Determine cause of leakage and repair* (see recovery measure introduced for consequence 18 under b).
- e. *Install/use leakage detection and H<sub>2</sub>-gas presence monitoring equipment at surface* (see barrier description introduced for threat 10 under e), including the use of gas detectors by personnel as part of the Personal Protective Equipment.

### **30. Injury or death – occurring in combination with other consequences (fire, explosion)**

Injury or death of humans and/or animals are two of the most severe consequences of physical effects, like pollution, suffocation, explosion and heat radiation, and which can be caused by leakage of hydrogen at the surface. These two consequences are therefore explicitly included in the BowTie diagram.

Injury or death as a consequence of physical effects caused by leaked hydrogen can be prevented/mitigated by:

- a. *Perform a QRA* (quantitative risk assessment) to quantify the probability of occurrence of failure scenarios that lead to leakage, the nature, likelihood of

occurrence, and severity of their physical effects, and their impact on humans, animals, and the environment.

- b. *Reconsider ATEX zonation*, meaning that the current ATEX zonation, and which is based on QRA's for natural gas storage, must be reviewed for storage of hydrogen. Such a review has to consider the deburning risks associated with hydrogen versus the ones for natural gas.
- c. *Minimize presence of humans and animals in vicinity of site* (see recovery measure description introduced for consequence 26 under b).
- d. *Execute emergency response plan* (see recovery measure description introduced for consequence 26 under c).
- e. *Warn local stakeholders and authorities* when a calamity occurs such that people living in the area can be informed and advised to take preventive measures to get themselves and animals out of harm's way.
- f. *Record incidents and follow-up with additional measures* to learn from the past and further reduce risk.

## 2.5 Towards failure scenarios for hydrogen storage in a salt cavern

The BowTie analysis has resulted in the identification of 23 threats that may jeopardize the integrity of the hydrogen storage system studied and 7 possible consequences when leakage of hydrogen occurs. Most threats (15) pertain to integrity failure of the well or wellhead in one way or another (materials, components, interfaces). While only a few (4) are directly related to integrity failure of the cavern. As such, it can be concluded that the well is the most critical component of a storage system.

Experience from previous incidents at underground storage facilities for natural gas confirms that the biggest risks arise from well problems [Evans, 2008]. Well failure rates reported in cavern storage studies are in the order of  $10^{-5}$ /well/year in Europe and  $10^{-4}$ /well/year worldwide, including both above-ground and below-ground failure [Keeley, 2008]. Geological failure rates of salt caverns worldwide are in the order of  $10^{-5}$  failures/cavern/year [Keeley, 2008]. No relevant failures of salt caverns have been recorded in Europe that led to leakage. This is in contrast to the USA where a few incidents did take place during the decades of storage operations [Evans, 2008]. In [Keeley, 2008] it is reported that for natural gas this type of failure leads to a slow release of the stored gas with a mass flux of  $10^{-6}$  to  $10^{-7}$  kg/s/m<sup>2</sup>. If the gas would reach the surface the discharge rate will be in the order of  $10^{-4}$  kg/s, which equates to a risk that can be considered negligible. When leakage from the well occurs, discharge rates of up to 100 kg/s are possible for natural gas (i.e. effectively 6 orders of magnitude higher than for geological cavern failures), at least for above-ground failure. Similar leakage rates are reported for hydrogen due to well failure above-ground based on work reported in chapter 3: up to 87 kg/s for leakage through the tubing opening at the wellhead at a storage pressure of 220 bar). Leakage rates for well- or cavern failure below-ground have not been reported for hydrogen. Further research would be required to obtain such leakage rates, and to assess how these translate to mass fluxes of hydrogen migrating through the subsurface that may ultimately reach the surface. At the surface, this leaked hydrogen could, under certain conditions, potentially form a concentrated gas plume that could ignite to cause a fire or explosion (see chapter 3).

In [Van der Valk et al., 2020] a qualitative non site-specific comparison was made between underground storage of hydrogen and methane. The latter as a proxy for natural gas, which consists of 70-90% of methane. Although in general underground storage of natural gas and underground storage of hydrogen are expected to have a similar risk profile, there are also differences:

- Hydrogen is a smaller and more diffusive molecule that can more easily permeate through materials, especially when they contain defects and/or cracks. Additionally, the embrittling nature of hydrogen can lead to progressive growth of such defects and cracks when subjected to large fast-cyclic changes in pressure (and temperature).
- If hydrogen is released in an unconfined open environment it will typically rise and disperse more rapidly (several meters per second) compared to the heavier CH<sub>4</sub>, [H2Tools, 2020]. This rapid dispersion of H<sub>2</sub> in open spaces (atmosphere) makes it less likely that significant amounts of hydrogen could accumulate to form a concentrated gas plume.
- Hydrogen has a much wider flammability range, and a much lower ignition energy compared to methane, and is therefore more prone to ignite when released.
- Hydrogen radiates little infrared heat when ignited to form a flame, but emits substantial UV radiation, in contrast to methane, which radiates heat and creates a flame that is clearly visible. The lack of infrared gives little sensation of heat, but the exposure to a hydrogen flame will still cause severe burns because of the UV radiation. Because a burning hydrogen flame is also not easily detectable (contrary to methane), it increases the risks associated with hydrogen when it ignites to form a flame.
- When a mixture of hydrogen and air explodes, the higher flame propagation speed potentially generates high pressures that could result in a pressure shock wave that causes massive burst damage, (i.e., building damage or even collapse). In contrast, when a mixture of methane and air explodes, the potential for burst damage is lower, but the longer duration of the flame, in combination with the heat that it radiates, can potentially lead to lasting harm. In the absence of confinement and congestion though, no overpressures are generated, and the consequence of an explosion is limited to a flash fire.
- Hydrogen is a reactive gas, in contrast to methane, that has the ability to react with minerals and fluids and may interact with microbes in the cavern. This could result in loss of hydrogen and/or contamination of the production stream due to the formation of hydrogen sulphide, a toxic, corrosive gas that degrades wellbore materials and poses a threat to human health when released to the atmosphere.

A logical next step following the BowTie analysis is to define failure scenarios for the storage system, in which the causal relationships between a threat or a combination of interdependent threats and its consequences is further detailed with the aim to identify when, where and how to intervene to prevent a failure from happening. In the BowTie diagram, failure scenarios are expressed by the horizontal connection between one or more threats and the top event on the left side of the BowTie diagram and one or more consequences on the right side. In a quantitative risk assessment, the quantified physical effects of the defined failure scenarios and their probability of occurrence are used to calculate risk contours that indicate the probability of injury or death per year and how this changes with distance of a person or group of persons from (read: exposure to) the hazard. While such assessments have been done many times before for underground natural gas storage in salt caverns, this methodology

has not been applied yet to failure scenarios for underground storage of hydrogen in salt caverns.

Failure scenarios can be defined that focus on failure of the well leading to leakage below surface. In the BowTie diagram for leakage of hydrogen in the subsurface, 10 threats are present that may lead to leakage below-ground due to failure of the well. However, for most threats, their occurrence alone will not directly lead to leakage, because of the double-barrier design of the well.

A first example of a failure scenario is when failure of the packer occurs (primary barrier), hydrogen will leak from the cavern into the annular space between the tubing and the casing, and will rise upward to accumulate at the top of the annulus at the wellhead. If the annulus is monitored, this would be detected at an early stage, and actions can be taken to replace the packer, if only at significant cost. However, if the annulus is not monitored, or the monitoring fails, then the leaking packer is not detected, and hydrogen can keep accumulating in the annulus directly against the casing (secondary barrier). If a casing connection is not hydrogen-tight, which is also a threat in the BowTie diagram, then the hydrogen is no longer contained and leaks out of the storage system. It is important to study this failure scenario in more detail to quantify the rate of leakage, and map plausible leakage pathways through the subsurface. Examples of such pathways are leakage along the interface between the casing and the cement, or through the cement into the surrounding rock, from where it may migrate upward through the overburden towards the surface.

A second failure scenario that is important to study is related to failure of the LCCS. At the LCCS, hydrogen is in direct contact with interfaces between salt and cement, and between cement and casing. Long-term exposure to hydrogen in combination with fast-cyclic changes in pressure and temperature may cause formation of micro-annuli (i.e. circumferential fractures) at these interfaces which could lead to leakage. With a wellbore geomechanical model, the damage (cracking) of the annular cement can be assessed, the probability of debonding and creation of micro-annuli at the interfaces can be predicted, and the width of the micro-annuli, as possible leakage pathways up the well, as created during the lifetime of the well can be estimated. In combination with transport modelling, the rate of hydrogen leakage along the micro-annuli and through annular cement can then be quantified.

Examples of failure scenarios used for natural gas storage are the scenarios that may lead to free outflow and/or leakage of natural gas at the surface. For such scenarios the quantitative risk assessment for natural gas storage in Zuidwending [Middel, 2010] makes a distinction between:

1. Blow-out (vertical free outflow) of a well during workovers,
2. Blowout of a well in combination with free outflow from a pipeline under pressure (horizontal free outflow) during injection and withdrawal, and
3. Leakage from the well (either vertically or horizontally).

In chapter 3 of this report, the results are detailed of a study to quantify the physical effects of the failure scenarios 1 and 3, but for hydrogen storage.

### 3 Physical effects of accidental hydrogen release at the wellhead

As introduced in the first chapter, and referred to in the second chapter, a modelling study has been performed to quantify the effects of uncontrolled outflow of hydrogen at the surface due to leakage at the wellhead (e.g. malfunctioning valve) or, as an extreme case, due to a blow-out whereby the wellhead is completely removed. Like in the second chapter, the study considers both a pilot phase and a subsequent second full-scale cavern phase for subsurface hydrogen storage in salt caverns. Therefore, outflow scenarios were considered for the generic hydrogen storage system as described in Section 2.2 that are representative for a pilot phase and for a full-scale cavern phase.

In the first section of this chapter the set-up of the modelling study, the modelling assumptions and the calculation methods are described, and in the second section the modelling results are discussed. This chapter is complemented with two appendices that provide more details and background to the contents of this chapter.

#### 3.1 Set-up of outflow and effect calculations

##### 3.1.1 Introduction

In order to perform a full Quantitative Risk Assessment (QRA) many factors are important such as frequency of the chosen failure scenarios, physical effects following failure, population density (and distribution) and atmospheric conditions at the time of failure. The result of such a QRA is a conclusion on whether the overall risk associated with a process or installation is acceptable or not.

In this study, rather than taking a probabilistic approach as in a full QRA, a deterministic approach is taken. The approach is aimed at quantifying the physical effects of accidental H<sub>2</sub> releases, which can be one or more of the following: 1) a high-concentration H<sub>2</sub> cloud in the atmosphere, 2) heat radiation of a H<sub>2</sub> jet fire and 3) explosion effects. Other factors that influence the risk, like population density and distribution, and frequency (probability) of the scenarios, are not taken into account.

This section will detail the scenarios that are chosen and the modelling approach that is applied to study the above-mentioned physical effects. These scenarios may be referred to as being of catastrophic nature and for which one may assume them to be worst-case scenarios. For the chosen scenarios an outflow calculation is first performed with the OLGA modelling and simulation software<sup>4</sup>, an industry-standard tool for this type of processes. The results from the outflow calculations then serve as input for the study of the physical effects and for which the HyRAM software tool is used [Groth et al., 2015].

##### 3.1.2 Scenarios

The hazard under study is the hydrogen that is stored under high pressure in the subsurface storage system introduced in the previous chapter. Accident scenarios are defined that represent hydrogen leakage through the tubing (217 mm diameter

---

<sup>4</sup> <https://www.software.slb.com/products/olga>

opening) or the casing (316 mm diameter opening), as would occur during a blow-out when the wellhead is completely removed, or through a small hole (1-10 mm diameter opening). Next to this outflow diameter, the geometric volume of a cavern is a second important parameter. For a pilot phase a representative volume of 117 m<sup>3</sup> is used for a small cavern. For a full-scale cavern phase, representative cavern volumes of 0.3 Mm<sup>3</sup> (demonstration scale) and 1.0 Mm<sup>3</sup> (commercial scale) are considered. Furthermore, for the outflow calculations the initial cavern pressure is varied between 50 and 220 bar. This leads to a set of representative scenarios, referred to further as cases, that have been studied with respect to both hydrogen outflow and physical effects and which are listed in Table 2.

The cases listed in Table 2 are the scenarios that have been studied throughout the research, of which some have been subject of detailed considerations while for others such considerations turned out to not have much added value. Hence, for only a subset of the cases this chapter reports and discusses results. All of the cases though have been used to consider the modelling assumptions via a study of the sensitivity for the well path geometry, grid cell size, and for the way two physical phenomena are being accounted for in the modelling approach. Therefore, Appendix B and Appendix C serve the reader with additional results obtained for the scenarios.

Table 2: Overview of scenarios. Underscore in Case ID of cases 7, 8, and 9 indicates size of leak.

Case ID	Phase	Pressure [bar]	Cavern volume [m <sup>3</sup> ]	Outflow diameter [mm]
Case 1	Pilot	50	117	217
Case 2	Pilot	135	117	217
Case 3	Pilot	220	117	217
Case 4	Pilot	50	117	316
Case 5	Pilot	135	117	316
Case 6	Pilot	220	117	316
Case 7_ <u>10</u>	Pilot	50	117	10
Case 8_ <u>10</u>	Pilot	135	117	10
Case 9_ <u>1</u>	Pilot	220	117	1
Case 9_ <u>3</u>	Pilot	220	117	3
Case 9_ <u>5</u>	Pilot	220	117	5
Case 9_ <u>10</u>	Pilot	220	117	10
Case 10	Full-scale	70	3*10 <sup>5</sup>	217
Case 11	Full-scale	135	3*10 <sup>5</sup>	217
Case 12	Full-scale	200	3*10 <sup>5</sup>	217
Case 13	Full-scale	70	1*10 <sup>6</sup>	217
Case 14	Full-scale	135	1*10 <sup>6</sup>	217
Case 15	Full-scale	200	1*10 <sup>6</sup>	217

### 3.1.3 Hydrogen outflow model

#### 3.1.3.1 Model description

Industry-standard transient multiphase flow modelling and simulation tool OLGA is widely used in the oil & gas industry. The tool concerns a one-dimensional flow simulator in which all constitute equations (mass, momentum and energy) are solved based on a finite difference method. It allows for the transient simulation of four phases (gas, oil/condensate, water and solids) including heat transfer. The tool can be used for both well simulations and flowline simulations. The well simulations range from production scenarios, such as for example start-up, shut-in, slugging, loading, injection simulations (gas lift, water injection, CO<sub>2</sub> injection), but includes also the

option to study blow-out (maximum open outflow) as important for this study. The tool allows process equipment to be included in the modelled flow system such as pumps, compressors, heaters, separators and valves, although in this study only pipes and valves are used.

In the current study outflow simulations have been done using OLGA v2018.1.0 with the goal to calculate the outflow rates in case of a full breach (either tubing or casing) or in case of a leak. This is done by first establishing a shut-in scenario with a closed wellhead valve. At a given time, the downstream boundary is changed to atmospheric conditions and the wellhead choke is fully opened. This will result in an open flow connection from the cavern to surface. In this scenario this flow path is kept open. That means, no actions at the surface are taken, such as for instance closing the subsurface safety valve. This allows the cavern to fully empty.

In the simulations for this study the following two steps are therefore modelled:

1. OLGA simulation model is initialised at a starting cavern pressure with the wellhead choke closed;
2. A transient run is subsequently started during which the wellhead valve is opened in 10 seconds (i.e. the valve is set from fully closed to fully open in 10 seconds) starting at  $t = 1000$  s.

Table 3: Well path coordinates

Along length (md)	TVD (m)
0	0
205	205
240	240
587	566
590	568
937	895
942	900
1263	1219

### 3.1.3.2 Modelling of system

For the study the system is modelled as consisting of two elements, being the well path and a section of topside piping and the cavern. The well path coordinates applied are found in Table 3, whereas the well path is visually represented in Figure 8.

For the well path a single-diameter well is used (either based on tubing size or casing size), extended with 20 m topside piping with the wellhead choke situated halfway this section. The 20 m topside is added for numerical reasons, because ending in a pure vertical section causes numerical instabilities in case of some temporary backflow. This may be the consequence of small pressure fluctuations due to numerical rounding and the back flow then occurring can be the cause for further (increased) backflow.

The cavern is modelled as a pipe section with a large diameter. As the actual flow rates in the cavern are very low there is hardly any pressure drop across these cavern elements and these pipe elements simply act as a volume. For the pilot phase, the cavern is modelled as a pipe with height of 10 m and a diameter of 3.86 m, resulting in 117 m<sup>3</sup> cavern volume. For the full-scale cavern phase, the total height is 338 m with either a diameter of 33.6, in case of the 0.3 Mm<sup>3</sup> cavern volume, or 61.4 m, in



case of the 1.0 Mm<sup>3</sup> cavern volume, see also Table 4. In the pilot phase a single pipe element is used, whereas in case of the full-scale cavern phase the cavern is modelled with 2 pipe elements referred to as 'top' and 'bottom'.

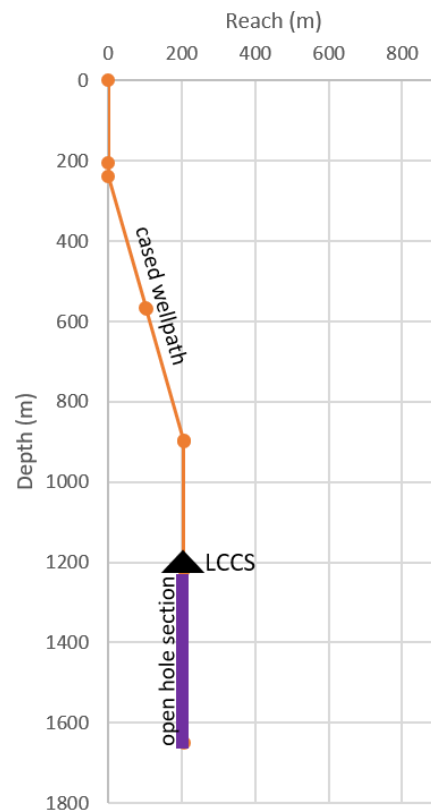


Figure 8: Visual representation of well path used in study

For the topside, 2 cells of approximately 10 m are used. For the well, the simulation cell length is at maximum 30 m, whereas for the cavern 5 cells are used for the pilot phase and for the full-scale cavern phase 5 cells for the top cavern part (9 m) and 11 for the bottom part (27 m). As the gradients in the topside part are large, some simulations were also performed with 4 cells of 5 m to check for consistency in the outflow results.

Table 4: Model parameters. (ID = Internal diameter; H = height; V = volume)

Parameter			
Tubing	ID = 0.2168 m		
Casing	ID = 0.316 m		
Cavern 'pilot'	H = 10 m	ID = 3.86 m	V = 117 m <sup>3</sup>
Cavern top 'full-scale'	H = 45 m	ID = 33.62 m	V = 40,000 m <sup>3</sup>
	H = 45 m	ID = 61.4 m	V = 133,000 m <sup>3</sup>
Cavern bottom 'full-scale'	H = 293 m	ID = 33.62 m	V = 260,000 m <sup>3</sup>
	H = 293 m	ID = 61.4 m	V = 867,000 m <sup>3</sup>
Cavern temperature	46.6 °C		
Topside temperature	10 °C		

### 3.1.3.3 Simulation cases

The outflow is studied for three leakage scenarios as discussed earlier in this section:

- Tubing leak: outflow through the tubing opening at the wellhead

- Casing leak: outflow through the casing opening at the wellhead
- Leakage through a small hole at or near the wellhead.

The tubing leak indicates a breach with the size of the tubing diameter and the casing leak indicates that the full tubing is lifted from the well. In case of a leak, the choke valve is not fully opened but is opened only until a leak size remains corresponding to a leak size of 1, 2, 3, 5 or 10 mm diameter. These scenarios are being studied for a pilot phase and full-scale cavern phase with either 0.3 Mm<sup>3</sup> or 1.0 Mm<sup>3</sup> volume.

Next to these scenarios several validations have been performed to assess the approach for this study and which include sensitivity towards the influence of:

- Choice of heat transfer methodology,
- Water saturation on the outflow, and
- Grid cell size.

For the modelling of the heat transfer two extremes can be chosen: adiabatic (no heat exchange, resulting in temperature change) or constant temperature. In case of outflow from a closed volume, the ideal gas law dictates that the temperature of the gas in the volume must decrease because the pressure decreases while the volume remains constant. This is a process independent of the Joule-Thompson (JT) effects of the gas. So even in case of hydrogen with inverse JT cooling, the hydrogen will cool down in the cavern. Heat transfer from the surrounding is in general a slower process, and for a pilot phase the assumption of adiabatic (no heat exchange) is therefore likely valid. However, for the full-scale cavern phase, the outflow period is long, and although the temperature of the gas will decrease due to expansion, it will also heat up due to exchange with the surrounding. To evaluate the sensitivity of the outflow on these extremes, two options have been studied as found in Appendix C, where one concerns a fully adiabatic situation and the other one a situation with a very high heat transfer coefficient for the cavern.

For this study on the outflow, dry hydrogen properties are being used. However, when brine is present in a cavern, hydrogen will become saturated with water (vapour) over a certain period of time. Under outflow conditions, i.e. pressure and temperature decrease, water potentially will condense out and influence the outflow.

For the presented cases of this study, only results obtained for dry hydrogen properties and a high heat transfer coefficient are shown and discussed and for the well path introduced earlier in this section. The sensitivity on heat transfer methodology, water saturation and grid size has been performed for a different well path. Therefore, Appendix B of this report discusses the differences in results obtained for the two well paths in order to conclude that these difference are minimal and that the sensitivity results of Appendix C obtained for the slightly different well path make sense for this study.

In Appendix C, the results obtained for the sensitivity analysis are presented and discussed. From the sensitivity analysis it is concluded that:

- The options for heat transfer methodology result in large differences in cavern and outflow temperatures but the effect on the mass outflow rate is minimal. In case of purely adiabatic flow (no heat exchange with the surroundings) the simulations show that the temperature of the hydrogen in the cavern drops to extremely low values of -150 to -200 °C. In the simulation representative of a pilot

phase with only a (very) small cavern this happens almost instantly, while for simulations representative of a full-scale cavern phase this happens gradually, reaching -150 °C after about 50 hours. When assuming a high heat transfer, the temperature of the hydrogen in the cavern remains fairly constant, with only a drop to about 0 °C immediately after the onset of outflow. A comparison of mass flows calculated with the adiabatic and high heat exchange assumptions shows that the differences in mass flows are small.

- The influence of the saturation of the hydrogen with water on the mass flows at outflow is small (less than 0.1%), although the numerical solutions become more unstable due to the effect of the choking (critical flow) behaviour in the well. The average outflow though is similar to the outflow obtained for dry hydrogen.

Therefore, the solutions generated with dry hydrogen and a high heat transfer coefficient are representative for more complex settings. Additionally, results have been obtained with a finer grid, and these do not differ much from the results obtained with the standard grid introduced earlier in this section. These additional results for a finer grid have been omitted from the sensitivity results found in Appendix C.

For the cases with high heat transfer and the well path shown in Figure 8, an overview is given in Table 5 of the outflow simulations relevant to be further discussed. In this table several settings define the specific simulations and these settings (which are also valid for and applied in Table 14 in Appendix B) are listed and explained below:

- **Sim name:** Concerns the simulation name *H2\_<number>\_<info>* and where *number* corresponds to the case number (see Table 2) and *info* refers to a setting for the heat transfer.
- **Phase:** Indicator for pilot phase or full-scale cavern phase.
- **Tubing/casing/leak:**
  - Tubing indicates that the flow path during blow-out is the tubing,
  - Casing indicates that it corresponds to the casing diameter,
  - Leak indicates that the valve is only partially opened resulting in a small leak size rather than a full breach.
- **Pressure:** Indicates the initial cavern pressure.
- **Volume:** Indicates cavern volume.
- **Leak size:** Indicates resulting leak size in case the valve is only partially opened.
- **Thermal:** Adiabatic indicates that the simulations are done at adiabatic conditions, whereas “U value” indicates that an effective heat transfer coefficient is used. In case of the marker
  - ‘\_U’ for the entire model a heat transfer coefficient of  $U = 9.5 \text{ W/m}^2\text{K}$  is used.
  - ‘\_U2’ a heat transfer coefficient ( $U = 1000 \text{ W/m}^2\text{K}$ ) at the cavern layers has been set such that the temperature is nearly constant for the fluid in the cavern.

Note that adiabatic is more appropriate for a pilot phase and ‘U2’ is more appropriate for a full-scale outflow when the outflow takes that long that heat transfer can occur in the cavern. However, the sensitivity analysis discussed in Appendix C revealed that there is not much difference for the mass outflow results.

- **Fluid:** Indicates that dry hydrogen properties are being used, whereas H<sub>2</sub>O saturated indicates that the fluid used was saturated at cavern conditions (at starting pressure and temperature).

Furthermore, the underscore ‘\_long’ indicates that the outflow is calculated for a long time, and which therefore not really captures the very first sharp peak in outflow but captures the long-term outflow. Results that have been obtained for the different simulations specified in the above table are discussed in section 3.2.1 and where for representation purposes the simulation names have been somewhat shortened.

Table 5: Simulation cases for well path shown in Figure 8

Simulation name	Phase	Outflow opening	Pressure [bar]	Volume [m <sup>3</sup> ]	Leak size [mm]	Thermal	Fluid
H2_1_U2	pilot	tubing	50	117		U value	dry
H2_2_U2	pilot	tubing	135	117		U value	dry
H2_3_U2	pilot	tubing	220	117		U value	dry
H2_4_U2	pilot	casing	50	117		U value	dry
H2_5_U2	pilot	casing	135	117		U value	dry
H2_6_U2	pilot	casing	220	117		U value	dry
H2_7_U2	pilot	leak	50	117	1, 2, 5, 10	U value	dry
H2_8_U2	pilot	leak	135	117	1, 2, 5, 10	U value	dry
H2_9_U2	pilot	leak	220	117	1, 2, 3, 5, 10	U value	dry
H2_11_long_U2	full-scale	tubing	135	3*10 <sup>5</sup>		U value	dry
H2_15_long_U2	full-scale	tubing	200	1*10 <sup>6</sup>		U value	dry

### 3.1.4 Physical effects modelling

With the use of results of the study on hydrogen outflow the following effects are studied:

- Plume formation of H<sub>2</sub> without ignition
- Jet fire and resulting heat flux for a direct ignition
- Explosion following a delayed ignition

The plume and jet fire are studied on basis of calculations with the HyRAM software as described in [Groth et al., 2015], whereas the explosion calculations are based on the BST-method described in [Sochet, 2010] and [Tang et al., 1999]. The most important characteristics of these calculations are found in the remainder of this section, whereas results obtained for different cases for the three effects are discussed in the next section.

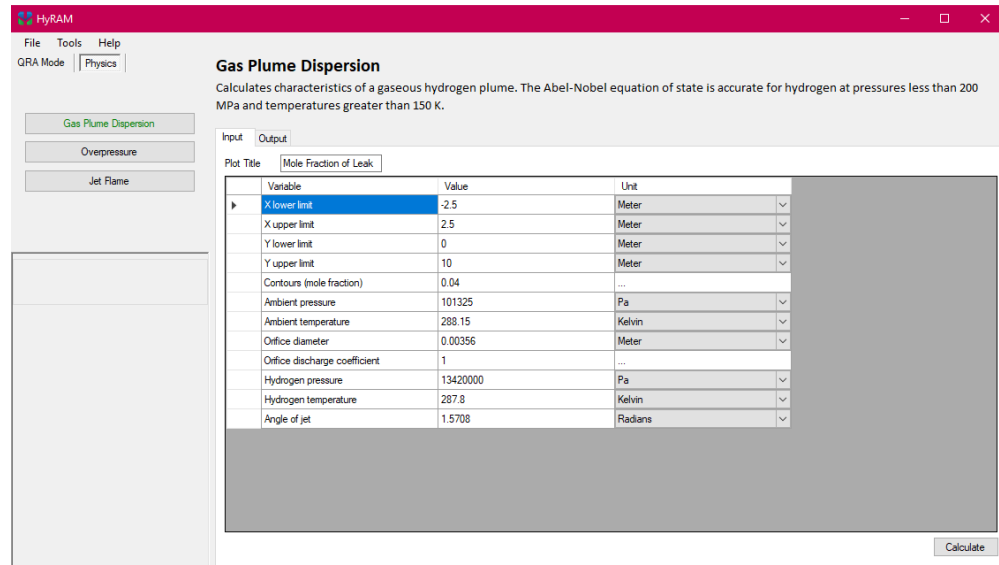
#### 3.1.4.1 HyRAM

The Hydrogen Risk Assessment Models (in short HyRAM) concerns a software tool that has been developed for assessing the safety of hydrogen fuelling and storage infrastructure. It has been developed by Sandia National Laboratories. It offers both a probabilistic approach and a deterministic approach. The latter option is used in the current study. The properties of the H<sub>2</sub> gas are described by the Abel-Noble equation of state [Groth et al., 2015]. This equation is valid for pressures lower than 200 MPa and temperatures above 150 K. The scenarios subject of this study fall within this validity range.

#### 3.1.4.2 Gas plume dispersion

To obtain results for the gas plume dispersion two calculations steps are performed, being the outflow through a nozzle and the mixing of air with the gas jet. When the pressure inside the tank/pipe is high enough, the flow through the exit is choked and will expand to atmospheric pressure through shocks in the outside atmosphere. These shocks are difficult to model in detail and for this reason the conservation of

mass and energy between the initial state and the expanded jet are used. Based on the conditions inside the tank/pipe, in such a way the velocity and temperature at the outside are determined.



**Gas Plume Dispersion**  
Calculates characteristics of a gaseous hydrogen plume. The Abel-Nobel equation of state is accurate for hydrogen at pressures less than 200 MPa and temperatures greater than 150 K.

Input Output

Plot Title Mole Fraction of Leak

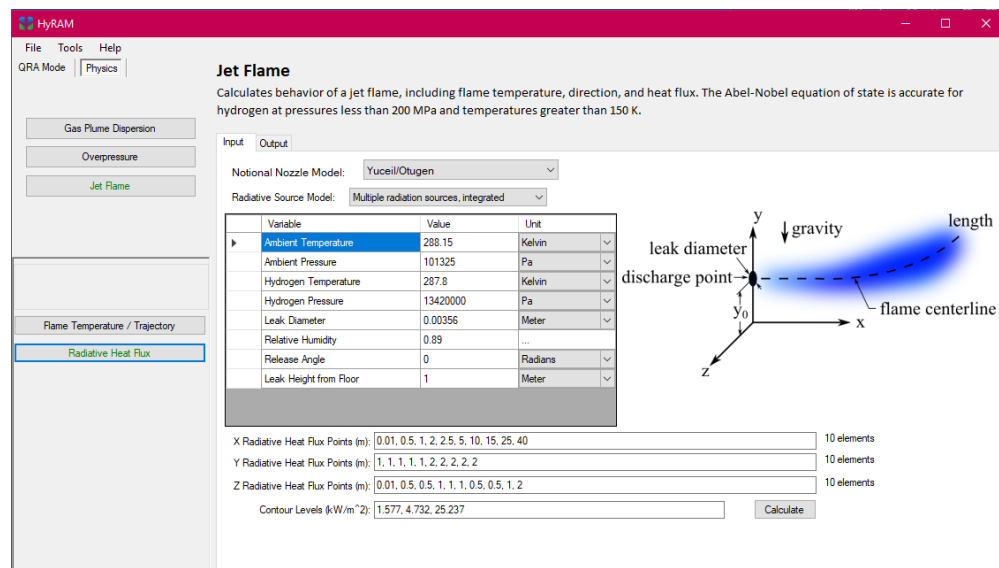
Variable	Value	Unit
X lower limit	-2.5	Meter
X upper limit	2.5	Meter
Y lower limit	0	Meter
Y upper limit	10	Meter
Contours (mole fraction)	0.04	...
Ambient pressure	101325	Pa
Ambient temperature	288.15	Kelvin
Orifice diameter	0.00356	Meter
Orifice discharge coefficient	1	...
Hydrogen pressure	13420000	Pa
Hydrogen temperature	287.8	Kelvin
Angle of jet	1.5708	Radians

Calculate

Figure 9: HyRAM user interface with input parameters for gas plume dispersion calculation.

After the jet has expanded to atmospheric pressure the surrounding air will start to mix with the hydrogen jet. This is done in the second step being the gas jet/plume calculation. It has to be noted that for this second step it is not possible to take the effect of atmospheric conditions (wind velocity, atmospheric stability) into account with HyRAM.

From the user interface with input parameters for the plume calculation in HyRAM, shown in Figure 9, several of the important parameters can be recognized. These parameters concern the  $H_2$  pressure and temperature, the orifice diameter and the outflow angle of the jet. An outflow angle of  $0^\circ$  means horizontal outflow, whereas an angle of  $90^\circ$  corresponds to a vertical outflow.



**Jet Flame**  
Calculates behavior of a jet flame, including flame temperature, direction, and heat flux. The Abel-Nobel equation of state is accurate for hydrogen at pressures less than 200 MPa and temperatures greater than 150 K.

Input Output

Notional Nozzle Model: Yuceil/Otugen

Radiative Source Model: Multiple radiation sources, integrated

Variable	Value	Unit
Ambient Temperature	288.15	Kelvin
Ambient Pressure	101325	Pa
Hydrogen Temperature	287.8	Kelvin
Hydrogen Pressure	13420000	Pa
Leak Diameter	0.00356	Meter
Relative Humidity	0.89	...
Release Angle	0	Radians
Leak Height from Floor	1	Meter

X Radiative Heat Flux Points (m): 0.01, 0.5, 1, 2, 2.5, 5, 10, 15, 25, 40 10 elements

Y Radiative Heat Flux Points (m): 1, 1, 1, 1, 2, 2, 2, 2 10 elements

Z Radiative Heat Flux Points (m): 0.01, 0.5, 0.5, 1, 1, 1, 0.5, 0.5, 1, 2 10 elements

Contour Levels ( $kW/m^2$ ): 1.577, 4.732, 25.237

Calculate

Diagram labels: leak diameter, discharge point, gravity, length, flame centerline, x, y, z,  $y_0$

Figure 10: HyRAM user interface with input parameters for jet flame calculation.

The output of the calculations is a contour plot of the hydrogen mole fraction, where the mole fraction of 4% is indicated by a white contour. This specific value represents the so-called Lower Explosion Limit for hydrogen-air mixtures.

#### 3.1.4.3 Jet fire

In our study, radiation is determined for a straight flame and which means that no influence of wind is taken into account. The user interface with input parameters for the jet fire calculation is shown in Figure 10 and from which it can be concluded that the same input as for the plume dispersion is required. In addition, though, some parameters for the output need to be specified and which e.g. concern several points (locations) for which the heat flux is calculated and specific values for the contour plots of heat flux. The values as applied for the current study are given in Table 6 and which are chosen on basis of [Veiligheidsregio Rotterdam-Rijnmond, 2013] for the first three values and of [PGS 3, 2005] for the last value.

Table 6: Values used for heat flux contour plots.

Heat flux level (kW/m <sup>2</sup> )	Description
1	Above this level the area should be evacuated.
3	Maximum level for long-term exposure for fire men
10	Cooling is needed to prevent spread of fire
35	100% lethal after 20 seconds exposure

#### 3.1.4.4 Explosions

Hydrogen can either ignite immediately upon release, or ignition can be somewhat delayed. Immediate ignition results in a jet fire or flame, whereas delayed ignition results in an explosion. The severity of such an explosion depends on the delay time, the mass released in the period until explosion, and the level of mixing with air. Together, these factors determine the size of the cloud and its concentration. Also, the amount of obstruction is important. In areas with little obstruction the explosive strength of a hydrogen cloud is lower than in areas with high congestion.

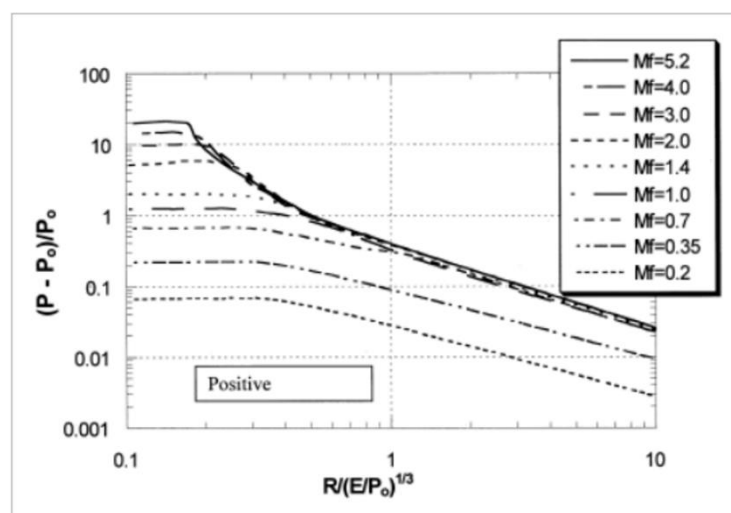


Figure 11: BST-curves representing scaled overpressure versus scaled distance. Diagram obtained from [Tang et al., 1999].

An ignition delay time of 3 seconds is assumed, i.e. the mass flow in the first 3 seconds of the release is taken as input for the explosion calculations. The explosion

effect has been determined using the BST-method described in [Sochet, 2010] and [Tang et al., 1999]. This is a multi-energy method in which the flame speed, expressed as the flame Mach number  $M_f$ , is used to obtain the properties of the blast wave. The effect of flame Mach number is shown in the different curves in Figure 11. The vertical axis represents the overpressure scaled with the ambient pressure, whereas the horizontal axis represents the distance scaled with the energy content of the cloud and the ambient pressure. At a certain scaled distance the curves for higher values for  $M_f$ , i.e. higher flame velocities, result in higher overpressures. This effect is most pronounced in the near-field, in the far-field the different curves collapse into a single curve for  $M_f$  values exceeding 0.7. It must be noted here that the effects of atmospheric mixing are not taken into account in this BST-method. Therefore, the concentration of hydrogen in the cloud is not explicitly included as a parameter in the calculation. The BST-method implicitly assumes that the mass in the cloud together with the size of the cloud result in a concentration that is between the Lower Explosion Limit and the Upper Explosion Limit.

The main input parameter for the explosion calculations is thus the mass in the hydrogen cloud after 3 seconds of delayed ignition. The outcome are the distances corresponding to certain overpressures values as listed in Table 7. Two publications have been used and which describe certain effects for these overpressure values: [Molkov et al., 2015 after Mannan, 2005] describes a study into the effects of hydrogen explosion on humans and buildings, whereas reference [Bevi, 2019] concerns safety norms from the Dutch government.

Table 7: Applicable overpressure values, 1<sup>st</sup> 4 columns: [Molkov et al., 2015 after Mannan, 2005]; last 2: [Bevi, 2019]

Molkov et al., 2015 after Mannan, 2005				Bevi, 2019	
Effect on humans	Overpressure (kPa)	Effect on buildings	Overpressure (kPa)	Effect	Overpressure (kPa)
1% lethality due to lung haemorrhage	100	Almost total destruction of house	34.5	100% lethality (in any case)	30 or more
1% eardrum rupture	16.5	Partial demolition of house	6.9	2.5% lethality (when inside) 0.0% lethality (in any other case)	10 or more. less than 30
No permanent damage	1.35	Minor damage to house	4.8	0% lethality (in any case)	10 or less

### 3.2 Discussion of study results

In this section the results of the study, for which the set-up was described in the previous section, are presented and discussed. First the results obtained with OLGA for the outflow of hydrogen are discussed. This is followed by the results obtained for plume and jet fire with HyRAM and the section concludes with a discussion of the results obtained from the explosion calculations.

### 3.2.1 Hydrogen outflow

As described in section 3.1.2 and 3.1.3 several cases have been simulated with OLGA among which for two different well paths. All simulations performed and main results obtained are provided in Appendix B and C. In this section the results for a selection of simulations found in Table 5, representative for all results obtained, are discussed. Here it has to be noted that for representation purposes the simulation names in the presentation of the results have been somewhat shortened.

In Figure 14 representative examples are given of the mass outflow rate for the pilot phase with a full tubing breach, the pilot phase with a small leak and a tubing breach at the full-scale cavern phase. A typical outflow consists of a sharp peak at opening of the valve followed by a gradual decline. The first sharp peak is a typical wellbore storage effect. This initial peak can for instance be observed in Figure 14 for case H2-11 (full-scale cavern phase). This initial sharp peak takes only 20 to 30 seconds after which the flow becomes more developed. For the developed flow, the mass flow rate outflow is limited by the frictional pressure drop and (frictional) choking occurring at the boundary or at the small leak. After the initial sharp peak, a normal depletion of the closed cavern follows. The depletion follows an exponential pressure decrease and shows a slow decrease in the outflow rate as can be observed in Figure 12 and Figure 14.

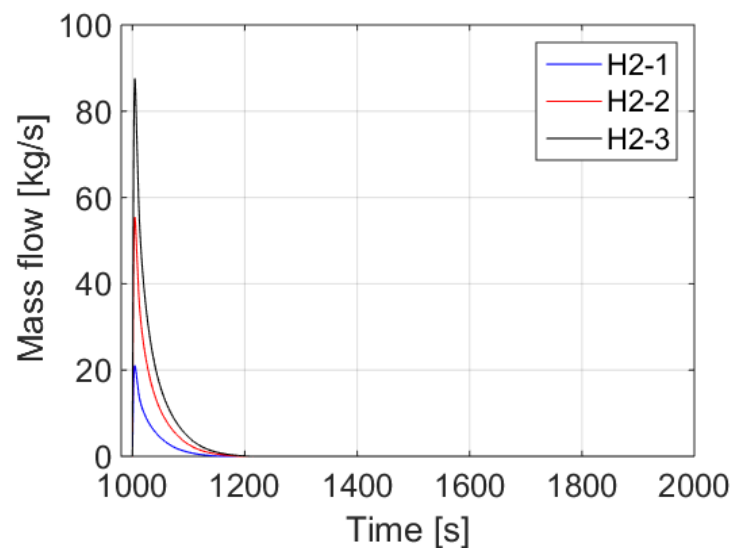




Figure 12: Mass flow rate as function of time for simulations H2-1, H2-2 and H2-3 (pilot phase, tubing leak, with 50, 135, 220 bar as starting pressure).

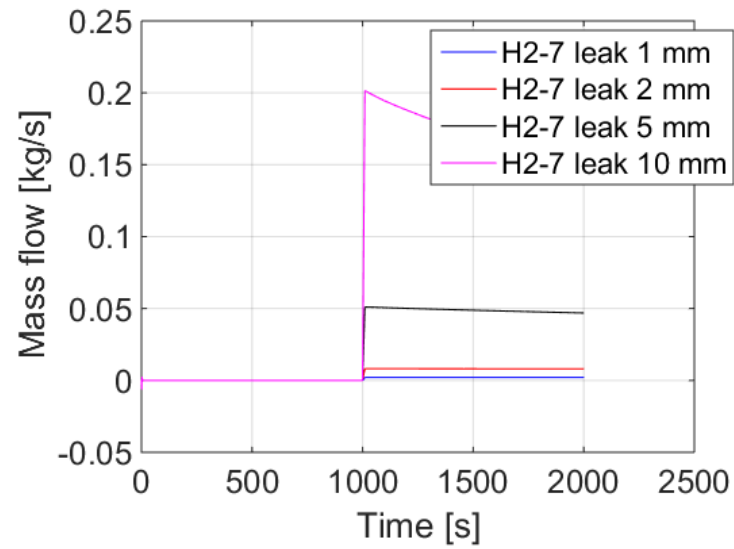
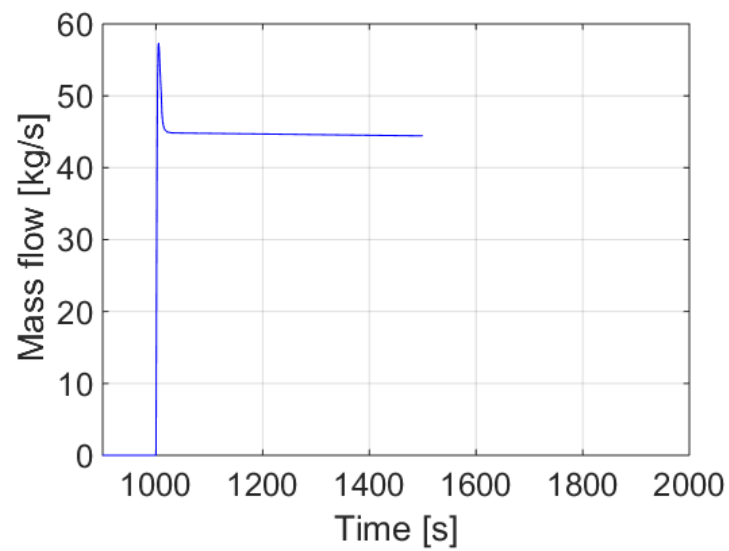


Figure 13: Mass flow rate as function of time for simulation H2-7 (pilot phase, leak holes, with 50 bar starting pressure).



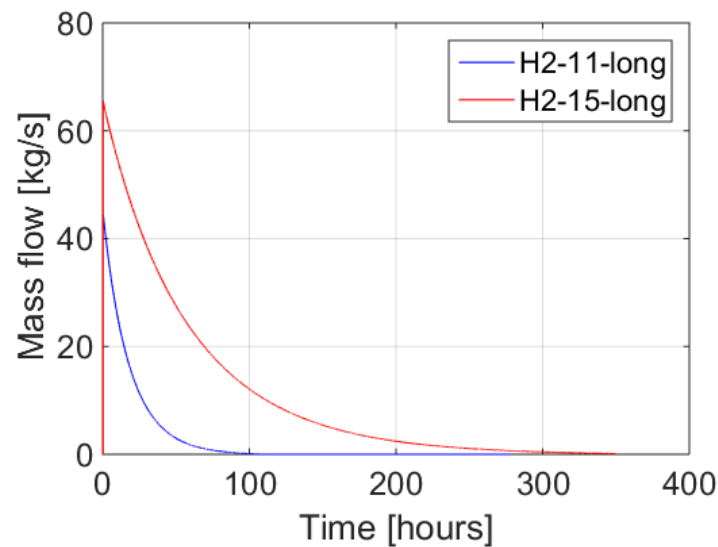


Figure 14: Mass flow rate as function of time for simulation H2-11\_long (full-scale cavern phase, 0.3 Mm<sup>3</sup>, tubing leak, with 135 bar starting pressure) and simulation H2-15\_long (full-scale cavern phase, 1 Mm<sup>3</sup>, tubing leak, and 200 bar starting pressure). Top figure zooms in at initial peak for H2-11.

As the outflow is governed by potential choking at the wellhead and by the frictional pressure drop in system, some trends are as expected, and which are:

- A higher initial pressure results in higher peak rates. For instance, in the pilot phase, the peak rates increase from 21 up to 87 kg/s with an increase in the cavern pressure from 50 to 220 bar.
- This outflow peak rate is basically independent on the cavern volume. The peak rate at the full volume (simulation H2-11) at 135 bar leads to an initial peak of 57 kg/s where the pilot phase reached up to 55 kg/s. The differences observed in these are due to the sharpness of the peak and due to the solution being solved in the simulation in steps of 1 seconds.
- Smaller leak sizes reduce the outflow significantly. At a tubing leak the outflow peaks at 21 kg/s (pilot phase, with 50 bar as starting pressure), whereas for a casing leak, the leak rate increases up to 38 kg/s. For small leaks (lower than 10 mm), the leak rates are limited to 0.2 kg/s (50 bar) and 0.9 kg/s (220 bar). As at these small leak sizes always critical flow occurs, this outflow scales with the leak size area. Note that for critical flow, the mass flow is restricted with a flow that is proportional to  $p \cdot c \cdot A$ , with  $p$  the upstream pressure,  $c$  the speed of sound and  $A$  the leak size area.
- Of course, larger volumes lead to longer depletion times. The depletion is defined here as the time for which the pressure in the cavern reaches 1.5 bar(a). In that case, the depletion is just 100 to 200 seconds for the pilot phase with tubing leak (as shown in Figure 12), but takes 311 hours for the largest cavern at the highest pressure (as shown in Figure 14).

A summary of peak rates and depletion times for selected cases is given in Table 8.

Table 8: Maximum leak rates and depletion times (pressure down to 2 bar)

Simulation name	Description	Depletion Time	Peak rates [kg/s]
-----------------	-------------	----------------	-------------------

H2-1	Pilot phase, tubing leak, starting pressure: 50 bar	124 s	21
H2-2	135 bar	158 s	55
H2-3	220 bar	175 s	87
H2-4	Pilot phase, casing leak, starting pressure: 50 bar	65 s	38
H2-5	135 bar	84 s	99
H2-6	220 bar	93 s	155
H2-7	Pilot phase, starting pressure 50 bar, leak size: 1 mm 2 mm 5 mm 10 mm		0.003 0.008 0.05 0.2
H2-8	Pilot phase, starting pressure 135 bar, leak size: 1 mm 2 mm 5 mm 10 mm		0.008 0.02 0.14 0.5
H2-9	Pilot phase, starting pressure 220 bar, leak size: 1 mm 2 mm 5 mm 10 mm		0.01 0.03 0.21 0.85
H2-11_long	Full-scale cavern phase, tubing leak, 0.3 Mm <sup>3</sup> cavern volume, starting pressure 135 bar	87 hr	57 45 (discounting initial peak)
H2-15_long	Full-scale cavern phase, tubing leak, 1 Mm <sup>3</sup> cavern volume, starting pressure 200 bar	311 hr	65 (discounting initial peak)

### 3.2.2 Plume formation

From the outflow simulation results discussed in the previous section as obtained with OLGA, the mass flow, pressure and temperature are used as important input for the gas plume calculations with HyRAM. The results obtained with these model calculations are discussed in the remainder of this section.

HyRAM calculates the mass flow rate from a tank based on its internal pressure and temperature. This is a different type of outflow than what is considered in case of a leakage of an underground cavern with piping. For this reason, the output data obtained with OLGA cannot be used directly as input for HyRAM. The pressure and temperature before the valve are used in combination with the mass flow rate. With this data, the outflow radius is therefore varied in HyRAM until the mass flow rate matches the one obtained with OLGA.

In Table 9, the input parameters for the plume and flame (jet fire) calculations are shown for the cases studied. It has to be noted that the values for the mass flow differ from the peak values reported for the corresponding outflow simulation in Table 8 and that we again refer to the case number as introduced in Table 2. As hydrogen is a flammable substance, this means that for a representative effect the first 20% of

mass outflow has to be taken. Over the related period of time the mass flow rate, pressure and temperature are averaged for the plume and jet calculation.

Table 9: HyRAM input parameters for the plume and jet calculations.

Case	$p_1$ ( $10^5$ Pa)	$T_1$ ( $^{\circ}$ C)	Diameter (m)	Mass flow (kg/s)
Case 1	24.9	-15	0.111	15.8
Case 2	66.4	-15	0.111	41.4
Case 3	107	-15	0.111	65.5
Case 7_10	49.6	10	0.01	0.24
Case 8_10	134	10	0.01	0.63
Case 9_1	218	10	0.001	0.010
Case 9_3	218	10	0.003	0.090
Case 9_5	218	10	0.005	0.25
Case 9_10	218	10	0.01	0.99
Case 10	8.6	14	0.204	17.6
Case 11	15.6	15	0.209	33.4
Case 12	22.8	16	0.208	48.1
Case 15	22.3	16	0.212	48.8

### 3.2.2.1 Pilot phase

For case 1 to 3 the resulting mole fraction distributions are displayed in Figure 15. It is observed that with increasing height, the  $H_2$  mole fraction decreases and which is a consequence of the mixing with air. The heights at which hydrogen content of the plume reaches the value of the Lower Explosion Limit (4% hydrogen) are 180 m, 290 m and 355 m, respectively. Furthermore, a higher cavern pressure comes with a higher mass outflow and therefore has a higher and wider plume as a consequence.

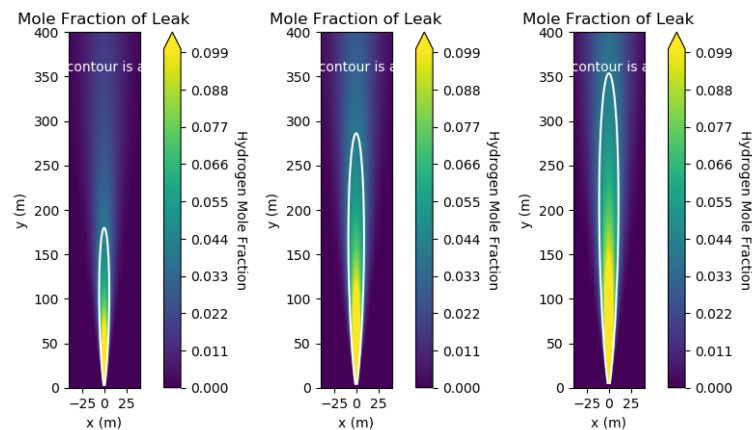


Figure 15: Hydrogen mole fraction for case 1, 2 and 3. The x-axis corresponds to the horizontal direction, whereas the y-axis corresponds to the vertical direction.

### 3.2.2.2 Full-scale cavern phase

The hydrogen plumes for cases 10, 11, 12 and 15 are shown in Figure 16, again via the distribution of the mole fraction. Here the same trend is visible for the height of the plume, i.e. the higher the cavern pressure, the higher the mass flow and the plume.

When compared to the plumes found for the pilot phase, it is clear that the plume for the full-scale cavern phase is lower. The reason behind this is that the pressure on which the outflow is based is lower for the full-scale cavern phase. For the pilot phase the pressure just before the valve decreases from initial pressure to atmospheric

pressure without reaching an equilibrium state. For the full-scale cavern phase the volume of the cavern is larger and therefore the pressure at the valve stabilizes at the value corresponding to the pressure drop over the valve. Hence, when averaged over the first 20% of mass outflow, the average pressure for the full-scale cavern phase is lower than the one for the pilot phase, leading to lower mass flow rates.

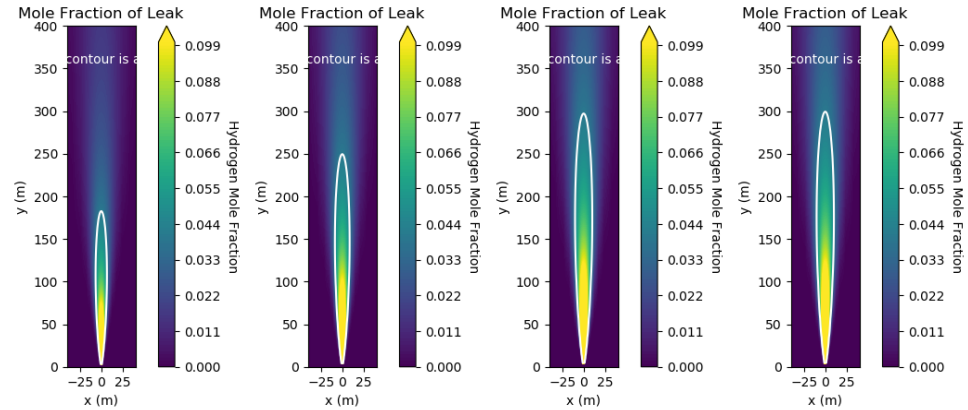


Figure 16: Hydrogen mole fraction for case 10, 11, 12 and 15. The x-axis corresponds to the horizontal direction, whereas the y-axis corresponds to the vertical direction.

### 3.2.2.3 Leakage

For the cases with leakage from the small cavern, the results are presented in two figures. Figure 17 shows the mole fraction distribution for case 9 with the leak sizes 1, 3 and 5 mm, whereas this distribution as obtained for the cases 7, 8 and 9 with leakage size of 10 mm is found in Figure 18.

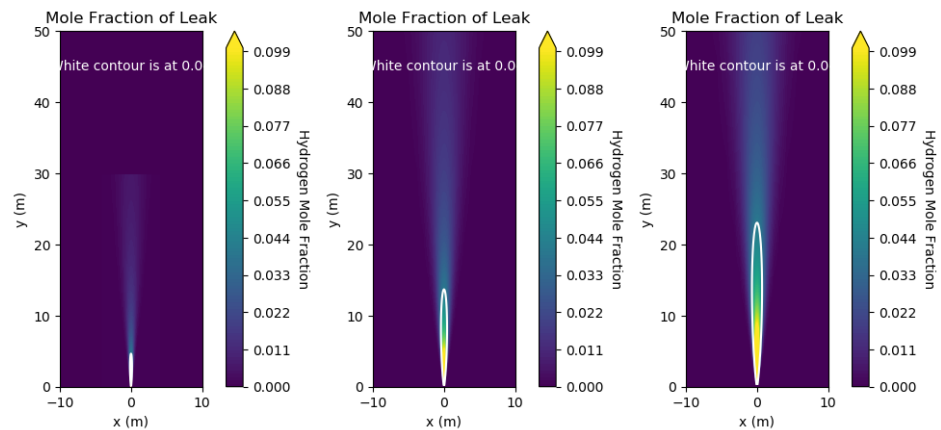


Figure 17: Hydrogen mole fraction for case 9, leak size 1, 3 and 5 mm. The x-axis corresponds to the horizontal direction, whereas the y-axis corresponds to the vertical direction.

When comparing these results with the ones provided in Figure 15 and Figure 16, it is observed that the plume heights for the cases with outflow through leaks are substantially smaller than those for outflow through the tubing. This is due to the significantly lower mass outflow. Furthermore, larger leakage sizes and higher cavern pressure also result in larger mass outflows and thus larger plume heights.

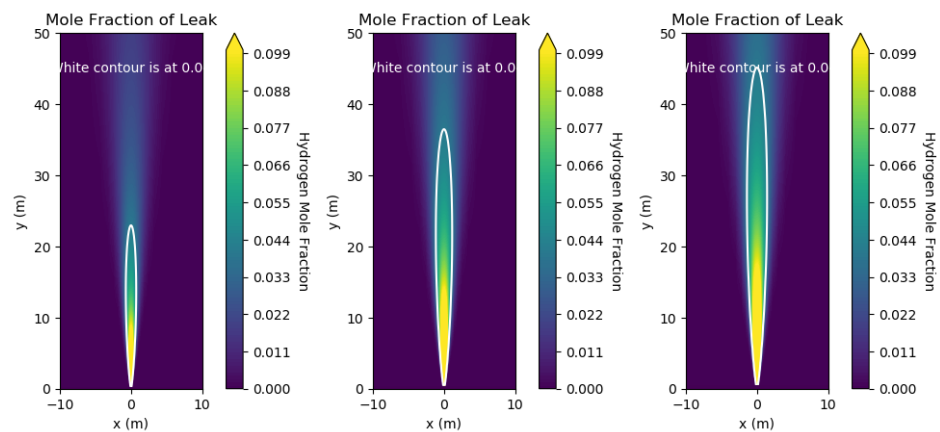


Figure 18: Hydrogen mole fraction for cases 7, 8 and 9 with leak size 10 mm. The x-axis corresponds to the horizontal direction, whereas the y-axis corresponds to the vertical direction.

### 3.2.3 Jet fire

The outflow results as discussed in the previous section, serve as input for the jet fire calculations with HyRAM. The results obtained are subject of this section.

#### 3.2.3.1 Pilot phase

For the pilot phase, i.e. cases 1-3, the calculated flame temperatures in K are shown in Figure 19. The blue/purple colour here indicates (relatively) low temperatures, whereas yellow indicates a high temperature. It is observed that a higher cavern pressure results in a higher and wider flame.

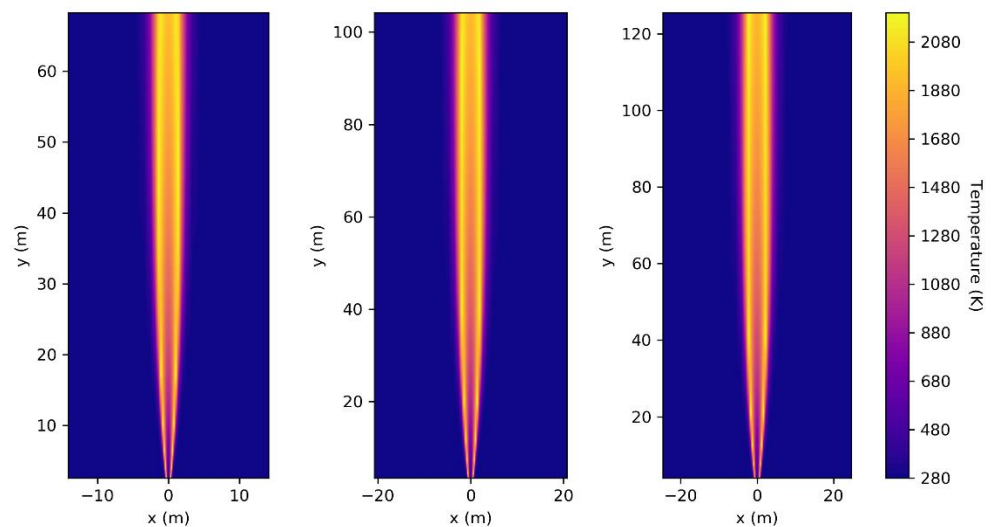


Figure 19: Flame temperature for case 1, 2 and 3. The x-axis corresponds to the horizontal direction, whereas the y-axis corresponds to the vertical direction.

Near the outflow at the bottom, it can be seen that only the outer layer of the flame is well mixed and has a high temperature. With increasing height the entire flame becomes well mixed and has a high temperature.

From the flame temperature the heat flux is determined and for case 1 this flux is provided in Figure 20. Two vertical cross sections through the centre of the flame are shown in the top part, whereas at the bottom a horizontal cross section is shown.

This cross section is taken at the height for which the heat flux contours are widest. At ground level the contours are slightly smaller. Please note that the border between the green area and the white area corresponds to the evacuation distance.

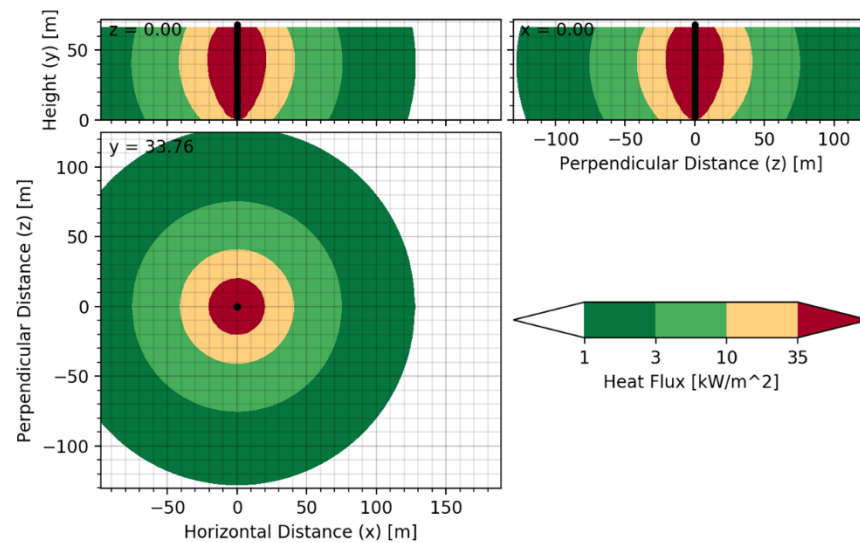


Figure 20: Heat flux contours for case 1. At the top two vertical cross sections through the centre of the flame are shown. At the bottom a horizontal cross section at the height for which the contours are widest is shown. The legend for the colours uses the values from Table 6. The x- and z-axes correspond to the horizontal directions, the y-axis represents the height/vertical direction.

For the pilot phase cases 1, 2, and 3 a horizontal cross section of the heat flux is shown in Figure 21. All these cross sections are not at ground level. From the figure it is clear that with increasing cavern pressure the heat flux contours become wider and the evacuation distance increases.

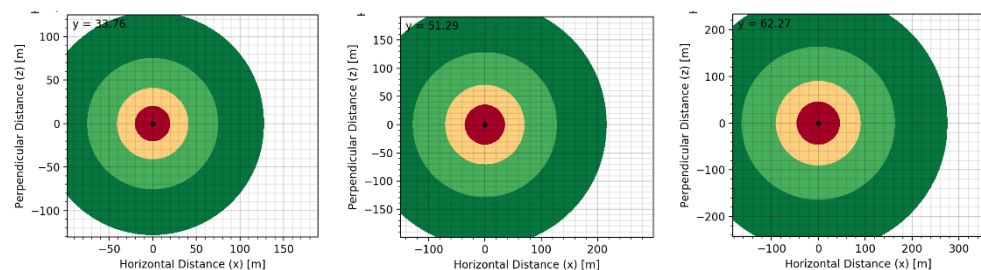


Figure 21: Heat flux contours for cases 1, 2, and 3. The contour levels are explained in Table 6.

A more quantitative representation of the heat flux results for the pilot phase (cases 1-3) is found in Figure 22. It shows the heat flux on a logarithmic scale at 1.5 m height above ground as function of distance from the outflow opening. The horizontal lines indicate the heat flux levels from Table 6. The evacuation distance ranges from 120 m for case 1 to 260 m for case 3. The 10 kW/m<sup>2</sup> contour, above which cooling is required to prevent the fire from spreading, is at 25 m for case 1 and at 65 m for case 3.

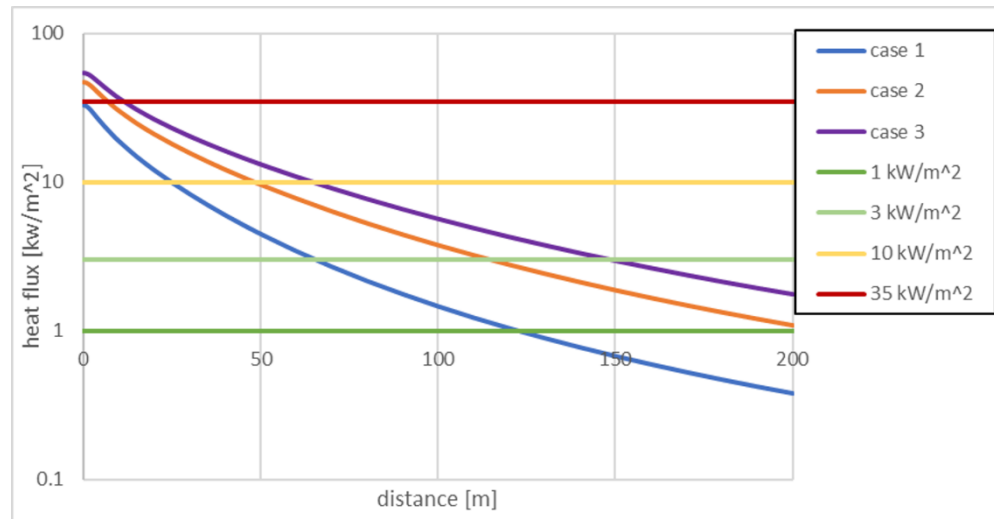


Figure 22: Heat flux at 1.5 m height vs. distance for cases 1, 2 and 3. The horizontal lines correspond to the values from Table 6.

### 3.2.3.2 Full-scale cavern phase

For cases 10, 11, 12 and 15, only heat flux data is shown and the flame temperatures are omitted, because these are very similar to the results for case 1 to 3 and do not add extra information. The heat flux as a function of distance is shown in Figure 23, where the curve for case 15 almost coincides with the one for case 12. The evacuation distance is 130 m, 185 m and 220 m for case 10, 11, and 12 & 15, respectively.

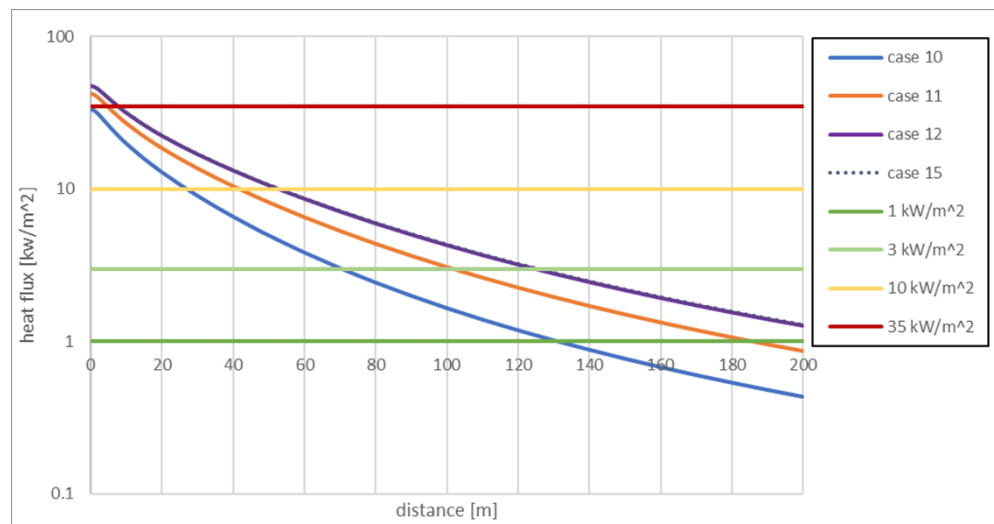


Figure 23: Heat flux vs. distance for cases 10, 11, 12 and 15. The horizontal lines correspond to the values from Table 6.

The value of 220 m for case 12 & 15 is less than the value of 260 m found for case 3 (pilot-phase). This is mainly due to the lower initial pressure inside the cavern. A second reason concerns the fact that for the larger cavern the mass flow rate stabilizes after an initial high peak. This results in a lower average mass outflow and hence in a smaller jet fire and lower heat flux for a certain distance.



It has to be noted that in the relation between heat flux and damage (represented by several heat flux levels) also the exposure time is important. Especially as the time scale for the outflow for the pilot phase cases is in the order of minutes, whereas for the full cavern phase cases it is in the order of 100 hours. The heat flux levels reported in this section occur directly at the start of the outflow of the hydrogen. As the outflow continues, the mass flow rate decreases and also the heat flux from the flame decreases. The time scale for the maximum heat flux at a certain location is minutes for the pilot phase cases and in the order of hours for the full cavern phase cases. This difference in time scale may therefore affect the appropriate measures that need to be taken in response to the occurrence of a hydrogen flame.

Next to display of the results in Figure 23, all relevant values for these cases are found in Table 10.

### 3.2.3.3 Leakage

The heat flux as a function of distance for the defined leakage cases is shown in Figure 24 and Figure 25. From these figures it is observed that the highest heat flux is found for case 9 with a 10 mm leak size. This is the only case for which a value of 10 kW/m<sup>2</sup> is found and all other cases have heat fluxes below this value.

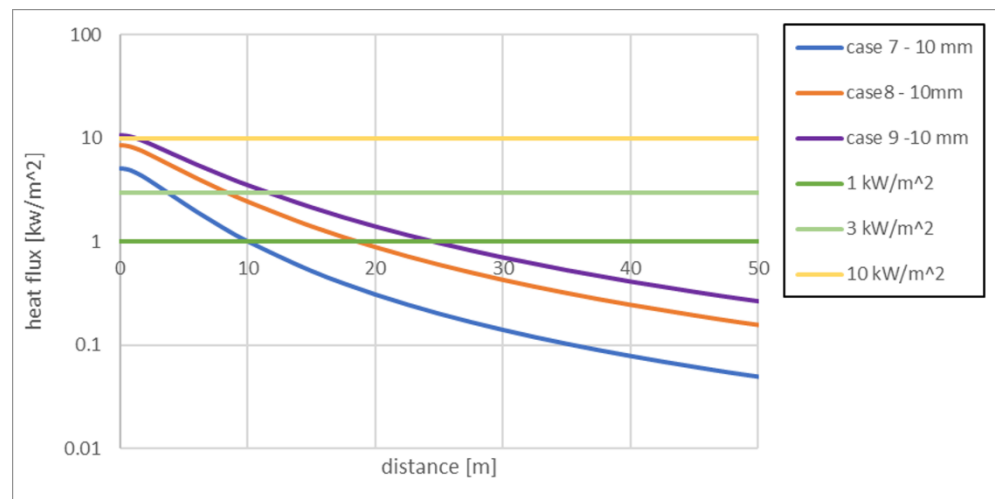


Figure 24: Heat flux vs. distance for cases 7, 8, and 9 with 10 mm leakage. The horizontal lines correspond to the values from Table 6.

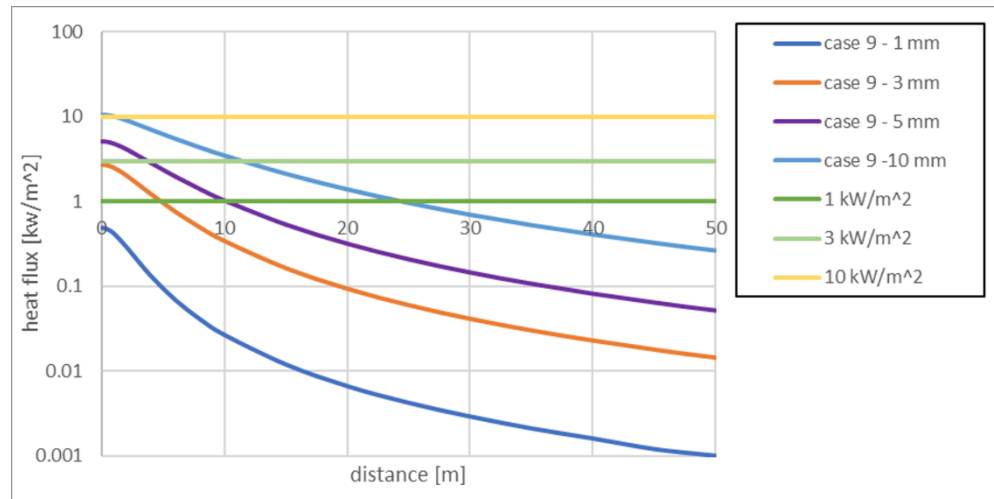


Figure 25: Heat flux vs. distance for case 9, with leak sizes 1, 3, 5 and 10 mm. The horizontal lines correspond to the values from Table 6.

#### 3.2.3.4 Summarizing table with results

The effect distances obtained for all cases are shown in Table 10 and where background colours of the columns correspond to the colours as applied in Table 6.

Table 10: Effect distances (in m) for heat flux. Interpretation of heat flux values is given in Table 6.

Heat flux	Effect on humans			
	1 kW/m <sup>2</sup>	3 kW/m <sup>2</sup>	10 kW/m <sup>2</sup>	35 kW/m <sup>2</sup>
Case 1	120	65	25	-
Case 2	200	115	50	6
Case 3	260	150	65	12
Case 9_10	25	12	1	-
Case 10	130	70	27	-
Case 11	185	100	42	5
Case 12	220	125	50	7
Case 15	220	125	50	7

#### 3.2.4 Explosion

The results for mass outflow from the cavern in the first few seconds as determined with OLGA in the outflow study (see section 3.2.1) are used to determine the explosive mass in the hydrogen cloud. A delayed ignition time of 3 seconds is assumed for this. The mass values used for the specific cases studied are given in Table 11 and which values are multiplied by a factor two to take into account the effect of ground reflection. The BST method is then used to obtain the distances corresponding to certain overpressure values.

Table 11: Input parameters for explosion calculations.

Case	H <sub>2</sub> mass in cloud (kg)
Case 1	62
Case 2	163
Case 3	259
Case 7_10	0.72
Case 8_10	1.89
Case 9_1	0.03
Case 9_3	0.27

Case 9_5	0.75
Case 9_10	2.98
Case 10	87
Case 11	165
Case 12	269
Case 15	242

In Table 7 several overpressure values of interest are presented, and in what follows the corresponding effect distances are further discussed. The effect distances for all cases are shown in Table 12. Two parameters determine the initial outflow and which are initial cavern pressure and the outflow area. And because of this both case 2 and 11, and case 12 and 15, have identical effect distances. From the data in the table it is seen that a higher cavern pressure leads to a higher mass outflow and results in more mass in the explosive cloud with larger effect distances as a consequence. The cases with leak outflow result in a smaller explosive cloud and thus in significantly smaller effect distances and only one such case is therefore listed in the table.

By comparing all summarized results from Table 12 as obtained for explosive overpressure with those obtained for the heat flux and summarized in Table 10, it is concluded that the effect of an explosion reaches further than the heat flux effects of a jet flame.

Table 12: Effect distances (in m) for explosions. The interpretation of the overpressure values is given in Table 7

	Molkov et al., 2015 after Mannan, 2005						BEVI, 2019	
	Effect on humans			Effect on buildings			Effect on humans	
Overpressure	1.35 kPa	16.5 kPa	100 kPa	4.8 kPa	6.9 kPa	34.5 kPa	10 kPa	30 kPa
Case 1	640	110	27	320	210	55	160	65
Case 2	880	150	37	440	290	75	220	90
Case 3	1020	170	43	510	340	85	255	100
Case 9_10	230	40	10	120	80	20	60	25
Case 10	710	120	30	360	240	60	180	70
Case 11	880	150	37	440	290	75	220	90
Case 12	1000	170	42	500	330	85	250	100
Case 15	1000	170	42	500	330	85	250	100

One of the assumptions for this explosion study is the delayed ignition time and for which a value of 3 seconds is used. A smaller or higher value will lead to smaller or larger effect distances, respectively. The upper limit is found for a steady state for which the content of the explosive cloud is constant in time, i.e. the amount of hydrogen added to the explosive cloud through outflow is equal to the removal of hydrogen from the explosive cloud through diluting with the surrounding air.

Based on the used methods for this report this upper limit of the explosive cloud size cannot be determined. For this reason the effect of the delay time on the effect distance (which is in the BST method scaled with the mass<sup>1/3</sup>) has been studied and the results are shown in Figure 26. Here, the effect distance for 3 seconds is used for normalisation. It is observed that an increase in delay time to 5 seconds results in 19% larger effect distances, whereas decreasing the delay time to 1 second results in 31% smaller effect distances.

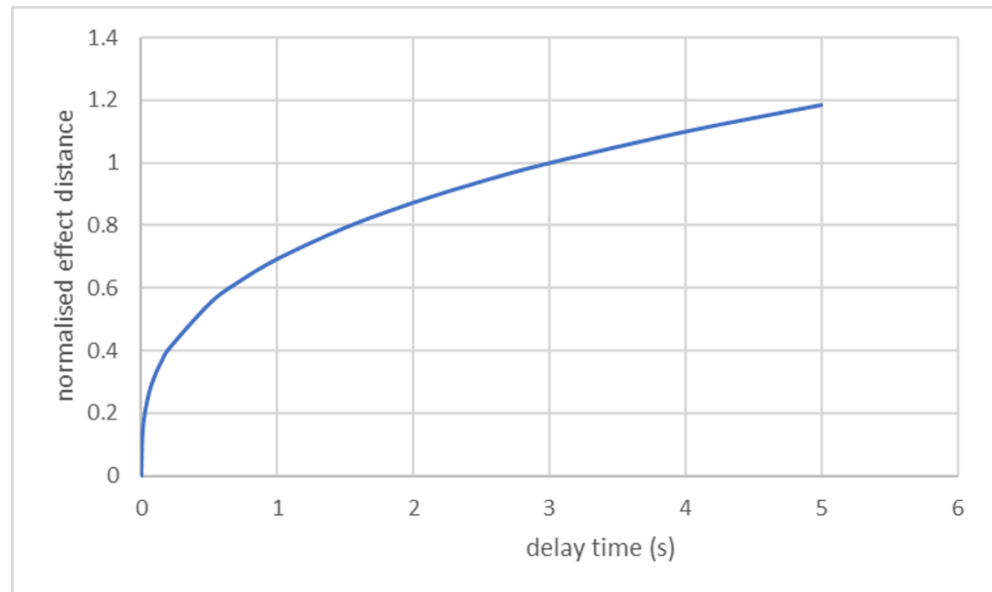


Figure 26: Normalised effect distance as a function of detonation delay time.

It has to be noted that for this explosion study a conservative approach has been chosen as e.g. for the flame Mach number the highest possible value is used. For an outflow that is unobstructed, therefore with little congestion, the Mach flame number can be smaller and which will reduce at least the near field effects. In addition, the cloud shape is assumed to be hemispherical at ground level, whereas in reality it will be more plume shaped with a certain elevation above the ground. Furthermore, the ground reflection effects may be smaller than the factor 2 that is taken into account in this study. Finally, it must be noted that the effects of atmospheric mixing are not taken into account. For further insight into the effects of atmospheric mixing on the shape, concentration and lift-off of the evolving hydrogen cloud, and how this influences the impact of a potential explosion, a more sophisticated method for explosion calculations has to be used.

## 4 Conclusions

In this study a BowTie analysis was performed for hydrogen storage in a salt cavern and physical effects of hydrogen release at the wellhead were quantified. The study, based on a notional design of a subsurface storage system introduced in section 2.2, was generic and did not consist of a location-specific evaluation. It has to be noted that the results from our analyses and models may be different when applied to a specific location, depending on the local situation and the cavern and well design criteria at the location. In the next two sections, the conclusions of both parts of the study are summarized, whereas this chapter concludes with a section where several recommendations for further research are provided.

### 4.1 BowTie analysis for hydrogen storage in a salt cavern

The BowTie analysis has resulted in the identification of threats that may jeopardize the integrity of a hydrogen storage system and possible consequences when leakage of hydrogen occurs. In total, on the left side of the BowTie diagram, 23 unique threats were identified, of which 16 may cause leakage of hydrogen in the subsurface when they occur, and 7 may cause release of hydrogen at the surface (above-ground). Most threats (15) pertain to integrity failure of the well (or wellhead) in one way or another (materials, components, interfaces), while only a few (4) are directly related to integrity failure of the cavern. As such, it can be concluded that the well is the most critical component of the storage system.

To prevent the identified threats from leading to damage, 69 unique barriers were identified that can be grouped into 6 types: material selection (9 barriers), design (21 barriers), test (6), protection (4), control (11) and monitoring (18). While most barriers in the first 5 groups are applied pre-operation, most if not all barriers of type “monitoring” are applied during operation. For some threats tests during a pilot phase provide an opportunity to gauge their significance in terms of risk level. These threats concern e.g. (i) “hydrogen dissolved in brine coming to surface during debrining”; (ii) the occurrence of large sub-zero temperatures while withdrawing; and (iii) the threats that are posed by geochemical and microbiological reactions (in particular the formation of highly-corrosive hydrogen sulphide). Likewise, for some barriers a pilot phase provide an opportunity to determine their significance. such as the Mechanical Integrity Test with hydrogen, the debrining procedure, and all barriers related to selection of materials, components and equipment. A pilot-phase allows for gaining experience under controlled conditions with significantly lower risks compared to a full-scale cavern phase. This is because of the small volume of hydrogen used and the fact that the test is done in isolation on a wellpad in an open field at considerable distance from infrastructure and not connected to above-ground facilities.

On the right side of the BowTie diagram, 7 consequences of leakage were identified, of which 2 relate to leakage of hydrogen in the subsurface, and 5 to leakage above-ground. In particular for above-ground leakage, fire or explosion stands out in terms of the ultimate consequence of injury or death. Here note that fire and explosion are both included as consequences as well in the BowTie diagram. In contrast, for below-ground leakage, the consequences appear to be less severe and also less probable for two reasons:

1. Shallow groundwater pollution would only occur when the leaked hydrogen actually reaches the shallow subsurface, whereby the location (depth) of the leak in the subsurface is an important factor;
2. The potential for explosion of hydrogen accumulating in the (shallow) subsurface must be deemed low.

To limit the (ultimate) consequences of leakage, 12 mitigation, 1 recovery, 1 remediation and 3 monitoring measures were identified. Measures to mitigate the consequences of leakage include amongst others minimizing the presence of humans and animals in the vicinity of the site, executing plans for responding to emergencies, and preventing leakage to actually cause fire and/or explosion. Recovery here is limited to locating the leak and repairing it, while this can be difficult especially in the full-scale cavern phase in case of fire or extreme noise (at high flow rate). Remediation relates to cleaning-up pollution of the soil and drinking water. Of the monitoring measures, the installation of leakage detection and gas presence monitoring equipment (at surface, in soil) is most effective in mitigating the consequences of leakage, in particular above-ground, because it allows early response.

#### **4.2 Physical effects of accidental hydrogen release at the wellhead**

A study was performed on the duration and rate of outflow of hydrogen from the tubing, casing, or from a small hole at or near the wellhead to the surface. The results obtained were subsequently used to study the physical effects that (may) occur when such H<sub>2</sub> leakage takes place, in particular those associated with gas plume formation (without ignition), formation of a jet flame and resulting heat flux (on direct ignition), and explosion (following a delayed ignition).

For the outflow study it is concluded that:

- Peak outflow rates are reached almost immediately after onset of outflow and decline afterwards due to pressure decrease in the storage.
- Outflow rates increase with the size of the outflow (leak) opening and initial storage pressure in the cavern (before release), but are not sensitive to the cavern volume.
- For the pilot phase scenarios, outflow rates are highest for the cases with the maximum storage pressure of 220 bar and outflow through tubing (87 kg/s) and casing (155 kg/s), respectively. Outflow rates for leaks from the cavern (sizes between 1-10 mm) are 2 orders of magnitude lower (range of 0.003-0.87 kg/s).
- For the full-scale cavern scenarios, a similar pattern is found. Peak outflow rates though are slightly lower (in the order of 5-10 kg/s) because of the 20 bar lower initial storage pressure.
- The duration of outflow depends on cavern volume and flow rate. For the pilot phase scenarios, outflow durations range between 124-175 seconds (2-3 minutes) for outflow through the tubing, and between 65-93 seconds (1-2 minutes) for outflow through the casing. In contrast, outflow durations in the full-scale cavern scenarios are much longer, for example in the scenario with a cavern volume of 1 Mm<sup>3</sup> and initial storage pressure of 200 bar the outflow lasts for 311 hours (13 days) before the pressure in the cavern can no longer sustain further outflow.
- In the pilot phase scenarios, for which the flow from the cavern to the surface is expected to behave more or less adiabatically (very small volume and very

limited time for exchange of heat with surrounding), the temperature of the hydrogen in the cavern drops to very low temperatures, i.e., -150 to -200 °C. However, this does not significantly influence outflow rates.

- The outflow rates of hydrogen obtained are not significantly influenced by water saturation.

For the subsequent study on the physical effects the following is concluded:

- Upon release, the height and width of the hydrogen plume that forms depend on outflow rate (which itself depends on storage pressure and hole size). For the pilot phase scenarios with outflow through the tubing, the maximum plume height reached is 355 m, and the maximum width is about 50 m. With increasing height, the H<sub>2</sub> content decreases due to the mixing with air.
- For the scenarios studied with leaks from the cavern of different small sizes (1-10 mm), plume heights are substantially lower (up to 40-50 m high) than for the outflow through the tubing or the casing. Clearly, larger hole sizes result in larger plume heights and higher storage pressures also result in larger plume heights.
- Higher and wider plumes result in higher and wider jet flames. Consequently, the heat flux is larger and therefore the effect contours become wider and the evacuation distance increases. In the pilot phase scenarios, the evacuation distance (for a heat flux of 1 kW/m<sup>2</sup>) ranges from 120 m at 50 bar initial storage pressure to 260 m at 220 bar initial storage pressure. The 10 kW contour, above which cooling is required to prevent the fire from spreading, is at 25 m for the 50 bar pressure scenario, and at 65 m for the 220 bar pressure scenario. In the full-scale cavern scenarios, the effect distances for heat radiation are slightly lower due to the 20 bar lower initial storage pressure. However, while the heat radiation effects only last a couple of minutes in the pilot phase scenarios, they last much longer in the full-scale cavern phase scenarios and this has not been taken into account in the calculations.
- Higher and wider plumes also lead to the formation of a (potentially) explosive cloud with more mass. Radii of the (circular) effect contours for explosive overpressure reach further than the contours for heat flux. This shows that the overpressure effects of an explosion reach further than the heat flux effects of a jet flame. A leak outflow results in a smaller explosive cloud and thus to significantly smaller effect distances.
- Explosion effect contours for both the pilot and the full-scale cavern phase scenarios range between 700-1000 m for overpressure levels (1.35 kPa) where no harm to humans is expected, and between 300-500 m for overpressure levels (4.8 kPa) where no damage to buildings is expected. Explosion effect contours for overpressure levels from [Bevi, 2019] of 10kPa (elevated risk of lethality only when inside) and 30kPa (100% risk of lethality in any case) range between 160-255 m and 65-100 m, respectively.
- An important assumption for the explosion calculations concerns the delayed ignition time. Here, a delay time of 3 seconds has been used as the baseline. A further analysis indicated for an increase in the delay time to 5 seconds effect distances that are 19% larger, whereas for a decrease in the delay time to 1 second effect distances are 31% smaller.

It has to be noted that the modelling performed for the studies comes with several assumptions. For a future follow-up study, it is recommended to include atmospheric effects to improve the accuracy of the plume shape and jet flames. Furthermore, for improved explosion modelling, the shape of the hydrogen cloud needs to be taken

into account, and more research must be done to accurately determine the expected delay in ignition (detonation).

### 4.3 Recommendations

To reduce the risks associated with underground hydrogen storage in salt caverns further research is recommended to focus on the following six topics:

- Effects of (long-term) exposure of well materials & interfaces to hydrogen under fast-cyclic pressure and temperature changes, to answer research questions like:
  - Will the integrity and/or durability of steels (embrittlement, corrosion), elastomers (hydrogen permeation), and cements (reactions with hydrogen) degrade?
  - Will the integrity and/or durability of interfaces between rock, cement and casing at LCCS degrade. And what is the associated risk of formation of leakage pathways for hydrogen, and what leakage rates can be expected?
- Effects of interactions of hydrogen with minerals and microbes in sump (insoluble at bottom of cavern) and brine in cavern, with the following research questions:
  - Will loss of hydrogen and/or contamination of hydrogen, such as with hydrogen sulphide, occur due to reactions (geochemical, microbiological)?
  - Will hydrogen dissolve into brine and how much? And to what extent will it come to surface when debrining?
- Effects of fast-cyclic pressure and temperature changes on tightness of salt, cavern integrity, and creep behavior, and where the research questions are:
  - How does this affect the width of the damage zone around the cavern, and is there a significant risk of leakage?
  - Does it impact cavern convergence rate and, consequently, subsidence?
- Quantification of risks and risk management, with the following focus. While further practical conclusions may be drawn executing a pilot phase (and from a full-cavern demonstration phase after a successful pilot phase) from the results obtained in this study, it is recommended to perform a full QRA with appropriate models. When performing such a study it is recommended to check whether the standard models that are used are sufficient appropriate for application for hydrogen. In particular the models for heat radiation of a hydrogen flame may have to be checked as hydrogen has a significantly lower surface emissive power than hydrocarbons. In the context of such a QRA, it is recommended to review which failure scenarios are most relevant, and what mitigation and monitoring measures can be put in place to minimize their risk of occurrence.
- Compatibility of equipment and procedures (such as compressors, piping, gas cleaners, and workover) and in particular those, such as for snubbing, that are standard in natural gas storage. The risks associated with those procedures, and mitigations, require further study to derisk their use for hydrogen storage.
- In our study we did not take into account the (additional) risks posed by activities in the direct surroundings of a cavern used for hydrogen storage, such as salt mining, storage of natural gas or compressed air, and storage of hydrogen in other caverns. Nor did we take into account the (additional) risk associated with collateral damage to facilities for such activities. While the results of this study provide insights into safety distances between activities to minimize the risk of collateral damage, it is recommended to further study the additional risks posed by surrounding activities.



## 5 References

Berta, M., Dethlefsen, F., Ebert, M., Schäfer, D., and Dahmke, A., 2018. Geochemical effects of millimolar hydrogen concentrations in groundwater: an experimental study in the context of subsurface hydrogen storage. *Environmental science & technology*, 52(8), 4937-4949.

Bevi, 2019. Handleiding Risicoberekeningen Bevi, versie 4.1 (1 oktober 2019)

Chabab, S., Théveneau, P., Coquelet, C., Corvisier, J., Paricaud, P., 2020. Measurements and predictive models of high-pressure H<sub>2</sub> solubility in brine (H<sub>2</sub>O+NaCl) for underground hydrogen storage application, *International Journal of Hydrogen Energy*, Volume 45, Issue 56, Pages 32206-32220

DBIGUT, 2017. The effects of hydrogen injection in natural gas networks for the Dutch underground storages. Publication number: RVO-079-1701/RP-DUZA

Evans, D.J., 2008. Accidents at UFS sites and risk relative to other areas of the energy supply chain, with particular reference to salt cavern storage. British Geological Survey, Nottingham, England. SMRI Fall 2008 Technical Conference, 13-14 October 2008, Galveston, Texas, USA.

Gonzalez-Diez, N., van der Meer, S., Bonetto, J., and Herwijn, A., 2020. North Sea Energy D3.1 Technical assessment of Hydrogen transport, compression, processing offshore. As part of Topsector Energy. <https://north-sea-energy.eu/static/ebe3cf344f4686a54a40de0d7ad1fe79/5.-FINAL-NSE3-D3.1-Final-report-technical-assessment-of-Hydrogen-transport-compression-processing-offshore.pdf>

Groth, K.M., Hecht, E.S., and Reynolds, J.T., 2015. Methodology for assessing the safety of Hydrogen Systems: HyRAM 1.0 technical reference manual, Sandia Report SAND2015-10216.

H2Tools, <https://h2tools.org>, page visited in December 2020

Hyde, K., and Ellis, A., 2019. Feasibility of hydrogen bunkering. Interreg North Sea Region Dual Ports.

Keeley, D., 2008. Failure rates for underground gas storage. Significance for land use planning assessments. Health and Safety Executive.

Koelewijn, R., van Dam, M., and Hulsbosch-Dam, C., 2020. North Sea Energy D4.2 Report on offshore structural integrity and safety performance of H<sub>2</sub> production, processing, storage and transport. [https://north-sea-energy.eu/static/84050b605af439a07d9806c763618802/10a.-FINAL-NSE3\\_D4.2-Report-on-offshore-structural-integrity-and-safety-performance-of-H2-production-processing-storage-and-transport.pdf](https://north-sea-energy.eu/static/84050b605af439a07d9806c763618802/10a.-FINAL-NSE3_D4.2-Report-on-offshore-structural-integrity-and-safety-performance-of-H2-production-processing-storage-and-transport.pdf)

Li, SY., and Urai, J.L. Rheology of rock salt for salt tectonics modeling. *Petroleum Science* 13, 712–724 (2016). <https://doi.org/10.1007/s12182-016-0121-6>

- Li, D., Zhang, Q., Ma, Q., and Shen, S. 2015. Comparison of explosion characteristics between hydrogen/air and methane/air at the stoichiometric concentrations, *International Journal of Hydrogen Energy*, Volume 40, Issue 28, pages 8761-8768
- Lopez-Lazaro, C., Bachaud, P., Moretti, I., and Ferrando, N., 2019. Predicting the phase behavior of hydrogen in NaCl brines by molecular simulation for geological applications. *BSGF - Earth Sci. Bull.* 190 7.
- Middel, M.T., 2010. Kwantitatieve Risicoanalyse Aardgasbuffer Zuidwending. KEMA.
- Molema, F., 2021. Reconnaissance study on the impact of leakage of subsurface-stored hydrogen on groundwater chemistry. TNO report 2021 S10234.
- Mannan, S., 2005. *Lees' Loss Prevention in the Process Industries*, 3rd ed., vol. 1. Elsevier Butterworth-Heinemann.
- Molkov, V., and Kashkarov, S., 2015. Blast Wave from a High-Pressure Gas Tank Rupture in a Fire: Stand-alone and Under-Vehicle Hydrogen Tanks, *International Journal of Hydrogen Energy*, Volume 40, Issue 36, Pages 12581-12603
- NOGEPa OPCOM, 2016. Industry Standard No. 41 – Well Engineering and Construction Process.
- Panfilov, M., 2016. Underground and pipeline hydrogen storage. In *Compendium of hydrogen energy* (pp. 91-115). Woodhead Publishing.
- PGS 3, 2005. Guidelines for Quantitative Risk Assessment.
- Reitenbach V., Albrecht D., Ganzer L., 2014. Influence of hydrogen on underground gas storage. Literature Study DGMK 752, DGMK Hamburg.
- Reitenbach, V., Ganzer, L., Albrecht, D., and Hagemann, B., 2015. Influence of added hydrogen on underground gas storage: a review of key issues. *Environ Earth Sci* 73, 6927–6937. <https://doi.org/10.1007/s12665-015-4176-2>
- Robertson, I.M., Sofronis, P., Nagao, A., Martin M.L., Wang S., Gross D.W., and Nygren K.E. 2015. Hydrogen Embrittlement Understood. *Metall Mater Trans A* 46, 2323–2341 (2015). <https://doi.org/10.1007/s11661-015-2836-1>
- Sochet, I., 2010. Blast Effects of External Explosions, Eighth International Symposium on Hazards Prevention, and Mitigation of Industrial Explosions, September 2010, Yokohama, Japan, hal-00629253
- Tang, M.J., and Baker, Q.A., 1999. A New Set of Blast Curves from Vapor Cloud Explosions, *Process Safety Progress*, 18(3):235-240
- Van der Valk, K., Van Unen, M., Brunner, L., and Groenenberg, R., 2020. Inventory of risks associated with underground storage of compressed air (CAES) and hydrogen (UHS), and qualitative comparison of risks of UHS vs. underground storage of natural gas (UGS). TNO report 2020 R12005.  
<http://publications.tno.nl/publication/34637695/1RqPrg/TNO-2020-R12005.pdf>

Van Wortel, J.C., 2019. Durability of steels for transmission pipes with hydrogen, EU project 'Naturalhy' (WP-3), report no.: R0096-WP3-C-0, (D32),".

Veiligheidsregio Rotterdam-Rijnmond, 2013. Rampenbestrijdingsplan, Brzo-inrichtingen Rotterdam-Rijnmond, Werkgroep Planvorming

## A BowTie diagram

### A.1 General, top-level bow ties

Available as separate document *TNOreport\_DEI4819001\_Annex\_Bow Tie - 1. General.pdf*

### A.2 Detailed, expanded bow ties

Available as separate document *TNOreport\_DEI4819001\_Annex\_Bow Tie - 2. Detailed.pdf*

## B Effect of well geometry

As discussed in section 3.1.3, the study on the outflow of hydrogen also considered a well geometry different from the one for which the results were reported and discussed in section 3.2.1. In general, it has to be noted that the well geometry is not critical as the flow is mainly determined by the choking behaviour at the outlet. Simulations have been performed though with both well geometries to study any differences and this appendix compares results obtained for the two well geometries. This will help us to present and discuss the relevance of further detailed results in Appendix C and which have been obtained for this other well geometry.

### B.1 Different well geometry

The well path as used in the outflow study has been given via Table 3 and Figure 8. Added to this well path in the OLGA model is a 20 m topside piping of 20 m as explained in section 3.1.3. The specifics of the different well geometry the study started with is given in Table 13. This different geometry was obtained because the measured depth (md) was interchanged with the reach. Next to this inconsistent well path all other geometrical parameters were the same as found in Table 4.

Table 13: Well path coordinates for different well path

Horizontal / reach (md)	Vertical / TVD (m)
0	0
205	205
240	240
587	566
590	568
937	895
942	900
1263	1219

### B.2 Simulation cases

For the well path of Figure 8 not as many simulations were performed as for the different well geometry given in Table 13. In section 3.1.3 (Table 5) the main set of simulations performed for Figure 8's well path has been provided and which simulations only concerned ones with a high heat transfer coefficient. This because simulations done with the different well geometry showed that the difference in mass flow obtained is negligible.

For the different well path three sets of simulations with OLGA have been done and which concern:

- Adiabatic scenario
- Heat transfer in the well
- Very high heat transfer in the cavern

Furthermore, for a selected number of scenarios a sensitivity has been done to study the effect of dry hydrogen versus water saturated hydrogen. In a last step sensitivity of the results has been studied with respect to grid size.

In Table 14, an overview is given of the large set of simulations performed for the different well geometry of Table 13, where the several settings that define the simulations have been explained at the introduction of Table 5 in section 3.1.3.3. For a subset of these simulations results are being discussed in this Appendix B and several results are compared with the corresponding ones for the well geometry of Figure 8.

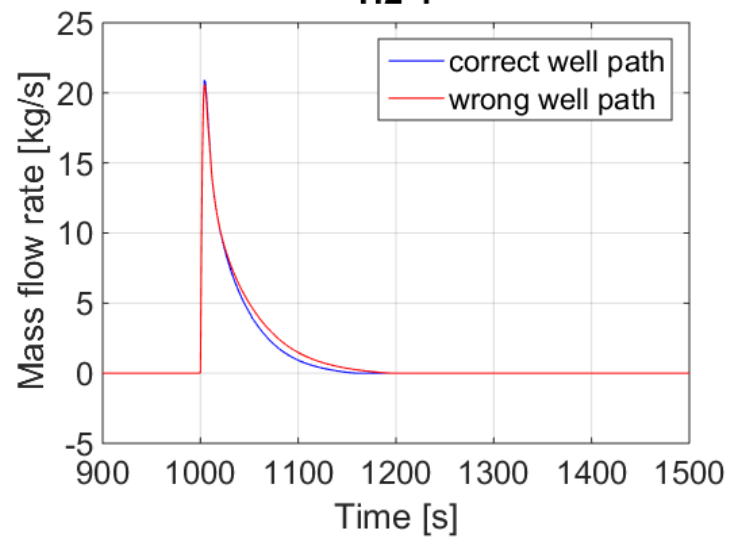
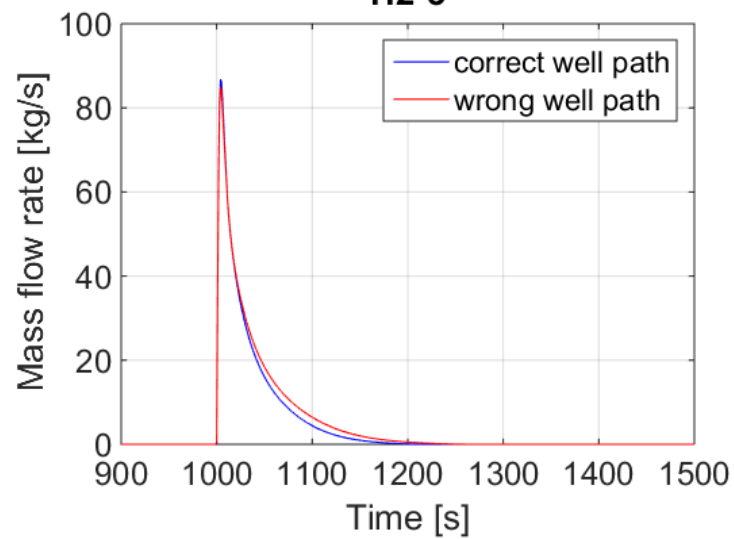
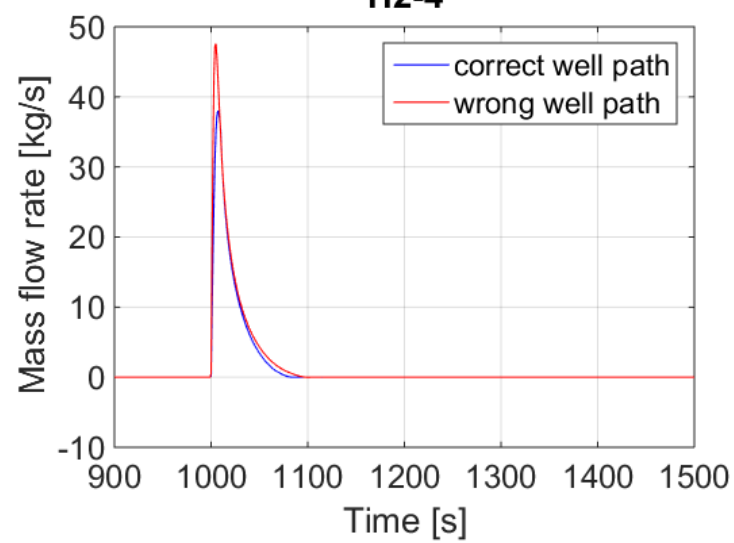
Table 14: Simulation cases for different well path given in Table 13

Simulation name	Phase	Tubing /casing /leak	Pressure [bar]	Volume [m <sup>3</sup> ]	Leak Size [mm]	Thermal	Fluid
H2_1	pilot	tubing	50	117		adiabatic	dry
H2_2	pilot	tubing	135	117		adiabatic	dry
H2_3	pilot	tubing	220	117		adiabatic	dry
H2_4	pilot	casing	50	117		adiabatic	dry
H2_5	pilot	casing	135	117		adiabatic	dry
H2_6	pilot	casing	220	117		adiabatic	dry
H2_7	pilot	leak	50	117	1, 2, 5, 10	adiabatic	dry
H2_8	pilot	leak	135	117	1, 2, 5, 10	adiabatic	dry
H2_9	pilot	leak	220	117	1, 2, 5, 10	adiabatic	dry
H2_10	full	tubing	70	3*10 <sup>5</sup>		adiabatic	dry
H2_11	full	tubing	135	3*10 <sup>5</sup>		adiabatic	dry
H2_12	full	tubing	200	3*10 <sup>5</sup>		adiabatic	dry
H2_13	full	tubing	70	1*10 <sup>6</sup>		adiabatic	dry
H2_14	full	tubing	135	1*10 <sup>6</sup>		adiabatic	dry
H2_15	full	tubing	200	1*10 <sup>6</sup>		adiabatic	dry
H2_1_U	pilot	tubing	50	117		U value	dry
H2_2_U	pilot	tubing	135	117		U value	dry
H2_3_U	pilot	tubing	220	117		U value	dry
H2_10_long	full	tubing	70	3*10 <sup>5</sup>		adiabatic	dry
H2_11_long	full	tubing	135	3*10 <sup>5</sup>		adiabatic	dry
H2_12_long	full	tubing	200	3*10 <sup>5</sup>		adiabatic	dry
H2_13_long	full	tubing	70	1*10 <sup>6</sup>		adiabatic	dry
H2_14_long	full	tubing	135	1*10 <sup>6</sup>		adiabatic	dry
H2_15_long	full	tubing	200	1*10 <sup>6</sup>		adiabatic	dry
H2_10_U	full	tubing	70	3*10 <sup>5</sup>		U value	dry
H2_11_U	full	tubing	135	3*10 <sup>5</sup>		U value	dry
H2_12_U	full	tubing	200	3*10 <sup>5</sup>		U value	dry
H2_10_U	full	tubing	70	1*10 <sup>6</sup>		U value	dry
H2_1_U2	pilot	tubing	50	117		U value	dry

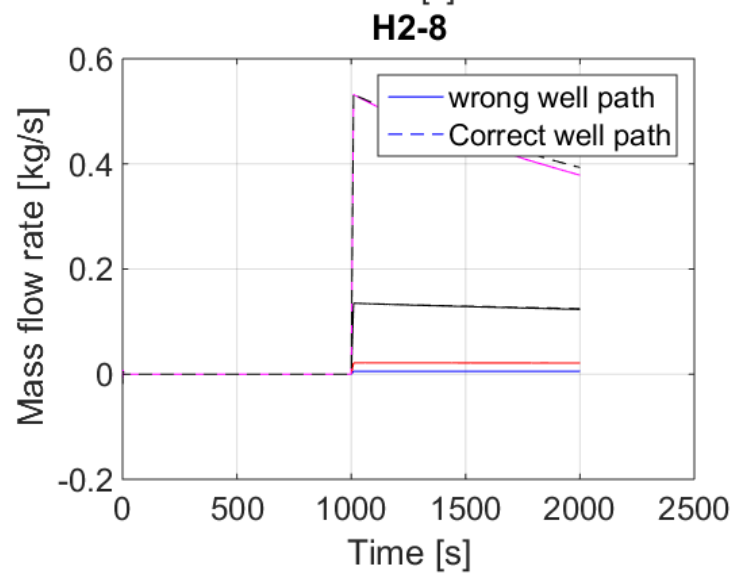
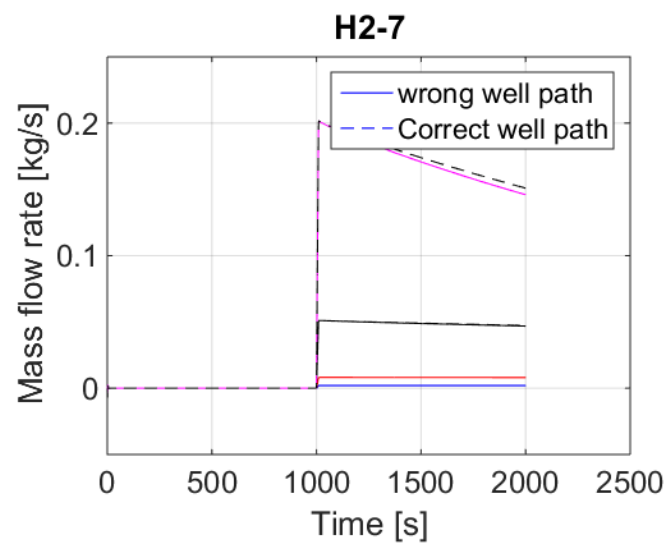
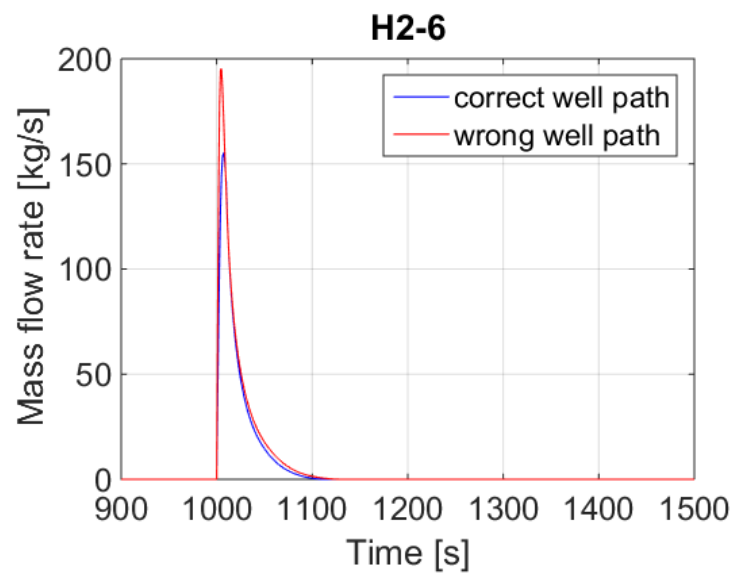
H2_2_U2	pilot	tubing	135	117		U value	dry
H2_3_U2	pilot	tubing	220	117		U value	dry
H2_4_U2	pilot	casing	50	117		U value	dry
H2_5_U2	pilot	casing	135	117		U value	dry
H2_6_U2	pilot	casing	220	117		U value	dry
H2_7_U2	pilot	leak	50	117	1, 2, 5, 10	U value	dry
H2_8_U2	pilot	leak	135	117	1, 2, 5, 10	U value	dry
H2_9_U2	pilot	leak	220	117	1, 2, 5, 10, 3	U value	dry
H2_10_U2	full	tubing	70	$3 \cdot 10^5$		U value	dry
H2_11_U2	full	tubing	135	$3 \cdot 10^5$		U value	dry
H2_12_U2	full	tubing	200	$3 \cdot 10^5$		U value	dry
H2_13_U2	full	tubing	70	$1 \cdot 10^6$			
H2_10_U2	full	tubing	70	$1 \cdot 10^6$		U value	dry
H2_11_long_U2	full	tubing	135	$3 \cdot 10^5$		U value	dry
H2_9_U2_alternative	pilot	leak	220	117	1, 2, 5, 10, 3	U value	dry
H2_16	pilot	tubing	50	117		adiabatic	H <sub>2</sub> O saturated
H2_17	pilot	tubing	135	117		adiabatic	H <sub>2</sub> O saturated
H2_18	pilot	tubing	220	117		adiabatic	H <sub>2</sub> O saturated
H2_19	full	tubing	70	$3 \cdot 10^5$		adiabatic	H <sub>2</sub> O saturated

### B.3 Comparison results influence well path

In Figure 27 simulation results obtained for the two well paths are compared for several main cases. In general, the conclusion is drawn that such results do not differ much. This specifically holds for the cases with a tubing leak and with a small leak hole, i.e. the cases 1, 2 and 3, and 7, 8 and 9. In these cases the peak height at opening of the valve is almost identical. For the cases with the casing leak, i.e. cases 4, 5 and 6, well path of Figure 8 does show a somewhat smaller peak height in comparison with the one for the different well path. This is likely due to the fact that in a larger diameter 'leak' frictional choking does occur with some more difficulties. The exact reason for the observed difference of 15% is unclear though at this stage. In case of a small leak the tubing does not play a role at all and the mass flow is fully determined by critical flow at the leak.

**H2-1****H2-3****H2-4**





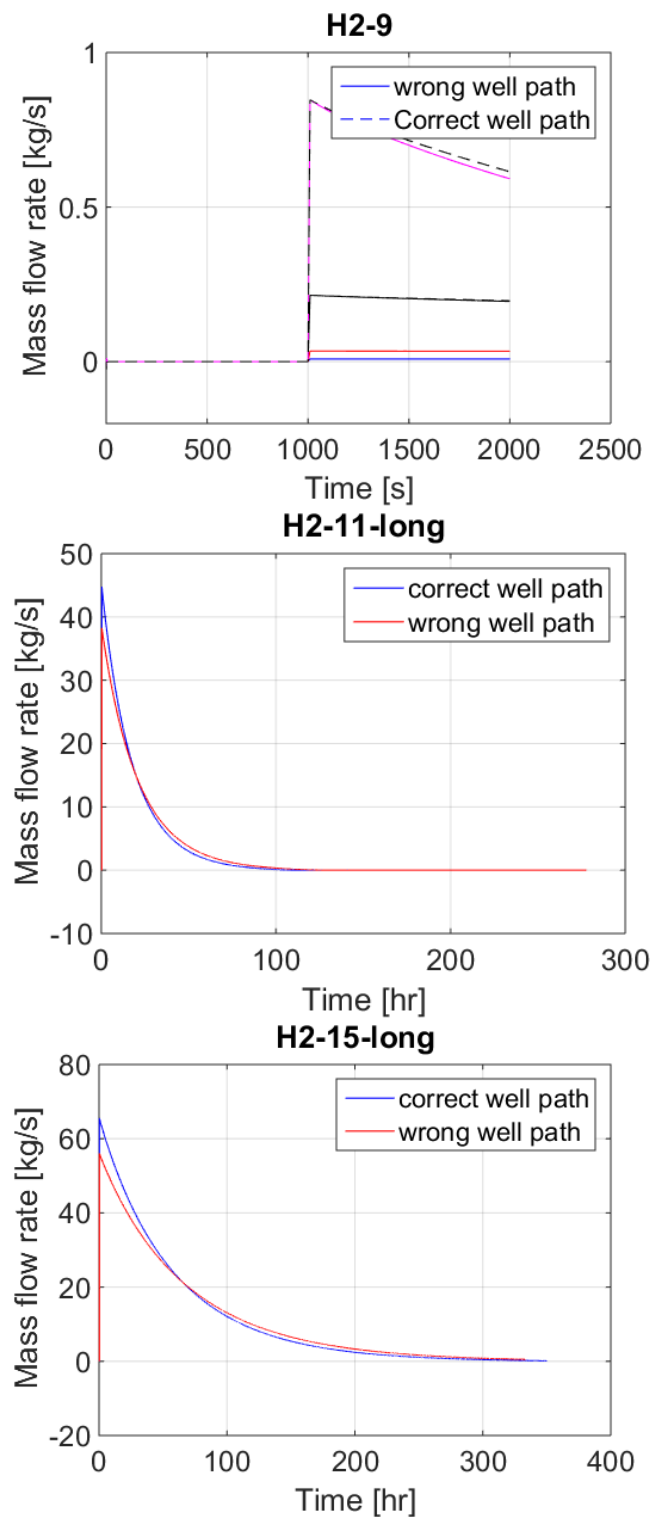


Figure 27: Comparison outflow mass flow rate updated and wrong well path. Cases 1,2 and 3 are pilot phase with tubing leak, cases 4,5 and 6 are pilot phase with casing leak, and cases 7, 8 and 9 are pilot phase with a small leak. Case 11 is a full-scale cavern phase with cavern volume 0.3 Mm<sup>3</sup> and starting start pressure 135 bar, and case 15 is a full-scale cavern phase with volume 1 Mm<sup>3</sup> and starting pressure = 200 bar.

## C Detailed results OLGA-old well path

Further to section 3.2 and to Appendix B, this second Appendix presents and discusses further results on mass outflow and cavern pressure drop obtain for the different well path.

### C.1 Mass flow rate

In Figure 28 to Figure 33 mass outflow rates in time are presented for several representative cases. For the pilot phase (with 50 to 220 bar as starting pressure) it is observed that the maximum leak rates are 20 to 86 bar, with a pressure depletion in approximately 200 seconds. In case of a full casing breach, the maximum leak rates increase up to 196 kg/s with depletion time drops down to approximately 100 seconds. At full pilot scale the leak rates are up to 80 kg/s at a starting pressure of 200 bar, and depletion takes 120 and 300 hours for the cavern volumes 0.3 Mm<sup>3</sup> and 1 Mm<sup>3</sup>, respectively. An overview of all leak rates and depletion times are given in Table 15.

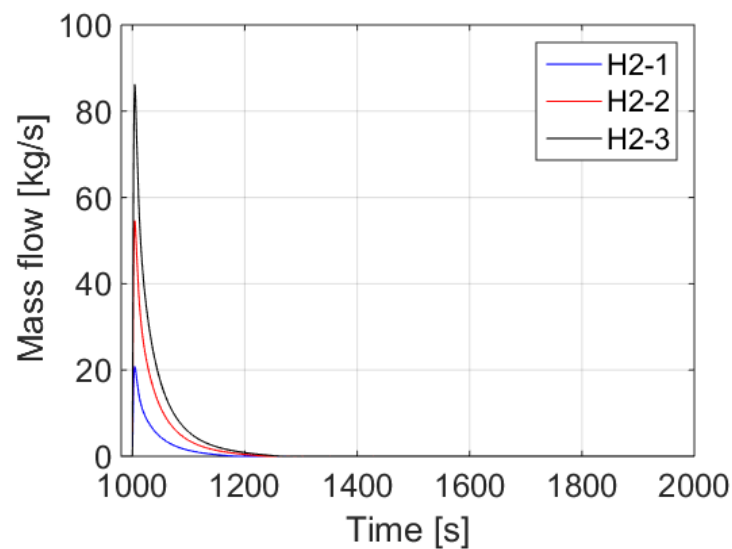


Figure 28: Mass flow rate as function of time for H2-1, H2-2, H2-3, i.e. pilot phase, tubing leak with 50, 135 and 220 bar starting pressure, respectively.

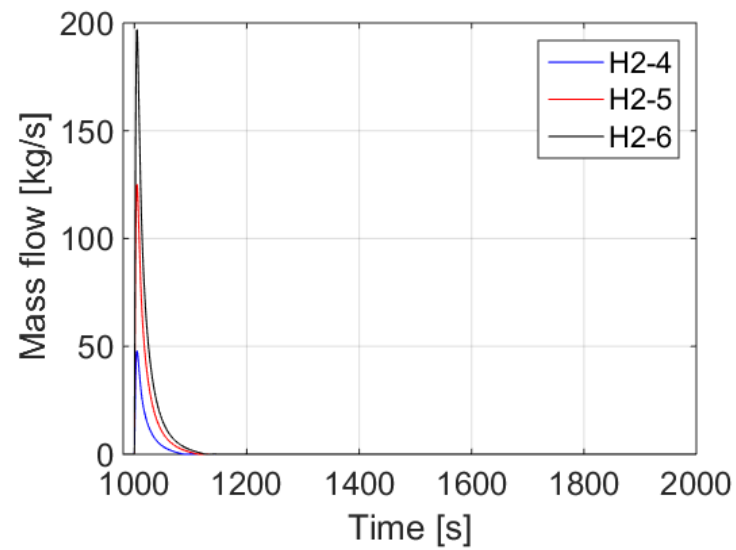


Figure 29: Mass flow rate as function of time for H2-4, H2-5, H2-6, i.e. pilot phase, casing leak, with 50, 135 and 220 bar starting pressure, respectively.

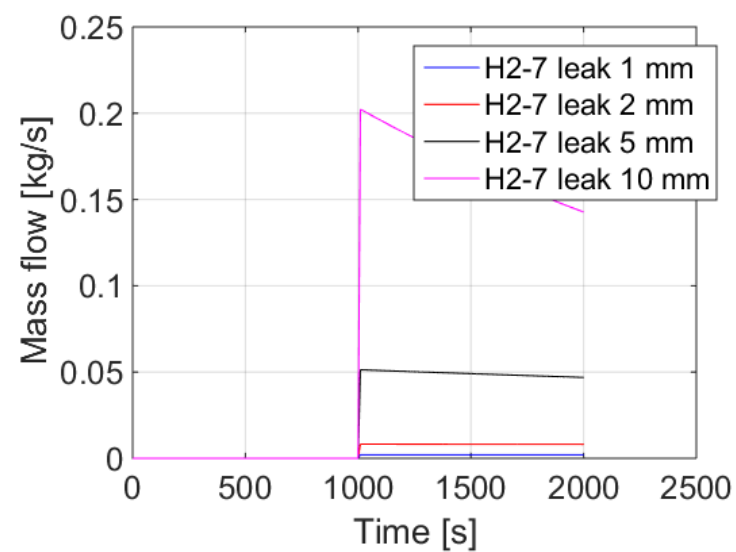


Figure 30: Mass flow rate as function of time for H2-7, i.e. pilot phase, small leak holes, and 50 bar starting pressure.

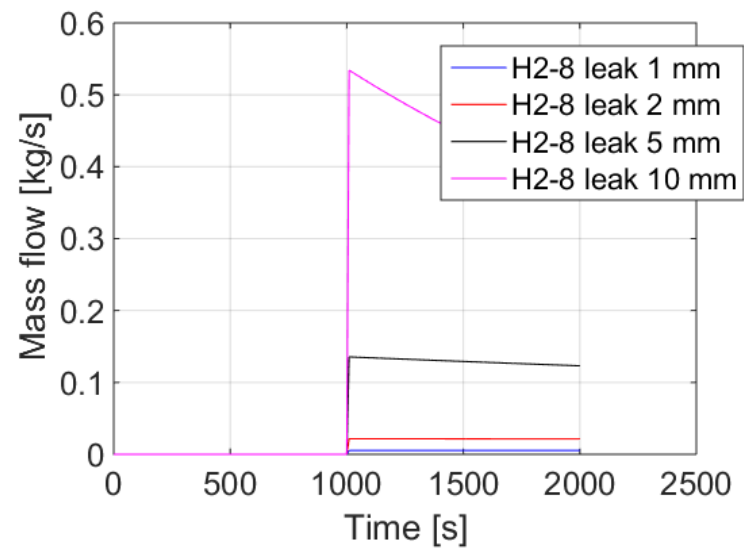


Figure 31: Mass flow rate as function of time for H2-8, i.e. pilot phase, small leak holes, and 135 bar starting pressure.

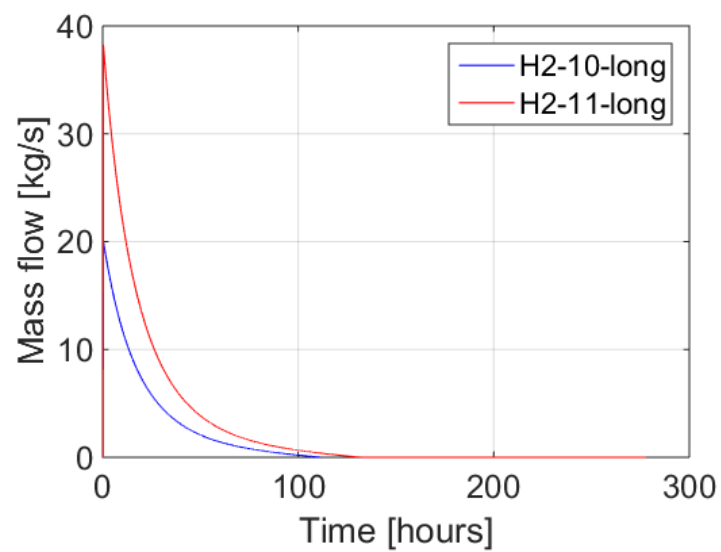


Figure 32: Mass flow rate as function of time for H2-10\_long, H2-11\_long, i.e. full-scale cavern phase, 0.3 Mm<sup>3</sup> volume, tubing leak, and 70, 135 bar starting pressure, respectively.

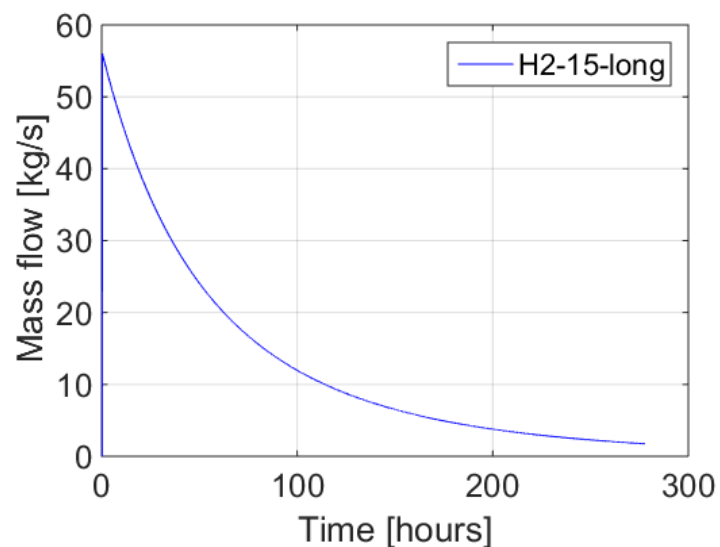


Figure 33: Mass flow rate as function of time for H2-15\_long, i.e. full-scale cavern phase, 1 Mm<sup>3</sup> volume, tubing leak, 200 bar starting pressure.

Table 15: Maximum leak rates and depletion times (pressure down to 2 bar)

Simulation cases	Description	Depletion Time	Peak rates [kg/s]
H2-1	Pilot phase, tubing leak, starting pressure: 50 bar	122 s	20
H2-2	135 bar	167 s	55
H2-3	220 bar	190 s	86
H2-4	Pilot phase, casing leak, starting pressure: 50 bar	60 s	48
H2-5	135 bar	81 s	125
H2-6	220 bar	92 s	196
H2-10_long	Full-scale cavern phase, tubing leak, 0.3 Mm <sup>3</sup> cavern volume, starting pressure: 70 bar	83 hr	29
H2-11_long	135 bar	91 hr	55
H2-12_long	200 bar	not calculated	80
H2-13_long	Full-scale cavern phase, tubing leak, 1 Mm <sup>3</sup> cavern volume, starting pressure: 70 bar	not calculated	29
H2-15_long	200 bar	243 hr (down to 5 bar)	56

## C.2 Influence water saturation

For a selection of cases found in Table 14 the difference in results obtained in the outflow study for dry hydrogen and for hydrogen with water saturated at cavern conditions is found in Figure 34 to Figure 37, and where each time the mass outflow as function of time is compared. In case of saturated gas, water will condense when flowing to surface due to the cooling effect of the pressure decrease of the cavern. Please note that, as no initial free water (brine) is in the cavern at the start of each simulation, effects of hydrogen taking free water to surface are not accounted for.

In case of the pilot phase, the mass outflow rate changes marginally between the two simulations. In case of the highest starting pressure (H2-3, Figure 36) the flow is somewhat more unstable. This is mainly explained by the effect of small traces of liquid on the frictional pressure drop and on the behaviour at the choking point. As the choking depends on the speed of sound and is affected by the liquid volume fractions, variation in these fractions will influence the choking behaviour slightly. However, for the simulations performed, the average outflow is not influenced.

This also holds for the full-scale cavern phase as shown in Figure 37. On the larger time scale the mass flow fluctuations are larger than for the pilot phase, but again, the average outflow is equal between the two simulations. This is due to the fact that the actual hold-up at the outflow is still very limited. For example, for case H2-19, the liquid volume fraction is just 0.023% (Figure 38).

Therefore, it is concluded that the simulations with the model with dry hydrogen are representative for the expected outflow and no corrections are required for any water saturation for the outflow study.

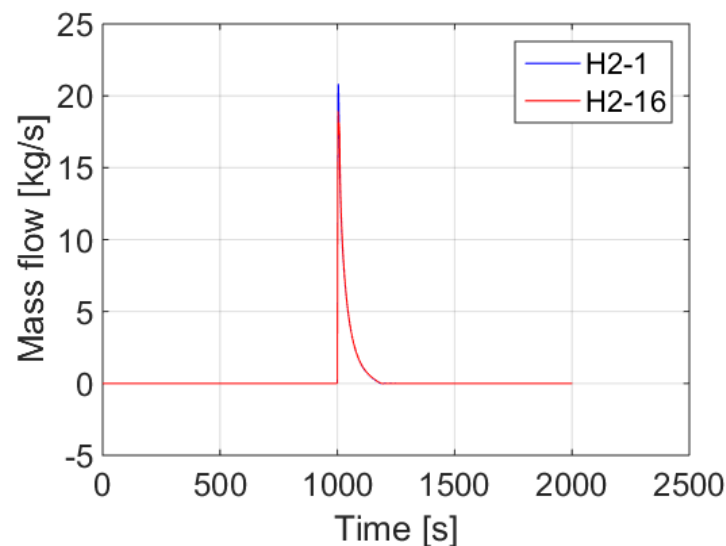


Figure 34: Comparison outflow mass flow rate dry gas (H2-1) and saturated gas (H2-16), i.e. pilot phase, tubing leak, 50 bar starting pressure.

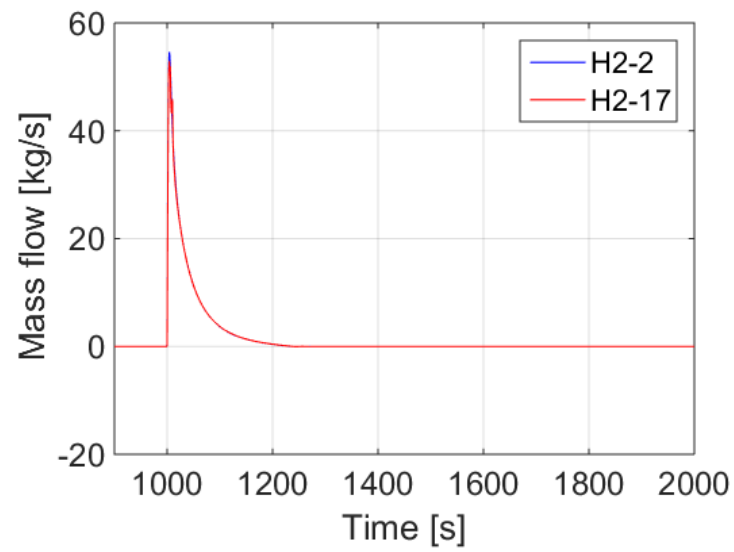


Figure 35: Comparison outflow mass flow rate dry gas (H2-2) and saturated gas (H2-17), i.e. pilot phase, tubing leak, 135 bar starting pressure.

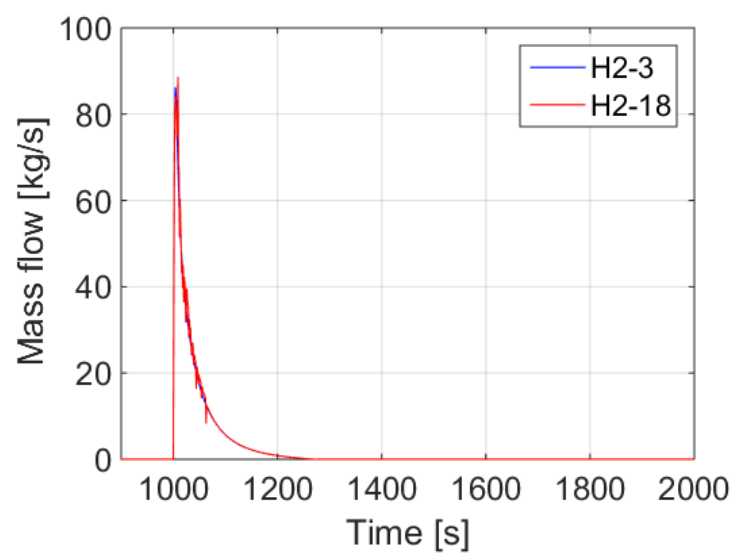


Figure 36: Comparison outflow mass flow rate dry gas (H2-3) and saturated gas (H2-18), i.e. pilot phase, tubing leak, 220 bar starting pressure.



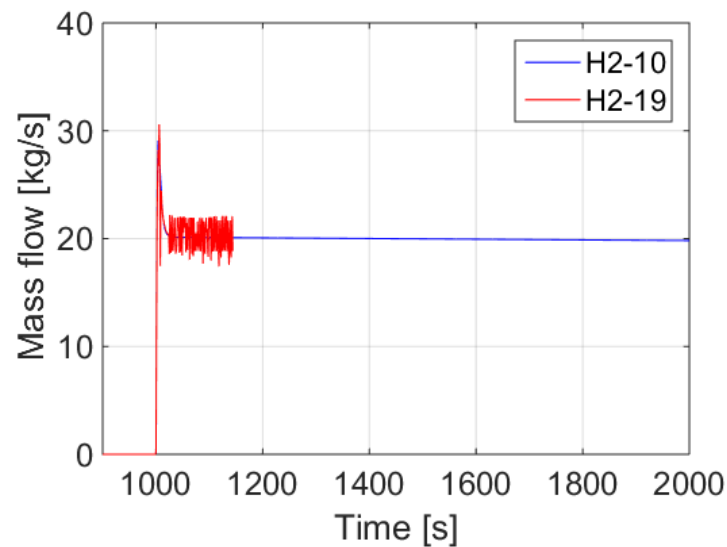


Figure 37: Comparison outflow mass flow rate dry gas (H2-10) and saturated gas (H2-19), i.e. full-scale cavern phase, 0.3 Mm<sup>3</sup>, tubing leak, 70 bar starting pressure.

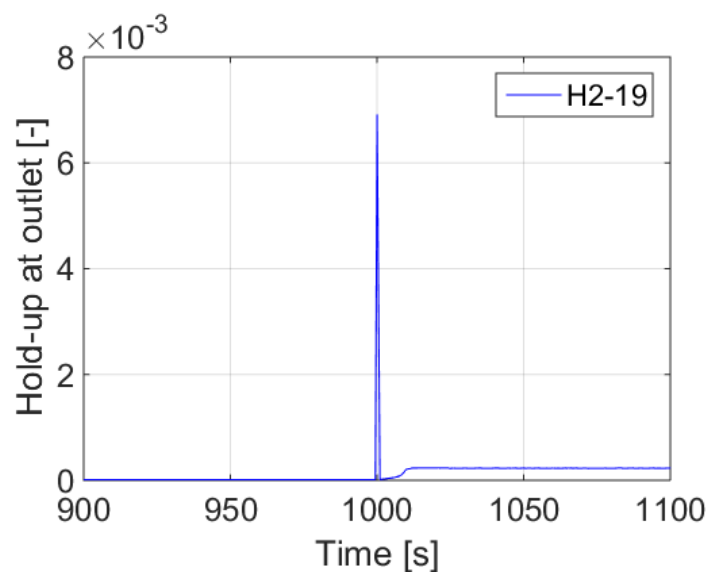


Figure 38: Hold-up (liquid volume fraction) as function of time for case H2-19, i.e. full-scale cavern phase, 0.3 Mm<sup>3</sup>, tubing leak, 70 bar starting pressure.

### C.3 Influence heat transfer

A physical effect to properly take account off in the outflow simulation concerns heat transfer in the well and cavern. At small time scales the system of flow from the cavern to the surface will behave adiabatic. This means that heat transfer to/from the surrounding is minimal. This has as consequence that the temperatures in the cavern will drop quickly down to potentially extreme low temperatures. This is due to the work done by the gas to flow from the cavern and is not dependent on the sign of the Joule-Thompson (JT) effect. That means even with a positive JT-coefficient for hydrogen cooling will take place.

On a longer time scale, the adiabatic assumption is not valid as the surrounding rock structure of and any brine present in the cavern will heat up the hydrogen. However, it must be remarked that as the actual flow rates in the cavern are low, the actual heat transfer between the brine and hydrogen and between the hydrogen and the brine will not be very high.

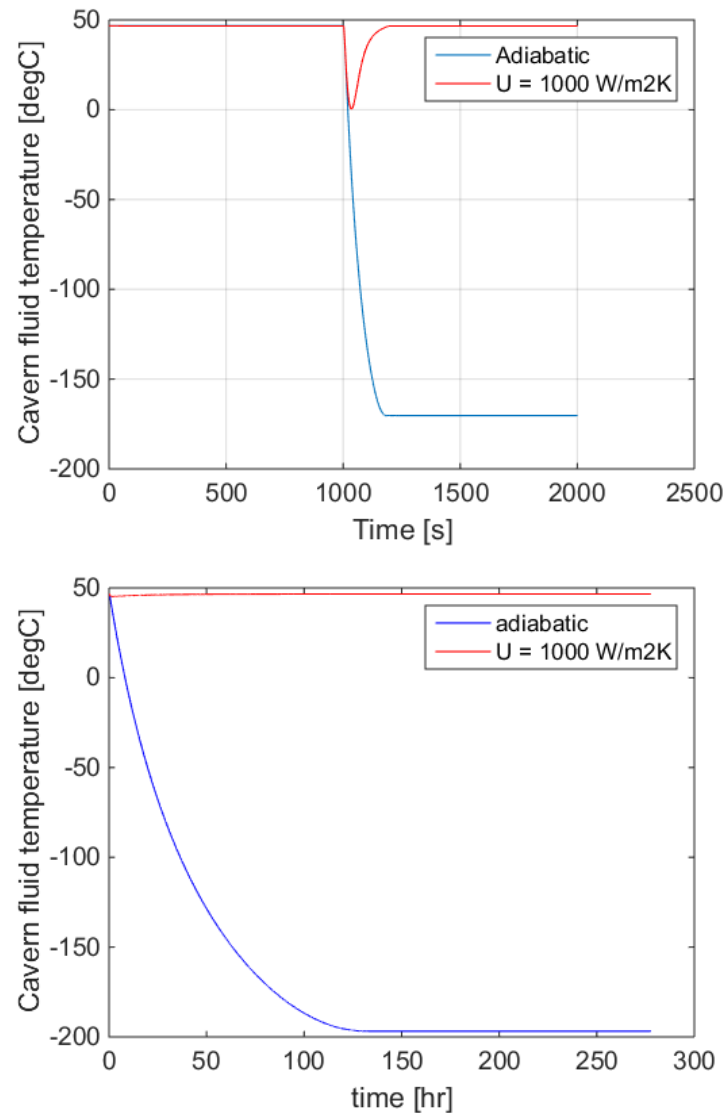


Figure 39: Comparison cavern temperature H1 (top) and H11-long (bottom) with adiabatic (blue) and  $U_{\text{value}} = 1000 \text{ W/m}^2\text{K}$  (red), i.e. pilot phase, tubing leak, 50 bar starting pressure, and full-scale cavern phase,  $0.3 \text{ Mm}^3$  cavern volume, tubing leak, and 135 bar starting pressure.

For a selection of cases the results obtained with an adiabatic assumption and with a heat transfer coefficient are compared via Figure 39 to Figure 42. Here a very high heat transfer coefficient of  $U = 1000 \text{ W/m}^2\text{K}$  is set for the cavern. This results in a more or less constant temperature, and it has to be noted that this value may lead to an overestimation of the heat transfer.

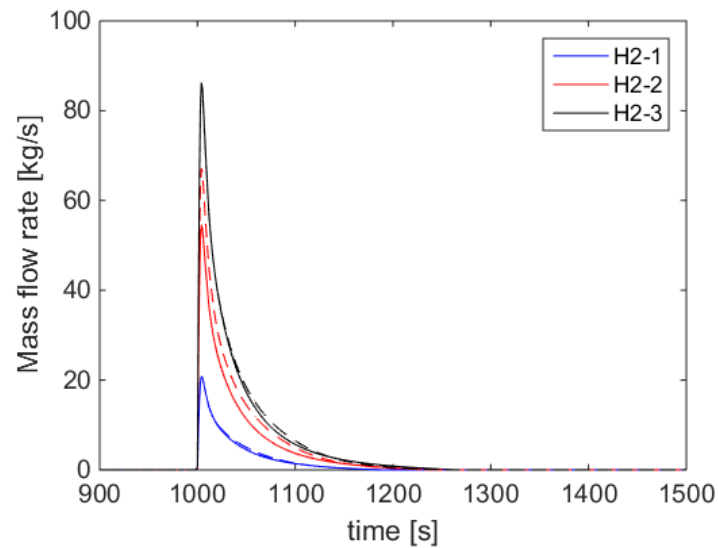


Figure 40: Mass flow rate as function of time for H2-1, H2-2, H2-3. Comparison adiabatic (solid lines) with Uvalue (dashed), i.e. pilot phase, tubing leak, and 50, 135, 220 bar starting pressure, respectively.

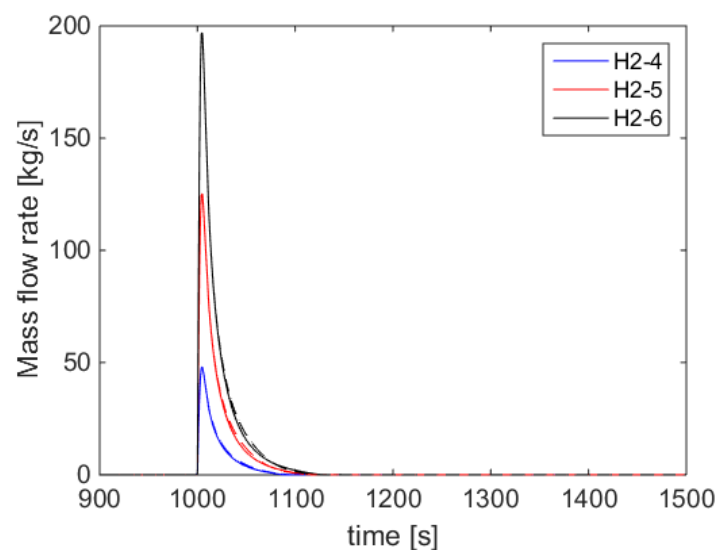


Figure 41: Mass flow rate as function of time for H2-4, H2-5, H2-6. Comparison adiabatic (solid lines) with Uvalue (dashed), i.e. pilot phase, casing leak, and 50, 135, 220 bar starting pressure.

For the pilot phase and full-scale cavern phase, the temperature in cavern is compared for each of the two assumptions for heat exchange, and which is shown in Figure 39. In case of an adiabatic flow, the temperatures drop down to unrealistic low values of  $T = -150$  to  $-200$  °C. In case of a high heat transfer, the resulting temperatures are more realistic and constant in time.

The resulting outflow for the assumptions for heat exchange are shown in Figure 40 and Figure 41 for the pilot phase, with tubing leak and with casing leak, and in Figure 42 for the full-scale cavern phase with tubing leak. It is observed that the difference in the outflow results is relatively small. Therefore, the choice between the different heat transfer solutions is concluded to be not very critical.

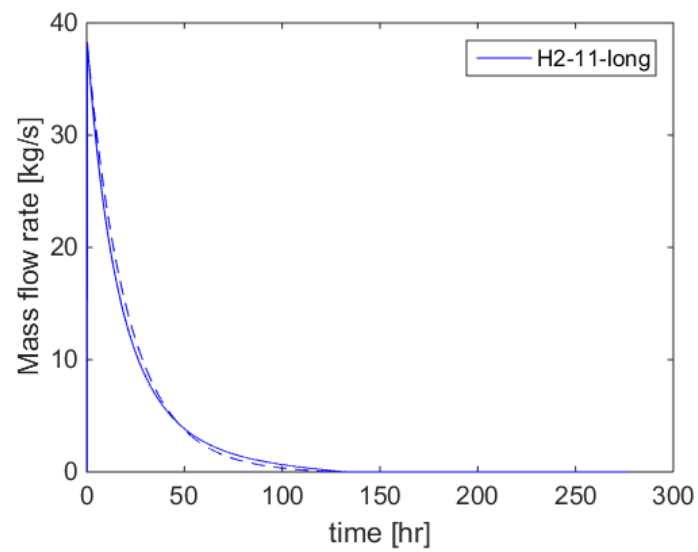


Figure 42: Mass flow rate as function of time for H2-11\_long, i.e. full-scale cavern phase, 0.3 Mm<sup>3</sup> cavern volume, tubing leak, 135 bar starting pressure. Comparison of adiabatic (solid lines) versus Uvalue (dashed) showing that results match very well.